University of Reading

Department of Cybernetics

Behavioural and Neural Correlates of Emergent Proto-Languages and Joint Action

Nicolas Thorne

Abstract

Haptic communication between humans plays a vital role in society. Although this form of communication is ubiquitous at all levels of society and human development, little is known about how synchronized coordination of motion between two persons would lead to higher-order cognitive functions used in haptic communication. During this project, a novel experimental paradigm was developed. In it, participants used their hands to control the rod to collect the coins on the screen. The aim was to investigate the neural and behavioural correlates of emergent haptic communication between paired participants. During the experiment, haptic interactions and neural synchronizations between paired participants were recorded and compared to baseline pairs. Baseline pairs were created from non-interacting single participants. During the Ph.D., two experiments were conducted. The first focused on haptic interactions and characterising the emergent proto-language that participants used to communicate. The second experiment used a novel hyperscanning methodology to isolate the synchronization characteristics of emergent proto-languages and social interactions. The EEG experiment presented here explores the interbrain synchronization between interacting participants systematically. This paradigm allows participants to interact with each other freely. This genuinely novel paradigm allows researchers to study pairs of participants in truly social situations. By comparing pairs with single participants, it has been possible to identify behavioural and neural characteristics related to the emergent proto-language that participants are using as a means of communication. Both of the experiments detailed here describe pioneering work in the study of social interactions and the emergence of proto-languages.

Acknowledgements

List of Publications

Thorne, N., Honisch, J. J., Kondo, T., Nasuto, S., & Hayashi, Y. (2018, Dec 5-6). Emergence of long range temporal correlations in cooperative tasks [Conference poster]. The 2nd International Symposium on Embodied-Brain Systems Science (EMBOSS), Tokyo, Japan.

Thorne, N., Honisch, J. J., Kondo, T., Nasuto, S., & Hayashi, Y. (2019). Temporal structure in haptic signalling under a cooperative task. Frontiers in Human Neuroscience, 13, 372.

Contents

List of Figures

Chapter 1

Introduction

For social animals, moving bodies in a coordinated manner plays an essential role in facilitating social interactions. Such coordinated actions are common in human group activities and include playing music, dancing, and jointly carrying objects, to name a few [1, 2, 3, 4]. Social interactions rely on exchanging information to identify a shared objective and create a closed-loop between the two individuals and their environment.

This project aimed to identify the behavioural and neural correlates of coordinated motion between paired participants. It was divided into two experiments. The first was a behavioural experiment, focused on identifying the force-force interactions' temporal structures that occurred while participants jointly lifted an object. The second experiment focused on calculating the correlations between inter and intrabrain electrodes between paired participants and surrogate pairs.

To study the social interactions between individuals while they coordinate their bodies in space and time, we need to move away from traditionally

held assumptions that say that high-level cognitive processes can be studied in isolation. Instead, it is essential to study how the mind and body are embedded in the world [5]. Embodied dynamics focuses on self-organising dynamic systems and claims that cognitive processes emerge from the continuous sensory-motor interactions involving the brain, body, and environment that form a closed loop[6]. The central idea is to look at the mind as an embodied dynamic system in a changing world. In the past, creating an adequate experimental setup to study embodied dynamics was extremely difficult. However, researchers can use human-computer interfaces to reduce the parameters used in social expression and overcome some of the difficulties of studying complex human-to-human interactions in real-time. For example, using the cursor motion and objects on a computer display, Auvray et al. developed the Perceptual Crossing Experiments (PCE) in which participants were to move their object and identify the other active player's avatar [7]. Using the PCE, Froese et al. found that social judgments were not based on one individual recognizing the other, but rather, on a mutually shared recognition of each other, i.e., on an interactively shared cognitive process [8].

In physical human-human interactions, haptic sensory feedback between participants could be used as a channel to share the mutual intentions between interacting participants. This channel could play a primary role in the construction of a shared motor plan. Van der Wel et al. showed that paired participants created a haptic channel by overlapping their forces[9]. This channel was used to transfer haptic information and to facilitate coordination between participants. Although the use of haptic channels was previously identified, the dynamic properties remain to be explored.

Investigations into haptic interactions typically focus on skill transfer between participants. They have shown that participants improve their task performance when coupled with each other, even if one is more proficient than the other. Results from skill transfer experiments done by Ganesh et al. suggest that subjects subconsciously used haptic information to enhance their performance[10]. Pairs of participants followed a target along a circular path using a mechanical interface. Participants could see their partner seated across from them but could not see their hand movements nor their screen. Two different conditions were tested, single, and connected. During the single condition, participants followed the target on their own. During the connected condition, the participants' hands were connected by a weak virtual elastic band using the mechanical interface. Results showed that dyads achieved significantly better results when haptically coupled with a partner than when they participated alone. Research by Mireles et al. further investigated the transfer of skills between interacting participants. They showed that pairs of naive participants could complete the task more quickly than pairs consisting of naive and expert participants [11]. Mireles et al. concluded that. They concluded that it is essential for naive participants to properly explore the space to learn a complete representation of the dynamics of the task [12, 11, 13]. Although haptic communication has been studied in the context of skill transfer, the main focus has been the characterization of motor performance as a result of haptic communication. Thus, the question of what is transmitted between partners that allows them to coordinate their movements remains.

Haptic communication uses the action-perception loops in which each participant moves their body and feels the force transmitted by their partner.

The key to this haptic communication is the coupling of the haptic action-perception loops of each participant. This project was aimed at studying these dynamic processes from behavioural and neurological points of view.

To this aim, a joint coin-collecting paradigm was developed. In this paradigm, participants moved in a 2D space using a peripheral device that allowed for the recording of position and the force applied to the device. Paired participants applied horizontal pressure on a rigid object to overcome gravity and lift it off the ground. The application of concurrent forces generated a haptic channel that participants used to communicate with each other [14, 9]. I hypothesize that this haptic channel was used to transmit bi-directional haptic signals carrying information about the participant's next target. The temporal patterns of the recorded forces were analysed to extract features of haptic signalling between paired participants. It was important for the paradigm to be genuinely social, meaning that participants were free to interact and work together to achieve a common goal.

The second experiment presented in this project added hyperscanning to the original coin collecting paradigm. By recording synchronous activation of neural circuits, both within and between different brains, it was possible to identify complex networks that characterised paired participants. Neural synchrony has been shown to play a central role in many brain functions, including binding neural information from different regions [15]. I hypothesize that synchronous brain oscillations between paired participants are being used to coordinate their movements, and that increased synchrony will be correlated to increased communication between participants.

Quantification of the inter and intra-brain synchronization between partici-

pants required a method robust enough to the false positives typically associated with calculating neural synchrony between participants taking part in the same task. Burgess's work shows that circular correlation was more robust to false positives than the other alternatives. It also gave a lower root mean squared error when compared to known synchronizations [16]. The synchronization between electrodes will be calculated using Burgess's method, and a complex network will be created for each trial. By comparing the networks calculated from paired participants with a baseline composed of two single participants, it is possible to identify network characteristics associated with social interactions and emergent forms of communication called proto-languages. Proto-languages refer to the communication that emerges from the interactions between two or more participants when they interact without using a common language.

The following sections will describe my work throughout this Ph.D. They include a comprehensive literature review, a description of the paradigm I developed, a description of the behavioural experiments as well as their results and conclusions, a description of a set of EEG experiments that were built on the previous experiments, and finally, a conclusion that relates both experiments to each other.

Chapter 2

Literature Review

2.1 Introduction

The research presented in this project lies at the intersection of six different fields of research: synergetics, joint action, haptic interactions, non-extensive entropy, EEG hyperscanning, and complex networks. This chapter will introduce each field and give a review of relevant publications.

Joint action paradigms study how animals create shared mental representations, predict their partner's intentions, and integrate those intentions with their own. Past research into joint action has purposely studied people in isolation. As such, the role of social interactions in joint actions is not yet understood. In this paradigm, it was essential to limit interaction between participants to a modality that could be accurately measured. Ultimately, force-force interactions were chosen as the means through which participants would communicate.

Research on force-force interactions has mostly focused on understanding the circumstances that lead to a complimentary transfer of skills between two people. Although the participants were unaware that there was a haptic connection between them, the results showed that even weak coupling increased the pair's performance. Some forms of coupling, such as visual coupling have been found to have a profound effect on the execution of rhythmic movements. The mechanisms and the means of information exchange that allow for this coupling have not been investigated.

Research into identifying important words or combinations of DNA letters has found that analysing their temporal patterns gives better results than previously used methods. This method uses the q-exponential, calculated using the concept of Tsallis entropy, to characterize the proportion of short and long-range temporal correlations. It is hypothesized that combinations of symbols with more long-range correlations are more likely to be important in transmitting information. How does this communication change the connectivity within a single brain and between two interacting brains?

Recording EEG from more than one participant is called hyperscanning. Hyperscanning paradigms typically restricted the degree of interaction that participants can have during the experiment. Hyperscanning paradigms have studied human interactions during various activities such as musical performances, card games, and imitation. However, few of these experiments gave the participants the freedom for new behaviours to emerge without outside drivers. For example, in the experiments with musical performances, researchers used a metronome to keep a steady tempo.

Analysis of the data collected from hyperscanning experiments has proven

to be challenging to interpret. The challenge is primarily due to the presence of outside drivers, such as flickering light, rhythmic background noise, and even repetitive movement. These can affect neural oscillations and create spurious correlations. Past research has looked at neural synchrony as a possible method of analysing inter and intra brain correlations. Many different methods have been used, in the literature, to characterize the correlations between one time series with another. These methods range from simple phase differences to more complex analysis, such as circular correlations. With these methods, it is possible to represent neural synchrony as a graph where each node is a region of interest (ROI), and the connections are the average correlations between the two or more ROIs.

2.2   Synergetics and Coordination Dynamics

Synergetics is a field of research that was first studied by Herman Haken in 1969. Synergetics studies how the cooperation of many microscopic elements produce a unified function at a macroscopic level. Haken created the tools to study the general principals governing the generation of these functions. Synergetics states that the formation of self-organized patterns in systems far from thermal equilibrium depends on external control parameters. When the control parameter reaches a critical value, the system's parts become unstable and change their configuration to adopt a new macroscopic state. The order parameter is a variable that characterizes changes in macroscopic states. Haken also introduced the slaving principle that states that near critical points, the behavior of a system is completely governed by the order parameters [17]. The concepts outlined by Haken

allow very complex systems to be described using only its order parameters, which are of much lower dimensionality than the original state space. Using the concept of synergetics, Haken, Kelso, and Bunz studied the coordination between two individuals. In their first experiment, participants were asked to flex their fingers in an out of phase pattern at increasing frequencies. They found that subjects showed only two stable states: one in-phase and one out of phase. Transitions from one state to another were abrupt and influenced by the movement frequency. Haken Kelso and Bunz studied these phase transitions in human finger movements and proposed a model of the potential function that describes the phase transitions[18]. These principals are known as the HKB model and have been used to study many other human behaviours such as reaction and anticipation.

Engstrom et al. asked paired participants to coordinate their finger flexions with each other in one of three patterns, reactive, synchronised, or syncopated [19]. During the experiment, participants were asked to increase their movement frequency. They found that manipulating the frequency could induce an involuntary change from a reactive state to an anticipatory one. These results suggested that reaction and anticipation are stable modes of a dynamic system and not two separate behaviours.

The shifts from reaction to anticipation based on target frequency are consistent for a wide array of tasks. Hayashi et al. asked participants to track a target around a circular path at different speeds. Three conditions were tested in the experiment:

1. The target was fully visible during the whole trial.

2. The circular orbit included two regions where the target was invisible

(30% of the top and bottom).

3. Subject was asked to track a previously recorded trial under condition 1.

The target frequency was increased from 0.1 Hz to 0.7 Hz in steps of 0.2 Hz during all three conditions. The experiment also included a mechanical tracking section, where participants tracked a tracer controlled by the PC, and a mutual tracking one, where a single participant controlled both tracers.

The results showed that in both the mutual and mechanical tracking conditions, there was a change in behaviour at 0.3Hz. In the case of singles, it marked the change between a reactive error correction mode to an anticipatory one. In paired subjects, it marked the change between a mutual error correction mode to a synchronised one.[2] Previous research also identified this frequency region as the critical area for transitions between reactive and anticipatory modes and has also been shown to hold for other paradigms such as finger tapping.[20, 1]

Other forms of coupling have also been shown to profoundly affect a person's tendency to synchronize with others. For example, Shockley et al. investigated the effects of verbal and visual coupling on postural sway [21]. Participants were asked to find the differences between two cartoon pictures. During the experiment, each participant could only see the picture directly in front of them. To learn about their picture, participants must communicate and describe the picture to each other. The experiment consisted of four different testing conditions that manipulated the participant's

body orientation and the task partner. Body orientation refers to whether the participants can see their partner's bodies while talking. Task partner refers to whom the participant is talking; this could be the other participant or an out of sight experimenter. This experiment suggested that it was verbal interactions and not visual information that synchronised the postural sway of both participants. Although the field has progressed over the years, the mechanisms that facilitate the coupling between participants are still poorly understood. In a similar experiment, Richardson et al. tried to confirm Shockley's findings. In Richardson et al. experiment, the cartoon face was located on a pendulum attached to either participant's wrist. They found that it was only visual information that coupled the participants and not the verbal interactions.

2.3 Interpersonal Coordination and Joint Action

How humans coordinate with others, and our environment is studied under the name of joint action. It has been formally defined as "... any form of social interaction whereby two or more individuals coordinate their actions in space and time to bring about a change in the environment" [14]. Studying joint action requires us as researchers to move away from traditionally held assumptions, which say that high-level cognitive processes can be studied in isolation. Joint action is thought to depend on three important abilities: 1) sharing representations of the outside world between partners, 2) predicting the actions of your partners, and 3) inte-

grating predictions about your partner's possible actions with your own. Previous research showed that joint action relies on directing our attention to where our partner is directing theirs and infer our partner's goal from this information [22, 23]. Several studies have shown that the prediction of our partner's actions could be due to a representation of our partner's actions being activated. It has also been shown that these actions are not entirely coded in terms of the observed movement but also in terms of the goal of the action [14]. The last piece of the joint-action puzzle is understanding how participants adjust their actions in response to a partner's. Task sharing and our representation of our partner's actions allow us to understand their final goal but do not adequately explain how we choose an appropriate reaction. Embodied cooperation has motivated the study of how a partner's presence can affect the possible actions, "affordances" of an individual. Studies by Richardson et al. have shown that the affordances available to each participant during a cooperative task are influenced by what they think they can do on their own and with their partner [24]. The mechanism behind this influence appears to be linked to changes in each participant's internal forward model. Ikegami et al. showed that an expert's abilities to predict outcomes of a practised task could be affected by how well they could predict another participant's actions [25].

Visual feedback is not the only way in which humans can couple their movements with each other. Experiments in joint action have also studied other modalities such as auditory [26] and force coupling [27, 9, 28, 29, 10, 30, 31],as well as coupling through emergent languages [32, 33]. Experiments investigating affordances have also shown that our set of possible actions is influenced by our abilities and the abilities we percieve in poten-

tial partners. In this context, all of the sensory modalities are important, given that they influence the affordances that we have at our disposal. In a novel environment where the traditional means of interaction, such as verbal communication, are not possible, this set of possible actions becomes a possible means of communication.

Experiments on emergent language and joint actions have typically used virtual environments to limit the interactions between participants. This limit allows new forms of communication to emerge organically during the experiment. The flexibility and control that virtual environments give researchers have also made them popular in experiments investigating other sensory modalities such as the force coupling experiments by DeSantis et al. [30] and Ganesh et al. [10]. These experiments use virtual environments and haptic devices to virtually link participants without their knowledge. DeSantis et al. used the virtual environment to model a virtual tool with unstable dynamics. Other attempts at limiting the types of interactions between participants have also included specially made mechanical systems through which participants interact; one example is the inverted pendulum[9]. In other experiments, participants interacted via other preexisting social interactions, such as playing music[26]. This research has shown that coupling between humans can happen due to information exchange in all sensory modalities. In this project, I focused on understanding the role that touch and haptic feedback can have on social interactions.

Touch holds an important place in human and animal communication. It is thought to have both phylogenetic and ontogenetic primacy [34]. Phylogenetic primacy means non-verbal communication preceded language in

evolutionary time. Ontogenetic primacy means that non-verbal communication comes before verbal communication during our lifetimes. However, touch has not been as well studied as other modes of communication. For example, vision has been studied about thirteen times more than touch and auditory communication about three times as much [35].

2.4   Force-force interactions

Research on touch has focused on the benefits of haptic feedback and has shown that it can improve performance in many manual tasks, both in singles and pairs [28, 29]. Two independent studies both found that physically coupling pairs of participants to each other, via a weak virtual spring, was mutually beneficial even if one participant was less proficient at the task than the other [10, 30]. Although both experiments looked at the effects of physical interactions between partners, each one looked at specific aspects of partner interaction. Ganesh et al. looked for differences in task performance when coupled to real participants or behavioural recordings played back on a haptic device. They showed that the benefits were strictly tied to the physical interactions between real participants. De Santis et al. looked at the effectiveness of different strategies used to stabilise a virtual object under the influence of a destabilizing force field. They found that the performance of pairs was closely tied to the predictability of the instability. Other studies, such as those by Bosga et al., showed that if participants were given a mass stabilization task, dyads performed the task slower than single participants. In this study, participants lifted a virtual object and held it in a target area for 2 seconds. To do this, they produced an upwards

force with their left and right index fingers on a load cell. No feedback was given to the participants apart from the visual feedback from the computer screen. This task was done once as a single and once with a partner. In the dyad condition, forces on the same side of the virtual object were added together. Results showed that even though dyads had no force feedback from their partners, the success rates were the same as for singles [36]. They also found that dyads formed synergies between participants that indicated the presence of force sharing. These studies show that tasks where both members of a dyad have the same possibilities for action are more positively affected by the presence of a partner [31].

However, it is not yet fully understood how physical coupling can profoundly affect the outcome of an action. The HKB framework suggests that the coupling is serving as a means of information exchange, which allows dyads to coordinate their movements correctly. Van der Wel et al. proposed that haptically linked dyads create haptic communication channels by simultaneously applying force to an object, which they referred to as overlapping forces. The overlapping forces served as a transmission channel for haptic information between participants[9, 31]. Results showed that pairs overlapped their forces twice as much as singles performing the same task. The forces also tended to be larger in the dyad's case. Because the characteristics of the overlapping forces did not change with the task's requirements, it was thought to be a characteristic of coordination between pairs.

Although numerous research projects have shown the importance of human-human force interactions in skill sharing, the dynamics of these interactions

remain unexplored. This project focuses on opening this new field of research and proposes a novel paradigm and methodology to capture emergent haptic interactions and analyse their dynamics. The paradigm I have developed takes care to limit the means of communication but, at the same time, give the participants enough freedom so that new forms of communication can emerge organically.

The role of haptics in information transfer and communication has been largely studied from a user interface design perspective. Haptic feedback has been of interest for researchers trying to identify a possible method of offloading some of the cognitive load placed on the auditory and visual systems by modern technology. Research into haptic communication has been focused on investigating the use of haptic symbols to convey abstractions [37]. One main focus of this research has been developing a system that will facilitate turn-taking in collaborative tasks [38]. In these studies, haptic symbols signal certain important states of the queuing system, such as changes of control or requests to change control. Work done by Chan et al. looked at the design process of haptic icons and their usefulness compared to visual ones. In these experiments, participants were asked to play a commercial computer game together. During the game, only one participant was in control at all times. To gain control, a participant needed to request control from their partner by either gently requesting, urgently requesting, or by taking control. If someone is in control, the requests are queued. Requests for control and their urgency were passed to the participant currently in control. When they released it, control passed to the first person in the queue. Participants were made aware of the state of the queue and their own state by the haptic icons developed and tested by

Chan et al. They investigated three conditions: 1) Information was given to the participants using only haptic icons. 2) Both haptic and visual icons were used. 3) Only visual icons were used. This study showed that participants preferred the haptic and haptic/visual conditions more than the visual-only condition.

These studies represent the limit of our knowledge about haptic communication and its ability to couple humans together. They have shown that humans can quickly learn to associate haptic feedback with specific actions and states[38] and that the force-force interactions which make haptic feedback between humans so beneficial cannot be recorded and played back[10]. There must be something in the dynamics of these force-force interactions, which is essential to the positive effects of sharing control over an object. This study focuses on characterising these dynamics in the context of an emergent proto-language.

2.5 Long range temporal correlations

Statistical analysis of language was first popularized by the work of George Zipf in 1932. He found a relationship between the frequency of a word and its location in a list of words ranked by frequency, where the most frequent word is ranked as 1. Zipf's law states that the rank and frequency of a word are proportional. It is expressed mathematically in the following way,

$$f(s) = \frac{A}{s^\alpha} \tag{2.1}$$

where s is equal to the rank, $f(s)$ is the normalised occurrence frequency, A is a normalising constant, and α usually takes values greater than 1. As originally stated, Zipf's law only holds for a small range of ranks, but it has been modified and successfully used to describe a wide array of phenomena, including a city's population growth, scientific citations, and word usage in languages. Zipf's law does have its drawbacks; first, in its original form, it can only model the statistical properties of a small range of frequencies. Secondly, it is limited in explaining the underlying mechanisms that create the pattern described by Zipf's law.

Since then, many different methods have been used to statistically characterise language and the same wide array of phenomena investigated with the Zipf law. The first of these was work by Peng et al. on analysing the long-range correlations found in nucleotide sequences[39], and later used by Schenkel et al. on written texts[40]. Peng et al. were interested in calculating the statistical properties on DNA sequences. During their study they treated each DNA sequence as a DNA walk which could be followed using a one dimensional walk, the number of steps taken by the walker is represented as l. By investigating the fluctuation measure, $F(l)$, of that random walk they found three different types of behaviour. 1) Random: if neucleotides were arranged randomly $F(l)$ would tend to $l^{1/2}$). 2) If there were local correlations up to a characteristic length the asymptotic behaviour of $F(l)$ would again be similar to $l^{1/2}$). 3) If there is no characteristic length then $F(l)$ would be similar to a power law l^{α} with $\alpha \neq 1/2$. They found that long-range correlations, where $\alpha > 1/2$, are characteristic of intron-containing genes and non-transcribed regulatory elements. Introns are defined as a nucleotide sequence inside a gene

that gets removed during the final product's maturation. Non-transcribed regulatory elements determine important characteristics of genes, such as determining when and where they are activated or deactivated. Sequences without intron-containing genes were characterized by $\alpha = 1/2$, which indicated the absence of long-range correlations. This research introduced a new method that could characterize the types of correlations present in a sequence. This method was later used by Schenkel et al. to identify correlations in written texts. Schenkel et al. chose to represent 32 symbols, including all 26 English letters and 6 punctuation symbols, empty spaces, and any extra symbols were ignored. Each of the 32 symbols was then represented with a 5-bit binary number; for example, a was represented as "00001". Using this method, the text was converted to a binary string. A random walk was then performed using the new binary string as the input. For every 0, the walker took a downward step, and for every 1, the walker took an upward step. In this study Schenkel and his colleagues analysed the α exponent of the function which describes the fluctuations in the one-dimensional walk. Their findings, although inconclusive, spark some interesting questions about long range correlations in language. They found the largest exponents were associated with computer programs, which had $0.7 < \alpha < 1$, texts such as the Bible or the Koran only had $0.5 < \alpha < 0.7$.

Given the difficulty of fitting Zipf's law to the full set of frequencies, some researchers looked for new ways of reformulating Zipf's original intuition. Research in statistical mechanics provides us with an interesting set of tools that can help us understand systems where not every state is equally possible. For example, in language, some combinations of letters will be repeated very often because they correspond to an important word, while

others with no meaning will possibly only appear by accident. This generalization of Boltzmann-Gibbs entropy was proposed and developed by Tsallis and has been proven to be a good method to characterize complex systems with long-range correlations [41, 42, 43]. Tsallis entropy is defined as

$$S_q = -k\frac{1 - \sum_{i=1}^{N} p_i^q}{q - 1} = -k\sum_{i=1}^{N} p_i^q \ln_q p_i \qquad (2.2)$$

, where k is a positive constant related to the Bolztmann constant, in this case the constant can be set to 1 for simplicity in future calculations[44]. p_i is the probability for the occurrence of the i'th state, NN is the total number of states and q measures how non-extensive the property we are measuring is. The q value is directly related to the proportion of long and short-range distributions present in the data. $\ln_q x$ is the q-logarithm, defined as:

$$\ln_q x = \frac{x^{1-q} - 1}{1 - q} \qquad (2.3)$$

.

An extensive property of a system is a property which is additive, such as the mass or the Boltzmann/Gibbs definition of entropy. If $q \leftarrow 1$, the system is extensive and has the additive properties of the Boltzmann-Gibbs measure of entropy. The cumulative distribution of events resembles a logarithmic distribution. This is also illustrated by equation 2.4, which shows the equation for the addition of Tsallis entropies.

$$S_q(A + B) = S_q(A) + S_q(B) + (1 - q)S_q(A)S_q(B). \qquad (2.4)$$

, where A and B are two systems, S_q is the entropy as defined by Tsallis (eq 2.2) and q is the non-extensive measurement. When $q = 1$, all states are independent as in Boltzmann-Gibbs entropy. As q increases, the influence that one state has on another also increases,this makes Tsallis entropy a powerful tool that can be used to study a wide variety of complex systems where not every state is equally likely.

It is important to note that Tsallis entropy makes no assumptions about the system's underlying microscopical properties, and as such, Tsallis entropy includes possible interactions between the systems being analyzed. The non-extensive parameter q measures how much influence one state has on another. This can be seen from the equation 2.4, which describes the addition of two systems under Tsallis entropy. The maximization of Tsallis entropy under certain constraints, such as probability normalization and expectation value constraints, lead to the q-exponential form for the probability distribution of the microstates associated with a given macrostate[45]. A microstate is defined in thermodynamics as a specific microscopic configuration of a thermodynamic system. The q-exponential is defined as

$$\exp_q(x) = [1 + (1 - q)x]^{\frac{1}{1-q}}, \qquad (2.5)$$

where q is the non-extensivity measure and $x = \in [0, \infty)$. One of this method's strengths is its ability to characterize a wide array of phenomena with a single number. Abe and Suzuki's work has focused on finding q val-

ues for different measurements relating to earthquakes and comparing them to already established theories such as the Omori law, Gutenberg-Righter law, and the Zipf-Mandelbrot law in particular. By generalizing the Zipf-Mandelbrot law, using Tsallis entropy, Abe and his colleagues were able to calculate the q values for distributions of calm times between successive earthquakes and distributions of distances between successive earthquakes. Temporal distributions were found to be less than 1, while spatial distributions were always found to be more than 1 [43, 42]. These results revealed that q values larger than 1, such as those found in the spatial distribution of epicentres, characterize systems with long-range correlations. On the other hand, temporal distributions are more closely packed around the moment when a big earthquake is detected. These results fit with what we already know about earthquakes and the successive aftershocks. Interestingly the Zipf-Mandelbrot law is also extensively used in linguistics to rank the importance of words in a text. However, the modifications done by Abe allow us to get a more detailed picture of temporal distributions of those words. Using these techniques, Mehri et al. ranked all the words in a selection of texts by calculating the q value for their temporal distribution. Words with q greater than 1 characterized ones that held more information [44]. For example, in the Origin of Species by Charles Darwin, system, 'why' and 'genera' all have q values above 3 while 'by','thus', and 'its' all have q values near 1. This same technique has been used to identify functional DNA words. Using the non-extensivity measure, researchers showed that as organisms evolve, the clustering level, measured by the q value, of CG dinucleotide increases [46].

2.6   EEG Hyperscanning

Interest in emergent phenomena and in pushing neuroscience towards taking advantage of more ecologically relevant experiments naturally led to an interest in recording data from multiple participants simultaneously. Although behavioural data can tell us a lot about the interactions between participants, a clear understanding of these research areas will require a detailed analysis of the emerging relationships between people. This section introduces a new technology that allows researchers to record activity from two brains simultaneously. This technology is vital so that researchers can start to approach questions related to joint actions, social cognition, and dynamic coordination. The first recorded attempt of using hyperscanning in a study was in the 1960s using EEG. The original experiment used hyperscanning to investigate the existence of extrasensory perception [47]. It was later re-introduced in 2002 by Montague et al., who used fMRI to study pairs of participants interacting with each other[48]. A large majority of hyperscanning studies utilize fMRI as their means of recording neural data. However, the size of the scanners restricts the type of task that can be studied. Previous studies showed that humans modulate behaviour depending on a variety of social factors such as proximity of a partner, knowledge of the presence of a partner, and even the gender or relationship they have with a partner. For these reasons, it is essential to employ a paradigm that allows for manipulating these variables [49, 50].

EEG hyperscanning has been used in various paradigms, including musical performances, card games, and imitation. One crucial paradigm has looked at the synchronisation of hand movements between participants.

In a study by Dumas et al., participants sat in separate rooms while performing meaningless hand gestures. Participants were able to see their partner's movements through a TV screen in real-time. The experiment was divided into 2 conditions, a spontaneous imitation condition where participants were told to imitate their partner whenever they wanted, and an induced imitation condition where one participant was told to imitate their partner. No view/no motion baselines were also taken before each trial and a no view/motion baseline at the end of the trial [51]. Dumas et al found that phase synchronisation could be detected during moments of behavioural synchrony and turn-taking. synchronisation was found in three frequency bands: alpha-mu, beta, and gamma, while the participants hand movements were synchronised. Symmetric increases in phase-locking were found between right parietal electrodes (CP6, P8) of the model and imitator in the alpha-mu bands. Central electrodes (FC1, Cz) on the model's brain and the parieto-occipital (P8, PO2, PO10) region on the imitator's brain were synchronised in the beta frequency. Finally, the frontal, central areas (F4, FC2, C4, CP6) on the model's brain were synchronised with the parietal areas (CP2, PZ, P4, P8, PO2, PO10) of the imitator's brain, in the gamma band. This study was able to show both behavioural and neural synchrony during spontaneous non-verbal interactions.

This study indicates that the right temporoparietal regions of the brain play an important role in social interaction at different frequency bands. These results are consistent with previous research that found that the right temporoparietal regions are activated during social processes. Such as sense of agency, attention and self-other discrimination [52, 51, 53]. By comparing the different frequency bands, Dumas et al. found that the

alpha-mu frequencies were the most robust in differentiating behavioural synchronisation from non-synchronisation. The alpha-mu frequency bands are considered to be neural correlates of the mirror neuron system[54]. Specific frequencies in the alpha-mu frequency band, Phi1, and Phi2 have also been identified as markers of social cooperation[55]. These results allowed Dumas and his colleagues to identify that synchronous states were correlated with increases in the right centro-parietal region in the alpha frequency band. This region was also important in social interaction by Decety, and his colleagues [52] and is also consistent with the mirror neuron system's location.

To better understand the neural correlates of imitation Tognolli et al. developed an experiment where pairs of participants were seated across from each other with a liquid crystal display blocking their view (could be made transparent and opaque by changing the voltage applied to it). Subjects were asked to rhythmically move their finger while in or out of view of their partner. A stable phase-locked state characterized coordination after visual contact. Tognolli identified two interesting oscillatory components Phi1 and Phi2, located above the right centro-parietal cortex. Increases in Phi1 were associated with more independent behaviour, while Phi2 was associated with increased coordination. It is important to note that these results were obtained by only looking at the intra-brain connectivity and did not consider the connectivity between participants as Dumas did [51]. This body of research suggests that the right centro-parietal region is associated with the ability to decode another's movements.

Games have also been a popular way of implementing more ecologically

relevant paradigms for hyperscanning, one of the first modern experiments involving EEG hyperscanning investigated the neural signals of team members and non team members during a card game [56]. Babiloni and his colleagues recorded groups of participants while playing a game where people were put in pairs. The player to the left of the dealer begins the round by placing a card on the table. The other players must also play a card in clockwise order. They must place a card of the same suit as the previous card. The highest card in the suit won each round. The first player to place a card on the table had a unique role; they must put down a card that gives their partner the best chance of winning the round. EEG recordings were taken from all participants, with a particular focus on the frontal cortex (Broadman areas 8,9,10,6), part of the parietal cortex (Broadman area 7), as well as the Anterior Cingulate Cortex (ACC) and the Cingulate Motor Area(CMA). Connectivity was estimated using partial directed coherence (PDC) and compared to the PDC of participants in a rest state. The results showed that the first participant (referred to as the group leader for that round) to put down a card consistently had the largest activation of the ACC and CMA. Their partner, however, showed correlated activity in the right prefrontal and parietal areas in the moments before they play their card. Previous studies have shown that the ACC is associated with the interpretation of other people's intentions.

2.7   Neural synchronisation

How the brain can create a coherent world view from functionally and anatomically specialized parts has been difficult for neuroscientists to an-

swer. One framework that has helped understand how integration can happen in the brain is the neural assemblies' framework. They are defined as distributed networks of neurons that are momentarily linked by reciprocal and dynamic connections [15, 57]. Neurons that are part of an assembly can be connected either directly or indirectly. Direct connections tend to be monosynaptic, while indirect ones tend to be polysynaptic. Connections between assemblies can be within the same cortical area or between distant regions in the brain. One of the most popular ways of studying reciprocal interactions is phase synchronisation.

Synchrony between neural populations has been found at multiple spatial scales ranging from local (2 μm) to several cms. Evidence for these scales has been found in multiple different studies using invasive and non-invasive techniques[58]. With electrodes separated by 1mm, Destexhe et al. recorded cortical activity from the visual cortex (Brodmann areas 17 and 18) of sleeping cats. He recorded activity during three stages of consciousness: deep sleep, rapid eye movement (REM), and awake. They found correlated activity in the beta and gamma bands in electrodes up to 5mm apart. Strong evidence for larger-scale synchronisation comes from research by Roelfsema et al. [59]. They recorded local field potentials (LFP) from different areas in the cortex of cats. The cats were presented with a grating that signaled the beginning of the trial. When the grating changed, the cats had to press a button in order to get their reward. They found that a pattern emerged from the increase in correlation between LFPs while completing the task and disappeared during the reward period.

Synchrony measures the temporal structure in a signal; if the rhythms of

two signals are similar, they are said to be synchronised. Phase locking values (PLV) have also been used to measure synchrony in many different experiments. This measurement has proven to be of great use when analysing EEG signals' temporal structures both in single participant experiments and in hyperscanning experiments. By filtering EEG signals to a narrow frequency band and decomposing them into their phase and amplitude using techniques such as the Hilbert transform, it is possible to characterise the degree of synchronisation. Using equation 2.6, it is possible to quantify the similarity between the rhythms of two signals[60]. The PLV value is defined at a time t as:

$$\text{PLV}_t = \frac{1}{N}\left|\sum_{n=1}^{N}\exp(j\theta(t,n))\right| \tag{2.6}$$

where t indicates the time bin, n indicates the trial and $\theta(t,n)$ is the phase difference $\phi_1(t,n) - \phi_2(t,n)$. Phase locking has been used to measure information transfer between two brains in a wide array of paradigms [55, 61, 26, 51]. Lindenberger et al. investigated changes in phase synchronisation within and between the brains of pairs of participants. They recorded EEG from pairs of guitar players during two distinct phases[61]. During a preparatory phase, the timing of the piece was set via a metronome. The second phase was during the performance of the piece. They found that phase synchronisation both within and between brains was larger during the metronome preparatory phase and during the onset of playing. The presence of an outside driver, such as the metronome, makes the results from Lindenberger et al. paradigm difficult to interpret. They suggest that the observed neural synchrony is only due to the timings imposed by

the tempo. While developing the paradigm, it was important to design it to minimize sources of indirect synchronisation. To this end, participants were given no instructions about pacing during the experiment.

Although the use of PLV to assess neural synchrony has given some interesting results, it is not a proper measurement of covariance between two signals and does not imply an exchange of information between them. PLV is a measure of the consistency of the phase difference between two signals; this is analogous to measuring the variance of the difference between them. Analysing the variance of the difference in a bi-variate distribution given by:

$$\sigma_{x-y}^2 = \sigma_x^2 + \sigma_y^2 - 2\sigma_x\sigma_y\rho \tag{2.7}$$

where σ^2 is the variance and ρ is the correlation between x and y. A small σ_{x-y}^2 indicates a strong link between x and y, however, there are two possible ways of obtaining this result, ρ could be large or σ_x^2 and σ_y^2 could be small. This shows that the variance of the difference could be subject to false positives and makes a poor measure of correlation [16]. Burgess and his colleague compared the performance of various measures of hyperconnectivity using simulated data and pseudo pairs made up of individual participants taking part in an experiment as singles. They were able to show that the circular correlation coefficient was an unbiased measure of hyperconnectivity and had a low root mean squared error. The circular correlation coefficient is measured by:

$$\text{CCorr}_{\Phi,\Psi} = \frac{\sum_{k=1}^{N} \sin(\Phi - \bar{\Phi}) \sin(\Psi - \bar{\Psi})}{\sqrt{\sum_{k=1}^{N} \sin^2(\Phi - \bar{\Phi}) \sin^2(\Psi - \bar{\Psi})}} \qquad (2.8)$$

where $\bar{\Phi}$ and $\bar{\Psi}$ are the average phases for channels a and b. Φ and Ψ are the phases of channels a and b at a given time. In the case of related channels, if the phase of one is slightly ahead of its expected phase, the same will be true for the other channel. If perfectly correlated, the circular correlation will be 1, and two unrelated channels that do not co-vary, the circular correlation will be 0.

2.8   Network Analysis

Complex networks have been successfully applied to analysis in many fields, including social sciences, biology, and physics [62, 63] and is quickly being recognized as a powerful tool when used to reveal inter and intra-brain interactions. Networks are defined as a set of nodes connected by directed or undirected edges. Nodes and edges represent any definable unit (people, fMRI voxels, EEG electrodes) and their interactions. Research has shown that consistent organizational principals are found in networks across all domains. As humans interact with the world, long-range activation patterns involving different combinations of sub-networks are created within the brain. These interactions between subnetworks are at the heart of the interest of complex network analysis using neural data. In brain networks, in-degree (number of inputs to a node) and out-degree (number of outputs from a node) have been used as an initial characterization of functionality between emitters and receivers. Brain networks have also been shown to

display small-world properties such as short path lengths and high clustering coefficients (clustering coefficient is defined as the number of existing connections of a node divided by all possible connections) [64].

Using network statistics, Toppi et al. have distinguished moments where social interactions were taking place from moments where they were not [65]. In their experiment, two airline pilots, one a captain and the other a first officer, flew in a controlled flight simulation from an airport in Rome to one in Pisa. The flight consisted of three different phases: take off, cruise, and landing. During the takeoff phase, the captain was in control of the air plane. The cruise phase included a brain-computer interface (BCI) task completed by one of the pilots at a time. The BCI task was included to ensure that the pilots had to take turns controlling the plane during the cruise phase. Before the landing phase, an electrical failure was simulated. The failure forced the captain to relinquish control of the plane to the first officer during landing. EEG data was collected from both participants during the three flight phases. Networks were calculated using partial directed coherence as a measure of directed information transfer. Toppi et al. found significant differences in the inter-subject densities between the different flight phases and between real and formal pairs. Toppi et al. measured the interbrain densities of each pair of participants. Inter-brain densities(D_{IC}) were defined as,

$$D_{IC} = \frac{\sum_{i=1}^{N} \sum_{j=N+1}^{2N} A_{ij} + \sum_{i=N+1}^{2N} \sum_{j=1}^{N} A_{ij}}{2N} \qquad (2.9)$$

, where N is the number of channels for each subject, and A_{ij} is the adjacency matrix, which includes both participants.

Toppi et al. found that Inter-brain densities, in both the alpha and mu frequency bans, were largest during the experiment's cooperative flight phases. In particular, they found that the landing phase had a significantly larger inter-brain density than the other two phases. Further analysis showed a higher density of frontoparietal and centro-parietal inter-brain connections during the landing phase than the take-off phase. This experiment also introduced a baseline measurement by creating formal couples, which are couples that did not take part in the experiment at the same time. They found that the inter-brain densities between formal couples were significantly lower than that of real couples. They also found no significant differences between the different phases of informal couples. The results presented by Toppi et al. show that it is possible to use hyperscanning to create complex networks that characterize the degree of cooperation between pairs of participants taking part in a complex real-world task.

2.9   Conclusion

Large amounts of work have been done surrounding the question of how humans can cooperate. This work has been focused on the most apparent sensory modalities, such as verbal language and vision. The role of other modalities, most importantly, touch, has remained mostly unexplored. The research focused on force-force interactions has been done under very controlled conditions, such as the inverted pendulum experiment by van der Wel et al [9]. Previous research has typically focused on stripping down tasks to their most simple form[9] or in limiting the social aspect of the experiment[28, 29, 10, 30, 31] as an effort to reduce the number of con-

founding variables. These strategies have greatly advanced our knowledge of human interactions but they leave out important aspects of our everyday actions and give a limited view of how we may react. These limitations make it important to also study humans in more biologically relevant situations. This will help give a clearer picture of the organic emergence of cooperation between people. The study of emergent forms of communication using touch has mostly gone unexplored and is central to understanding the evolution of language and also opens up new methods of communication with technology. One important application is creating compliant robotics for home care and increasing the effectiveness of rehabilitation robots.

In this experiment participants will be asked to complete a task which requires both participants to coordinate their movements without talking. They will need to devise a way to exchange information about their plans on how to most efficiently complete the task. All communication between participants was done via force-force interactions which were recorded. Given that communication can be seen as a temporal sequence of symbols, it is possible to characterize these symbols by their temporal distributions [40, 44]. Using measurements of long-range temporal correlations such as the Tsallis q value [66], we can identify sequences of forces with longer range correlations. These sequences are good candidates for being key-words in an emergent non-verbal language which can be referred to as a protolanguage. To further understand emergent haptic languages and how they allow us to interact with other humans with no prior planning, it was also important to study its effects on the brain. By recording EEG from paired participants, called EEG hyperscanning, and calculating the functional connectivity between inter and intra-brain areas it was also possible

to study the connectivity patterns between participants. Previous studies have been able to show changes in functional connectivity between paired participants. However, these experiments either greatly limited the social aspect of the interaction[55, 67] or included an outside source of synchronization such as a metronome [61]. An experiment that addresses these two issues would greatly advance our understanding of this complex phenomenon, from both behavioural and neurological points of view.

Chapter 3

Experimental Paradigm

The literature review shows an abundance of research in either low or high-level cognitive functions such as coordination dynamics and internal models. Nevertheless, little is understood about how something like coordination dynamics and skill transfer can lead to the emergence of protolanguages or create the internal models that enable us to interact with each other organically. Past experimental paradigms, such as those outlined in chapter 2, imposed several restrictions in order to facilitate the analysis and interpretation of the experimental results. Many experiments either hid the partner's presence or forced participants to use minimal means of communication. However, to truly analyse the force-force interactions and the higher-order cognitive abilities they facilitate, such as planning and turn-taking, it is necessary to allow participants the freedom to explore all the available means of communication. In this paradigm, I tried to create a social experience where participants were given a task and allowed to communicate organically. It was essential to use a sensory modality

that could be quickly recorded and with enough resolution to capture a protolanguage's emergence. The paradigm was framed as a game to make the experiment engaging and encourage cooperation between paired participants.

The paradigm presented in this document put participants in a situation analogous to dancing or moving a heavy object in a complex and loud environment. Participants were asked to refrain from verbal communication during the trials and not talk about the experiment until it was completed. This obligated participants to use force-force interactions and some visual cues as to their only means of communication. This communication could take one of two forms: 1) Participants communicated by overlapping their forces and creating a haptic channel that allows them to transmit haptic cues[9]. 2) The force overlaps could be transitory, meaning that the communication is happening by discrete signalling [38]. The visual cues included posture from other members of the dyad and visual feedback from the shared screen.

Subjects were tested both alone and in randomly assigned pairs; special care was taken to ensure that all participants met three criteria:1) Each pair consisted of two strangers. 2) Each pair consisted of two individuals of the same sex. 3) Both participants were right-handed. During the experiment, participants navigated a two-dimensional playing field populated by a blue cursor and a specific number of randomly distributed yellow circles. The blue circle was the participant's cursor, and the yellow circles the targets that needed to be reached with the blue cursor. An example of the paradigm can be seen in Fig.3.1. During each trial, the total number of

yellow circles was constant. As soon as a target was reached it disappeared and a new one appeared at a random location on the playing area. The objective of the task was to collect as many targets as possible. The number of coins on the screen (one, two, five, or ten coins) was related to the level of interaction that was required between participants. For example, with only one target on the screen, there was little need for communication, and participants could limit themselves to only coordinating their movements together. With ten coins on the screen, participants needed to communicate with each other and possibly generate a strategy that allowed them to move through space as efficiently as possible and collect as many targets along the way. Each session lasted a total of an hour and a half including the set up for the EEG experiment. Each trial lasted 40 seconds during which a pre determined number of coins were shown on the screen. The number of coins corresponds to each of the 4 conditions. Each condition was repeated 10 times, making a total of 40 trials. The order of the conditions was chosen randomly once when the experiment was being planned, the same order was used in all the experiments.

To successfully move in the virtual world and collect targets, participants needed to couple their movements to each other. The HKB model [18] predicts that participants use some form of communication. In this experiment, communication was restricted to either movement of the cursor (visual feedback) or haptic signalling, transmitted through the rigid cylinder. Fig 3.2 shows a pair of participants taking part in the experiment. The cylinder used to play the game was lifted by applying pressure on both sides and lifting the device, with two hands or a partner's help. Participants were only able to push on the device. This meant that signalling
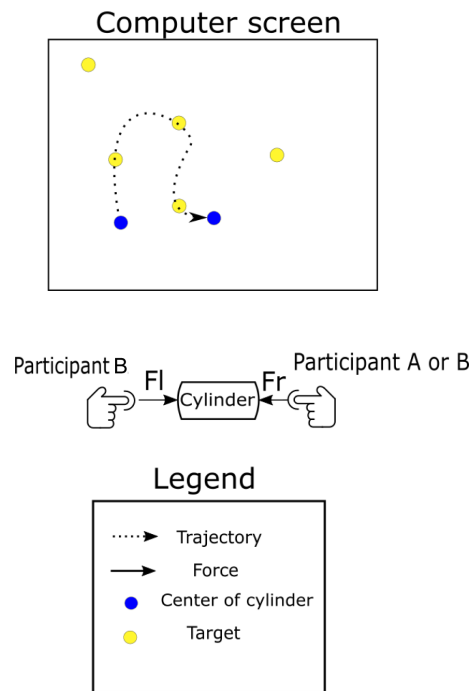
Figure 3.1: Example of the paradigm developed for this experiment. Participants are shown either 1,2,5 or 10 yellow targets on the computer screen at a time. When the blue tracer touched a target the target disappeared, and a new one appeared at a random location. One or two participants could play the game at a time. When played by paired participants, participant A was seated on the right side and used their right index finger. Participant B was to the left side and used their left index finger.

occurred via changes in force on either side of the cylinder. An example of the experimental setup can be seen in Fig.3.2. If the cylinder was dropped, participants were asked to lift the device and continued with the trial. These forces were analysed by binarizing the signal and noting the timings of the two binarized time series. These were then combined into four different signalling behaviours, known as haptic signals. The four haptic signals included, left: only the left force is above the threshold, right: only the right force is above the threshold, none: Both forces are below the threshold, and both: Forces are above the threshold. The threshold was defined as 10% of the maximum force for that participant. Haptic signals can then be combined to form sequences of intricate patterns hypothesized to be used in communication between participants. In linguistics, non-extensivity measures have been used to calculate the long-range dependencies of particular words in large texts [45]. This analysis showed that function words, which have more short-range temporal correlations, also had lower q scores. Function words are defined as words with little lexical meaning and express grammatical relationships between other words. On the other hand, essential words were characterized by larger q scores. It has been shown that essential words will have less to do with grammatical restrictions and therefore show less long-range dependencies than words like: and, of, the, which are more closely related to grammar. Using the non-extensivty statistic allowed for a characterization of the importance of certain signalling combinations.

The paradigm was programmed using Matlab 2017a and Simulink. Matlab was used to display the paradigm on the screen, and Simulink was used to collect and record data from the sensors. A copy of the Simulink/Matlab
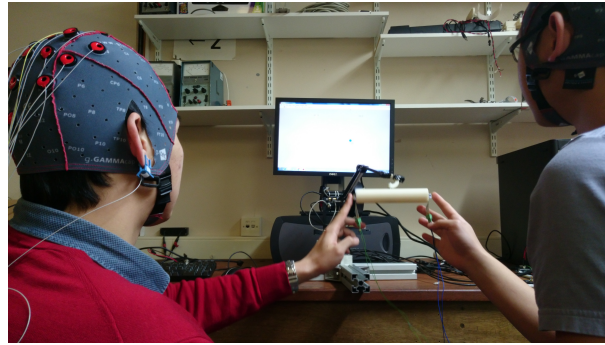
Figure 3.2: Two people participating in a trial run of the EEG experiment. This example shows that participants sat side by side. The haptic device was placed half way between both participants. In this photo, participants are wearing the EEG devices. However in the true experiments 32 electrodes were used.

program used in the experiment is shown in Fig.3.3 UDP was used to send data from the host to the target. For the UDP connection to function, it was essential to have an ethernet card with an 8139C chipset installed in the target PC. The coordinated movement of paired participants and solo movement from single participants is recorded using a haptic device. The device was physically restricted to move only in a vertical plane parallel to the computer screen. Forces are measured using an interlink fsr400 sensor with a minimum sensitivity of 0.98 newtons of force [68]. The output from these sensors was processed by an op-amp conditioning circuit designed to give a linear relationship between force and voltage. The circuit also allowed for both offset and gain calibration for each force sensor. The full testing procedure for fsr (force sensing resistor) sensors is given in appendix A.2. One thing to consider was that the fsr measures the pressure (force/area) applied to the conductive polymer inside. A rigid plastic dome was attached to each force sensor to reduce the possible errors introduced by participants applying force unevenly to the surface. The dome helped

distribute the force across the whole sensor, thus giving more accurate readings. Force sensors were also statically calibrated so that the minimum and maximum registrable forces were the same for both the left and right sides.

Movement was measured using a haptic device built at the university, a picture of the device can be seen in Fig 3.2. Signals from the haptic arm were collected by a Contec counter board, CNT32-8) and sent to Simulink for processing. Acceleration was measured using an adxl335 3-axis accelerometer with integrated amplifiers. Data from the two force sensors, accelerometer, haptic arm, and EEG amplifiers were synchronized and timestamped by a Contec PCIe expansion box. The timestamped data was streamed to the target pc for storage and the host pc to display it to the participant. The sampling rate for behavioural experiments was 1000Hz; for EEG experiments, the sampling frequency was dropped to 500Hz due to a lack of sufficient hard drive space on the target PC. All electrodes were tested to ensure proper EEG measurements; an overview of the method can be seen in the appendix A.4.2. Extensive testing of the data acquisition system was also necessary to ensure the proper recording of EEG data. Four different data acquisition methods were tested; ultimately, the method with least distortion of a sine wave was used. A full description of the method is found in appendix A.4.3.

During this project, two sets of experiments were completed. The first recorded behavioural data and was focused on identifying the behavioural characteristics of haptic communications. The second used the same paradigm but focused on identifying the neural correlations of social interactions us-

Figure 3.3: Copy of the Matlab/Simulink program used to run the experiment. This program was compiled on the host machine and took care of the display of the experiment to the participants.

ing the same paradigm. Using novel hyperscanning techniques, we recorded two participants interacting with a high degree of temporal accuracy and found clear differences in connectivity between paired participants and singles.

Chapter 4

Behavioural Experiment

4.1 Introduction

Haptic communication between humans plays a vital role in society [35, 69]. Although this form of communication is ubiquitous at all levels of society and human development, little is known about how synchronized coordination of motion between two persons could lead to higher-order cognitive functions used in communication. Past research has mainly focused on the effects that haptic feedback has on motor performance and skill transfer. Results from this research have reinforced what many have instinctively known that haptic feedback is an effective means of transmitting information between people. The paradigm introduced in chapter 3 has been designed to investigate the mechanisms that allow human participants to coordinate their movements, even when no verbal communication is taking place.

In the paradigm used throughout this project, participants were asked to

play a simple coin collecting game on the computer. They first played the game independently, as a bi-manual task, and later, as a randomly assigned pair. Participants were asked to lift a plastic cylinder and collect as many yellow targets as possible. During the experiment, the position of the cylinder and its acceleration and the forces exerted on it by both participants were recorded. Given that all communications were done haptically, the analyses of the force-force interactions' dynamics were a primary focus.

4.2 Methods

4.2.1 Subjects

In total, 30 participants took part in the experiment. Participants were recruited from the University of Reading student body and were all right handed between the ages of 18 and 35. Participants first completed the experiment in singles and returned a few days later to complete it as pairs. For the paired participant experiments, it was essential to keep all social conditions as equal as possible. To this end, pairs were chosen so that the participants were both strangers and of the same sex. The inclusion of pairs of friends or mixed sexes would introduce more complex social interactions. Complex social interactions such as those present between members of the opposite sex would make the results more challenging to interpret without a meaningful baseline measurement. Which participant would be A or B was chosen at random. The experiment was reviewed in accordance with the research ethics procedures of the University of Reading and was given a favourable ethical opinion for conduct. All participants gave their informed

written consent to participate in the experiment and have their data used for publication.

4.2.2   Experimental Task

The behavioural experiments consisted of 40 trials, each lasting 40 seconds. The trials were divided into 4 groups of 10. Each group corresponds to one of the four coin conditions (1,2,5 or 10 coins on the screen). Each trial lasted a total of 40 seconds, with a 5-second break in between trials. After every ten trials, the participants were given a 1-minute break to rest their arms. In between each trial, participants were presented with a 5-second countdown. During this time, the participant could see their tracer and a red circle that marked the centre of the playing area. The sequence of conditions was calculated randomly during the initial planning phase of the project. The same pseudo-random sequence was used for all participants. The entire experiment lasted a total of one hour, including the briefing and debriefing of participants.

Participants placed their index fingers on the plastic domes on either side of the cylinder. They lifted the device off the table by coordinating their pressure and moved it in a 2-dimensional vertical plane parallel to the computer screen. When the experiment was done with single participants, the task was bi-manual. Participants faced the computer screen and placed their left and right index fingers on the cylinder's corresponding side. When done by paired participants, each participant sits facing the same computer screen with the screen and the haptic device midway between both participants and at about an arm's length away so that they could both comfortably

move in a 2d plane in front of the screen. The participant to the left of the device used their left index finger, and the one to the right used their right index finger. Some participants were reluctant to apply pressure to the device. Typically, this was due to not wanting to appear too forceful with their partner. Special instructions were given to these pairs to press firmly on the device.

4.2.3 Defining Haptic States

All participants were able to lift the device, coordinate their movement and collect coins during the task. I hypothesize that paired participants exchanged information about their next target and formed a joint motor plan to get to that location without dropping the device by using force-force interactions as a means of communication. Van der Wel et al. identified a possible means of communication between participants that may be responsible for our ability to carry out this experiment [9]. They proposed that when pairs of participants apply a force on a device simultaneously, a haptic channel is created. In this study, the concept of a haptic channel was extended to include different combinations of forces by participants A and B. There are four possible combinations of forces between pairs of participants, as shown in Fig 4.1b. These combinations are known as haptic states throughout this thesis.

Haptic data was first low pass filtered using a Butterworth filter with a 25 Hz cut-off frequency using the Matlab zero-phase filter function. The first and last seconds of each trial were discarded to remove any sensor noise caused by picking up and putting down the cylinder. The data collected

from force sensors were first normalized by calculating the z-score for each trial,

$$F_N = \frac{F(t) - \mu F}{\sigma F} \tag{4.1}$$

, where μF is the average force, σF is the standard deviation of the force, and $F(t)$ is the force at time t. The threshold used to binarize the forces is chosen from the normalized force. The binarized force at time t, B(t) was calculated by comparing the average value of a 250 ms stepped time window to 10% of the maximum value of the normalized forces for a particular pair or single. B(t) was calculated as,

$$B(t) = \begin{cases} 0, & for \frac{1}{250} \sum_{i=1}^{250} F_N(i) < F_t \\ 1, & for \frac{1}{250} \sum_{i=1}^{250} F_N(i) \geq F_t \end{cases} \tag{4.2}$$

, where F_N is the normalized force, and F_t is the threshold calculated as 10% of the maximum F_N. B(t) was calculated for each time window t. The value for the threshold was chosen empirically. Different pressures were applied to the device while an assistant was holding the other end of the device. Voltages, where the pressure was noticeable to the assistant, were recorded. The least noticeable pressure was typically about 10% of the maximum pressure put on the device during a given trial. Any value larger than 10% of the maximum threshold was labelled 1, and anything below it was marked as 0. A stepped window was used in this process because it was hypothesized that this was the window of attention of each participant. Sliding windows were later implemented when calculating the haptic words, as shown in Fig. 4.1a. Binarized forces were then combined to create a single time series that encodes both A and B forces, as shown

in Fig 4.1b.

The different possible combinations of binarized forces are given the following labels:

1. Moments when no forces are above the threshold.

2. Moments when only participant A is applying an above threshold force on the device.

3. Moments when only participant B is applying a force that is above the threshold.

4. Moments when both forces are above the threshold.

A diagram showing the procedure is given in Fig. 4.1.

4.2.4 Haptic Signals

When analysing forms of communication between participants, it is necessary to define a window of time that corresponds to the participant's window of attention. Haptic states within this window make up the signal that each participant is reacting to and using to exchange information with their partner. Defining this window of attention is vital for analysing the temporal dependencies of the haptic signals. The upper bound for the window length was informed by research looking at the optimal presentation rate of haptic cues. Tan et al. presented a target haptic cue sandwiched between two masks, which were also haptic cues [70]. In their experiments,

participants were asked to identify the target cue. Haptic cues were a combination of single, double, and triple frequency waveforms presented to one of three fingers. By analysing the percentage of correct identifications as a function of the time before the target was presented, they concluded the optimal presentation rate was about 2.2 - 3 cues a second.

Haptic states were calculated using a 250ms window, and haptic signals were defined as two consecutive haptic states. These times were chosen so that a haptic signal's total time was within the 2 - 3 cues a second measurement. Although signals composed of one and three haptic states were also analysed, those composed of two states yielded the largest δq values when comparing pairs and singles. A list of signals consisting of two haptic states, and their corresponding states and signal numbers, are given in Figs.4.1b and c. With this definition, it is possible to investigate the longer and shorter-range temporal correlations found in the data and compare them with the two modes of communication identified by Uno et al. [33]. Dividing the force data into haptic states and then haptic signals resulted in a time series of 70 haptic signals for each trial.

4.2.5   Calculating non-extensivity measure for haptic signals

A generalized Boltzmann-Gibbs (BG) distribution, called the Tsallis distribution, was used to analyse the long-range temporal correlations present in the data. This distribution is described by Eqs. 2.2 and 2.3 [66, 41, 71]. Tsallis' generalization allows for the characterization of systems not properly described by BG, such as ones with long-range interactions. By fitting

a)

250 ms

Fa

Threshold

Fb

| 1 | 1 | 1 | 1 | 0 | 1 | 0 | 0 | 0 | 0 | 0 | 0 | Fa |
| 1 | 1 | 1 | 1 | 0 | 1 | 0 | 1 | 0 | 0 | 1 | 1 | Fb |

S_n S_{n+1}

| 4 | 4 | 4 | 4 | 1 | 4 | 1 | 3 | 1 | 1 | 3 | 3 | Haptic States |

| 16 | 16 | 16 | 13 | 4 | 13 | 3 | 9 | 1 | 3 | 11 | Haptic Signals |

b)

State	Fa	Fb
1	0	0
2	1	0
3	0	1
4	1	1

c)

Signal	S_n	S_{n+1}
1	1	1
2	1	2
3	1	3
4	1	4
5	2	1
6	2	2
7	2	3
8	2	4
9	3	1
10	3	2
11	3	3
12	3	4
13	4	1
14	4	2
15	4	3
16	4	4
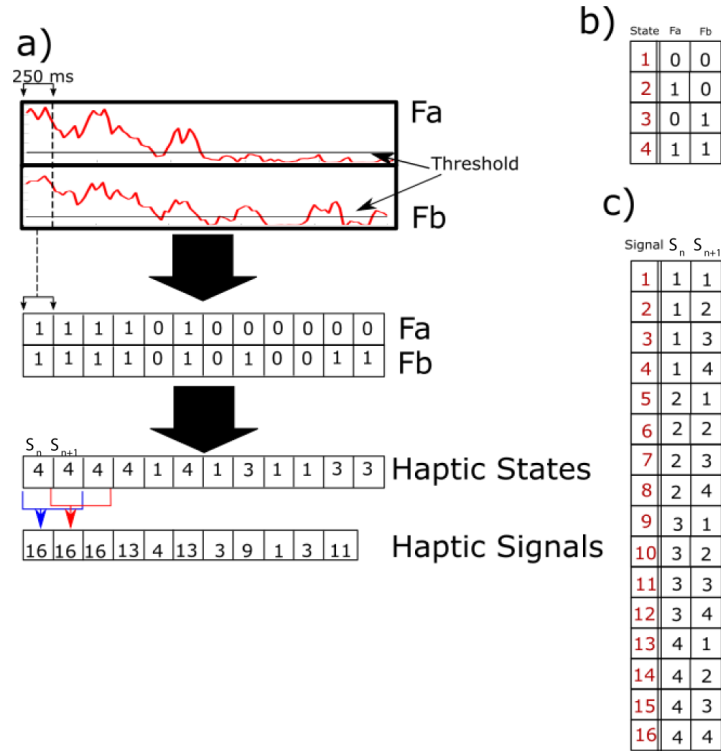
Figure 4.1: A) Method used to binarize the continuous forces recorded from force sensors A and B. Forces are first binarized by comparing to a threshold, this results in a binary time series for each force sensor. Binary signals are then combined to form a single time series of haptic states that encode both information streams. To uncover the signalling being used by dyads to communicate with each other haptic states were further combined into haptic signals using a sliding window. Signals of different lengths were tested with haptic signals of length, two giving the highest non-extensivity scores. b) Corresponding haptic states comprised of two binarized forces a and b. The resulting haptic state is shown in red. c) Haptic signals comprised of two consecutive haptic signals. Haptic signal numbers are marked in red, states at time t, and t+1 are marked as S_1 and s_2, respectively.

Eq. 2.5 to the distribution of the collected data, it is possible to calculate the q value associated with it and, in this way, characterize the proportion of long-range to short-range correlations.

Depending on its q value, known as the non-extensivity measure (shown in Eq. 2.3), the Tsallis distribution can fit a wide array of other distributions for those cases when the sum of the entropies of the systems is not linearly additive, the original BG equations can be obtained when $q \to 1$. q values larger than 1 describe systems with long-range interactions between two events of interest, and q values smaller than 1 with shorter-range interactions. This property of the Tsallis distribution has been used to characterize the spatial and temporal patterns in complex systems such as earthquakes. Abe and Suzuki's works have successfully detailed new laws relating to both the spatial and temporal distances between earthquake epicentres [43, 42]. They found that q values smaller than 1 indicated shorter range spatial correlations between two earth earthquakes; these are related to the aftershocks which accompany most earthquakes. On the other hand, Q values larger than 1 characterized the longer-range temporal correlations found in earthquake epicentre time series. Phenomena with long-range temporal correlations were previously found to be adequately described by the Zipf-Mandelbrot law [42]. Through this research, Abe et al. concluded that the non-extensivity measure was an appropriate and powerful way of characterizing phenomenon with different ranges of correlations.

The Zipf-Mandelbrot law has also been extensively used in linguistics research to identify keywords in a text [72]. Given that Abe and Suzuki were able to show a connection between non-extensive statistical mechanics

and the Zipf-Mandelbrot distribution, others have used the non-extensivity measure as an alternative way of identifying keywords in a text [45] and even as a way of distinguishing functional DNA words by looking at their distributions in the DNA sequence [46].

For this analysis I created a new time series that contained the temporal sequence of haptic signals for each trial. The number of signals between two successive entries of the same signal was taken as the distance between them. For example, if we are calculating the distances for signal 1, as shown in Fig. 4.2a, the distances would be D1 to D4. D1, for example, would be equal to 2. By fitting the Eq (2.5) to the cumulative distribution of d, the non-extensivity measure q was obtained for each signal during each trial. The influence of noise on the results was reduced by normalising q values calculated from the original data with ones from random permutations of the haptic signal time series [44]. Distances between consecutive entries of each haptic signal and q values were then calculated the same way as for the non-shuffled time series to create a set of surrogate q values. This procedure was repeated N times for each trial and averaged together, as shown in Eq. 4.3.

$$\Delta q = q_d - (\frac{1}{N} \sum_{i=1}^{N} q_s^i) \qquad (4.3)$$

where q_d is the q value calculated from the original data and q_s^i is the i'th surrogate q value. Positive values indicate signals with a larger proportion of long temporal distances than the same number of events distributed randomly in time. In contrast, negative values correspond to signals with

a larger proportion of short distances than the same number of events randomly distributed in time.

This procedure resulted in a single q value for each haptic signal for each trial. The q values of all trials of a given condition were averaged together to create one q value for each condition. The results from different participants were treated as separate samples from an underlying distribution of q values for a given signal and condition overall paired or single participants.

To identify the length of the window of attention for the haptic signalling taking place between paired participants, three different lengths of haptic signals were tested. Signals with a length of two gave the largest Δq values between pairs and singles and fit well into the time scale reported by Tan et al. [70]. An example of this process can be seen in Fig. 4.1, and a full table of all 16 haptic signals that were further analyzed is shown in Fig. 4.1c.

The positions of each entry of a haptic signal with m total entries can be denoted as $t_1, t_2...t_m$. Distances between two successive entries of a signal are written as $d_i = t_{i+1} - t_i$. By fitting the q-exponential, described in the Eq. (2.5) to the cumulative distribution function of distances for a particular signal, the non-extensivity measure for that signal can be calculated as shown in Fig. 4.2b. Any signals that appeared fewer than ten times were discarded and not fit with the q-exponential.
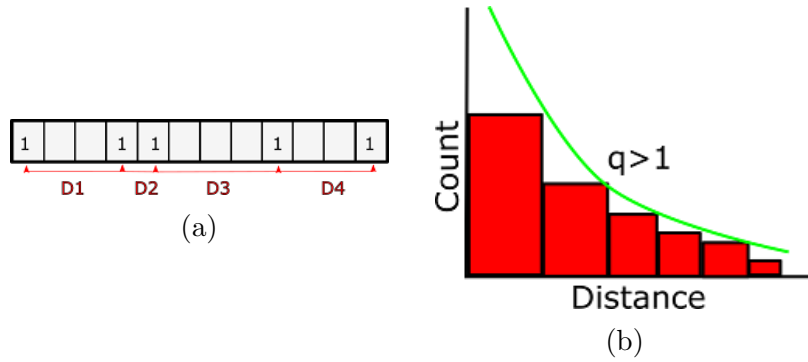
Figure 4.2: a) Distances between all consecutive entries of a particular signal are recorded. The distribution of these distances will then be fit by the q-exponential detailed in Eq. 2.5. b) Fit of q-exponential to distribution of distances. q values larger than 1 are similar to power laws. Surrogate data sets are created by randomizing the positions of each haptic signal and creating a distribution of the new distances as detailed in Eq. 4.3

To contrast findings from different participants, it was important to discard any undesired effect on the q value, which would be due only to the frequency of a particular signal. The effects of frequency on the q value were corrected by shuffling the haptic signal in time and calculating new q values. The procedure was repeated one thousand times for each signal, and the mean of each random distribution was recorded. Δq is then calculated as $q_d^i - <q_r^i>$ where q_d^i is the q value calculated from the collected data for signal i and $<q_r^i>$ is the average of the randomized q values for signal i. Data from each participant was analysed both as averages over all participants for a given trial and as probability distributions made up of averages over entire trials.

4.3 Results

4.3.1 Learning and increase in performance

The performance was measured by counting the total number of targets collected during a trial. The correlation coefficients were calculated using the corrcoef Matlab function with a significance level of 0.05. Two pairs and their corresponding singles showed negative correlations (pairs 3 and 8), two other pairs (pairs 7 and 9) had correlations below 0.5. All other paired participants had correlations above 0.5 for all conditions. These results show that the majority of paired participants could increase their level of coordination with their partner and perform better in the task. The increase in performance could be due to improvements in the internal models created by each member of the pair, which includes their partner.
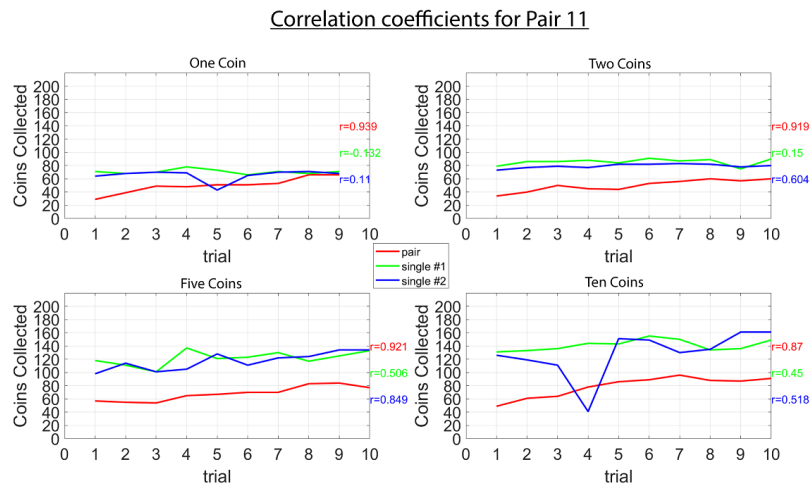
Figure 4.3: Correlation coefficients where paired participants have larger correlation coefficients (r) than singles. Due to an error in the recordings, one coin trials only have 9 trials instead of 10. Each graph shows the progression for a given condition and participant. The r values shown on the right of each graph correspond to the r value calculated for each plot.
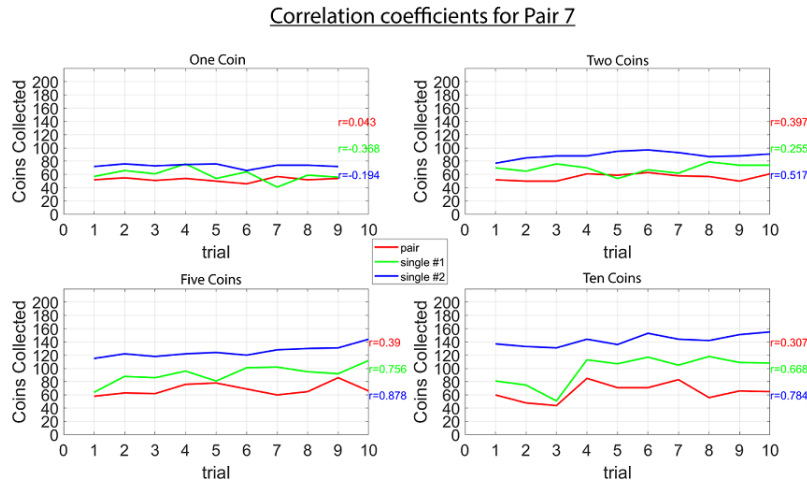
Figure 4.4: Correlation coefficients where paired participants have correlation coefficients (r) similar to those of singles. Due to an error in the recordings, one coin trials only have 9 trials instead of 10. Each graph shows the progression of a given condition and participant. The r values shown on the right of each graph correspond to the r value calculated for each plot.

4.3.2   Calculating haptic States from Recorded Forces.

As a first step, transition probabilities were calculated for each state. Transition probabilities were calculated as the average number of times a given sequence of states occurs in the time series. Figs. 4.5-4.8 show the average transition probabilities for all pairs, during 1, 2, 5 and 10 coin trials. The results indicate that single participants spent most of their time applying above threshold forces to both sides of the cylinder, labelled as state 4. This behaviour allows single participants to stabilize the cylinder and move quickly from target to target. On the other hand, paired participants could be in any of the four haptic states. States where one or more participants are below the threshold are considered receptive states given that participants are passively waiting for input. State 1 corresponds to a fully

receptive state where neither participant is applying an above threshold force on the device, states 2 and 3 correspond to unilateral receptive states where either F_a of F_b is above the threshold, and the other is below the threshold. By averaging over all participants, it was found that participant A was twice as likely to be receptive than participant B. This difference could be because participant A was using his/her non-dominant hand when playing the game. Future experiments could be done to investigate this point further.

Comparing transition probabilities in conditions 1 and 10 for paired participants reveals some similarities. Transitions to and from states 3 and 4 are unique to these two conditions. On the other hand, conditions 2 and 5 have no shared unique loops between states, but condition 5 has a unique loop between states 1 and 3, suggesting that the force-force interactions occurring in conditions 1 and 10 have some similarities. This similarity could be due to the density of coins on the screen and the communication needed to identify the next target. In the one coin case, participants only have one choice of a target at a time, which means that participants need only to exchange minimal amounts of information to determine the next target. In the ten coin case, participants are given many options. However, one of the ten will usually be closer to the participant's cursor than the others and thus be an obvious next target.
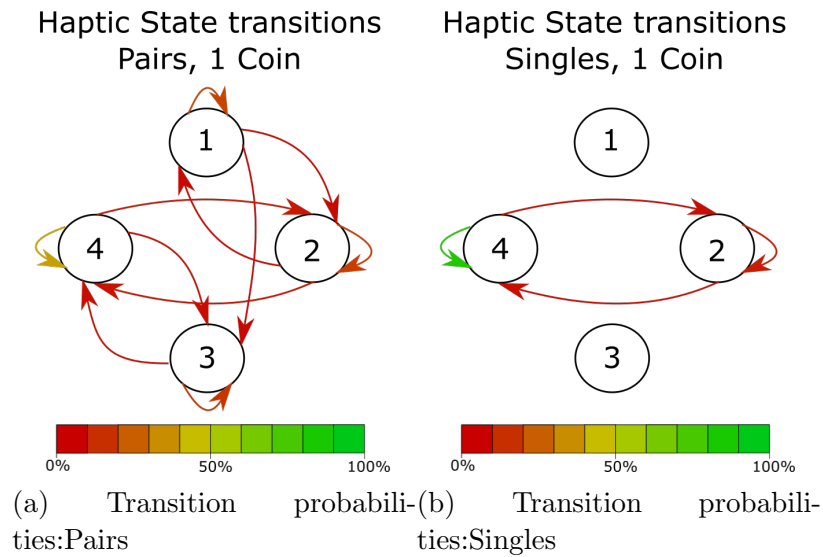
Figure 4.5: Average transition probabilities over all one coin trials. Each node corresponds to one of the haptic states identified above. These figures show the results for 14 pairs and 28 singles due to a recording error making impossible to analyse the data from one of the pairs. a) Average transition probabilities for all 14 dyads. b) Average transition probabilities for all 28 single participants.
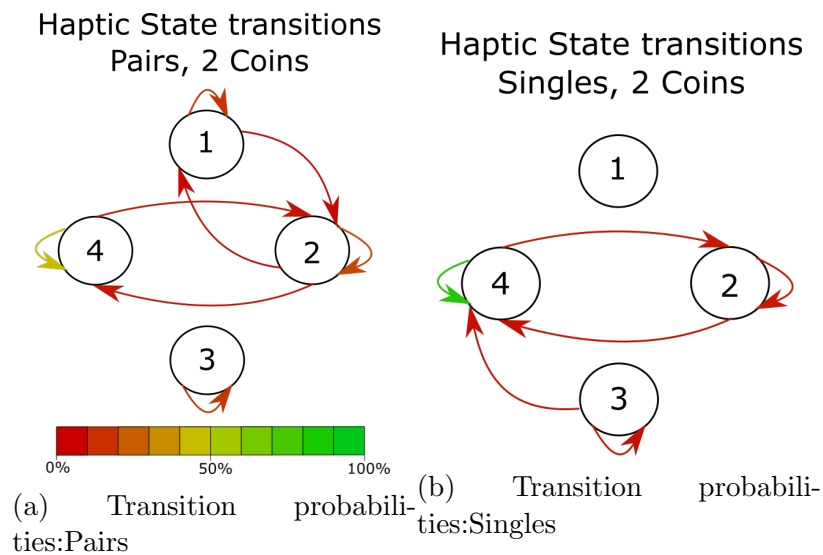
Figure 4.6: Average transition probabilities over all two coin trials. Each node corresponds to one of the haptic states identified above. These figures show the results for 14 pairs and 28 singles due to a recording error making impossible to analyse the data from one of the pairs. a) Average transition probabilities for all 14 dyads. b) Average transition probabilities for all 28 single participants.

(a)   Transition   probabili-
ties:Pairs

(b)   Transition   probabili-
ties:Singles
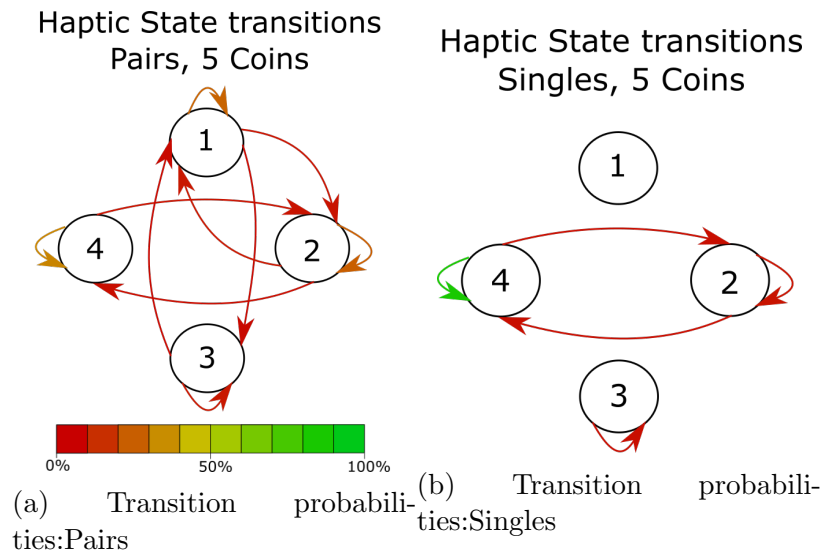
Figure 4.7: Average transition probabilities over all five coin trials. Each
node corresponds to one of the haptic states identified above. These figures
show the results for 14 pairs and 28 singles due to a recording error making
impossible to analyse the data from one of the pairs. a) Average transition
probabilities for all 14 dyads. b) Average transition probabilities for all 28
single participants.

(a)   Transition   probabili-
ties:Pairs

(b)   Transition   probabili-
ties:Singles
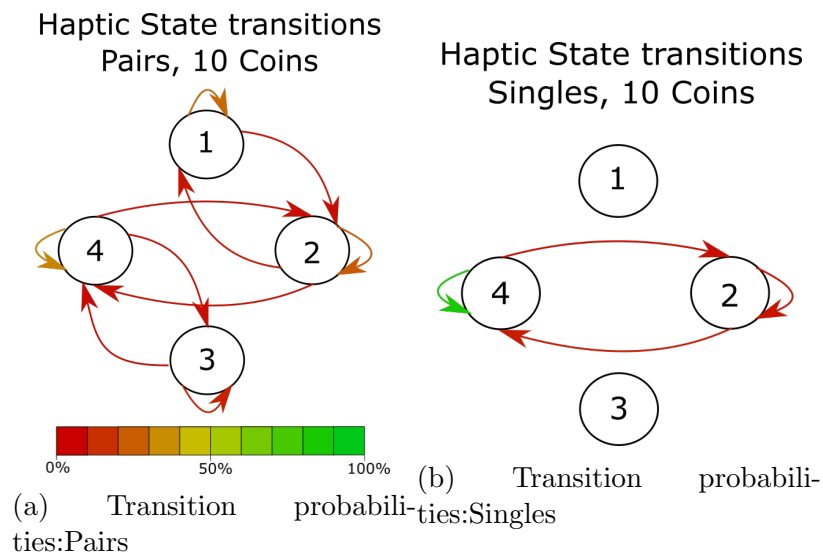
Figure 4.8: Average transition probabilities over all ten coin trials. Each
node corresponds to one of the haptic states identified above. These figures
show the results for 14 pairs and 28 singles due to a recording error making
impossible to analyse the data from one of the pairs. a) Average transition
probabilities for all 14 dyads. b) Average transition probabilities for all 28
single participants.

4.3.3 Characterizing the long ranged temporal correlations of haptic signals.

To further understand the exchange of information during mutual haptic interactions, it was necessary to analyse the long and short-range temporal correlations present in the haptic signal time series. As a first step, the immediate transition probabilities for each haptic signal were calculated and graphed, as shown in Figs.4.9-4.12. These figures show a clear difference between paired and single participants. Paired participants show a loop between states 6,8,14, and 16, which is consistent across all conditions. These haptic signals are ones where only participant B, or both participants A and B, are applying force on the device at times t and t+1. Singles also use the same haptic signals but in very different proportions. For example, in single participants, the probability of repeating signal 16 was about 80%, while in paired participants, it was about 40%. A key difference between pairs and singles is that single participants lack a loop in the transition probabilities. Instead, signal 16 acts as a powerful attractor. For paired participants, there are two clear loops; the first is present during all trials and is between signals 6,8,14, and 16 (figures 4.9-4.10). The second emerges during the 5 and 10 coin conditions and includes signals 1,2,5 and 6 (figures 4.11-4.12).These results show clear differences in the signalling behaviours of paired and single participants. However, this analysis only looked into the immediate future. Longer temporal correlations were also analysed by measuring the non-extensivity value q. By calculating each possible haptic signal's temporal correlations, it was possible to identify key behavioural differences between the paired participants and the single participants.

Calculating the q-values for paired participants, shown in figures 4.13 and 4.14, showed that 80% of the signals could be fit by the q-exponential. The distributions that could not be fit by the q-exponential function corresponded to signals with only short-range correlations. In single participants, only 30% of the signals identified in the time series had any long-range correlations.

More importantly, signals found between paired participants that are not found in single participant trials are ones where one state 1 is purely receptive (both participants apply a below threshold force). State 2 is unilaterally receptive (only one participant is applying a below threshold force). One example of a combination that meets these requirements is signal 2, which is a combination of $S_1 = 1, S_2 = 2$. Suggesting that combinations of purely receptive states and unilateral receptive states were being used as a means of transferring information between the paired participants.

In this study, methods from non-extensive entropy were used to characterize the distribution of long and short-range temporal correlations of what has been defined as haptic signals. By testing different lengths of haptic signals, it was found that signals with a length of two haptic states, on average, showed the largest non-extensivity values and had the most long-range temporal correlations, which is an essential feature of languages [33]. By analysing the temporal correlations in the haptic signals, I was able to identify a temporal structure that can indicate some association with other forms of coding which transfer information such as genetic nucleotides and in human language [44, 46]. The combination of long and short-range temporal correlations is critical features of the emergence of protolanguages

[33].

Haptic Signal Transition Probabilities
Pairs, 1 Coin Trials

Haptic Signal Transition Probabilities
Singles, 1 Coin Trials

(a) Counts for dyads.

(b) Counts for single partici-
pants
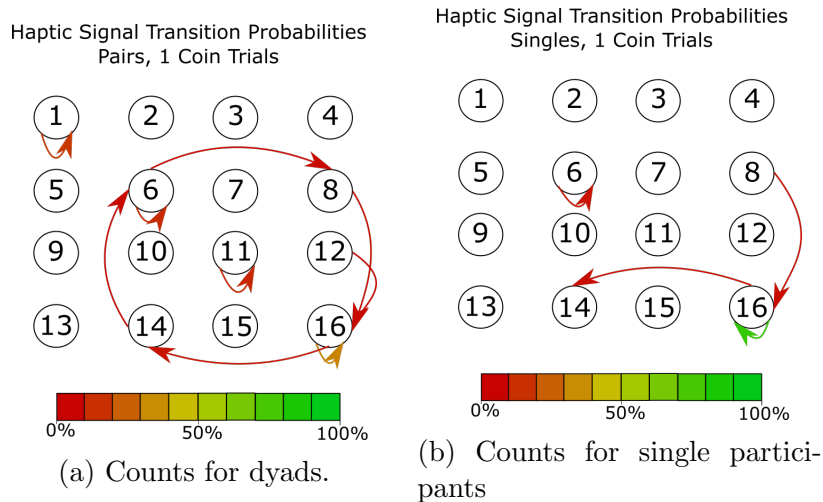
Figure 4.9: Transition probabilities for one coin condition over all par-
ticipants. The row number represents the state at t=1, and the column
number represents the state at t=2. For example, haptic signal 6 represents
haptic state 2 at t=1 and haptic state 2 at t=2. A full list of the haptic
signals and their corresponding states can be seen in figure 4.1. The colour
of the arrows shows the transition probability from signal to signal. Only
transitions above 2% are shown. The symmetry shown by dyads in states
s1 and s2 suggests that participants share control of the device to collect
as many coins as possible when taking all trials into account. Dyads also
use a wide array of signals, therefore, increasing the potential for commu-
nication, while single participants have no need to communicate and are
only using them as a means of stabilizing the device. Data shown here are
averaged over all 28 single participants and 14 dyads. One of the dyads
was disqualified due to errors in the data collection.

(a) Counts for dyads.

(b) Counts for single participants

Figure 4.10: Transition probabilities for two coin conditions over all participants. The row number represents the state at t=1, and the column number represents the state at t=2. For example, haptic signal 6 represents haptic state 2 at t=1 and haptic state 2 at t=2. A full list of the haptic signals and their corresponding states can be seen in figure 4.1. The colour of the arrows shows the transition probability from signal to signal. Only transitions above 2% are shown. The symmetry shown by dyads in states s1 and s2 suggests that participants share control of the device to collect as many coins as possible when taking all trials into account. Dyads also use a wide array of signals, therefore, increasing the potential for communication, while single participants have no need to communicate and are only using them as a means of stabilizing the device. Data shown here are averaged over all 28 single participants and 14 dyads. One of the dyads was disqualified due to errors in the data collection.

(a) Counts for dyads.

(b) Counts for single participants

Figure 4.11: Transition probabilities for five coin conditions over all participants. The row number represents the state at t=1 and the column number represents the state at t=2. For example haptic signal 6 represents haptic state 2 at t=1 and haptic state 2 at t=2, a full list of the haptic signals and their corresponding states can be seen in figure 4.1. The colour of the arrows shows the transition probability from signal to signal. Only transitions above 2% are shown. The symmetry shown by dyads in states s1 and s2, suggests that participants are sharing control of the device in order to collect as many coins as possible when taking all trials into account. A new loop emerges during the five coin condition among signals 1,2,5,6. This loop includes only signals that are made up of at least one receptive state.

(a) Counts for dyads.

(b) Counts for single participants
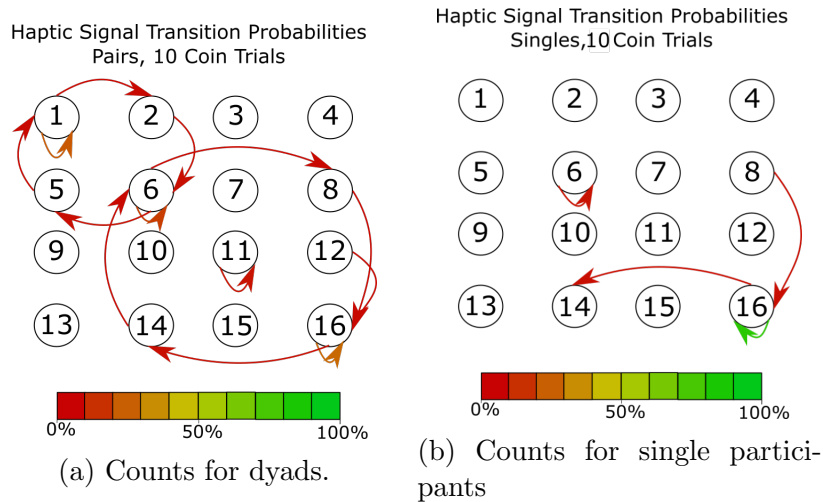
Figure 4.12: Transition probabilities for five coin conditions over all participants. The row number represents the state at t=1 and the column number represents the state at t=2. For example haptic signal 6 represents haptic state 2 at t=1 and haptic state 2 at t=2, a full list of the haptic signals and their corresponding states can be seen in figure 4.1. The colour of the arrows shows the transition probability from signal to signal. Only transitions above 2% are shown. The symmetry shown by dyads in states s1 and s2, suggests that participants are sharing control of the device in order to collect as many coins as possible when taking all trials into account. Here we see the same loop that emerged in the 5 coin condition among signals 1,2,5,6. This loop includes only signals that are made up of at least one receptive state.

4.4 Discussion

In summary, I was able to find behavioural characteristics unique to singles and paired participants. From the transition probabilities, it is clear that single participants spent most of their time applying pressure to both sides of the device (Fig. 4.5-4.12). Resulting in a low percentage of the identified haptic signals having any long-range correlations. Paired participants showed a variety of possible haptic signals, most of which included a receptive haptic state (Fig. 4.8 and 4.12).

Figure 4.13: Δq for all ten coin trials and over all paired participants. The red line shows the average of all data for a particular signal. The red outline shows the 95% confidence interval of the average value, and the blue outline shows the standard deviation. Signals that appeared less than 5 trials over all participants have been removed. Although both paired and single participants show temporal correlations that are longer and shorter than a random distribution, only pairs have long-range correlations in signals, including a receptive state (signals 1-5). Single participants only show long-range correlations for signals where pressure is put on both sides of the device and for signal 6 where participants are only applying force on Fa. It is important to note that only 30% of the identified haptic signals have any long-range correlations in single participant experiments, while 80% have long-range correlations in paired participant experiments.

Figure 4.14: Δq for all ten coin trials and over all single participants. The red line shows the average of all data for a particular signal. The red outline shows the 95% confidence interval of the average value, and the blue outline shows the standard deviation. Signals that appeared less than 5 trials over all participants have been removed. Although both paired and single participants show temporal correlations that are longer and shorter than a random distribution, only pairs have long-range correlations in signals, including a receptive state (signals 1-5). Single participants only show long-range correlations for signals where pressure is put on both sides of the device and for signal 6 where participants are only applying force on Fa. It is important to note that only 30% of the identified haptic signals have any long-range correlations in single participant experiments, while 80% have long-range correlations in paired participant experiments.

Results show that the paired participants' haptic signals have both long and short-range temporal correlations as indicated by the larger ΔQ values and a larger proportion of signals that could be fit by the q-exponential function as shown in Figs. 4.13 and4.14.This result indicates a rich nature of the temporal patterns unique to the haptic interactions between the paired participants due to the real-time coupling of the action-perception loops. The combination of longer and shorter-range temporal correlations suggests that forces applied to either side of the device are indeed being used as a means of transmitting information between paired participants.

In particular, signals combining purely receptive states and unilateral receptive states show longer and shorter-range temporal correlations. These characteristics are essential for the emergence of protolanguages [33]. The results suggest that the language that emerges from these interactions is used by participants to couple their movements to move the cylinder. Figures showing other conditions can be seen in the appendix, figs.A.5-A.7

In the past literature, we find three main computational models that explain how groups of participants can coordinate their movement: 1) "No computation" model proposes that paired participants follow their target independently. 2) "Follow the better partner" model supposes that haptic information allows members of the dyad to judge their partner's performance. If the partner is better than them, then they switch to following the partner. 3) "Multisensory integration" model assumes that the haptic forces allow partner's to estimate the other's position and track a weighted combination of this estimate and the target depending on how reliable the information is [73]. Takagi et al. proposed a fourth model that they showed could accurately reproduce experimental observations. They proposed that partners used the haptic forces to estimate their partner's target and improve their prediction of the target's movements. It is important to note that participants had some haptic information from their partner during these experiments but not enough to influence their movements or let them know that they were haptically coupled to another person. Another key difference is that no choices were presented to the participants; they followed the target or followed a simple instructions set.

In the context of control engineering, the internal model is often identified

as the feed-forward model in a control loop. Takagi et al. showed that paired participants could identify a common target using only the mutual force-force interactions [73], and they suggested that this ability is due to the creation of a feed-forward model which can not only be used to predict the outcome of one's movements but also to predict the outcome of a partner's movements. The same principals must also be present in the joint "coin-collecting" paradigm in this study. Paired participants need to build an internal model of their partner to simulate their movements and identify their intentions.

It is important to note a critical difference between Takagi's experiment and the joint "coin-collecting" paradigm. The joint coin-collecting paradigm is a genuinely cooperative task. Both participants jointly control a single cursor and are rigidly coupled to one another through moving a rigid rod. In Takagi's experiment, participants are unaware of each other. In principle, both participants are engaged in an individual reaching task. Even though their hands are weakly connected by a virtual spring, the interaction force is so small that the participants would not notice their partner's existence.

4.5   Conclusion

In conclusion, this experiment has shown that the coin collecting paradigm during this project has been able to show apparent differences, in transition probabilities and Δq values, between paired and single participants. Throughout the experiment, almost all participants showed signs of improvement over the trials, indicating that participants were able to learn

what strategies gave the best outcome. Due to the experimental design, all communication had to be done via haptic feedback. These haptic interactions were encoded into 4 haptic states and 16 haptic signals. Analysis of the transition probabilities between states showed that paired participants used all possible states. On the other hand, single participants only used stated 4 and 2. The reduced number of available states suggests that little or no information is being exchanged in the single participant experiments. This result is further supported by the low percentage of haptic signals that showed long-range correlations in single participant experiments. These promising results show that this paradigm can create conditions in which participants are encouraged to communicate via haptic interactions and create a simplified language. Using this language, participants negotiated which action to take next during the experiment. The next experiment will use the same paradigm and apply it to EEG experiments with more than one participant. This project will build on past experiments on joint action, which only investigated mechanical coordination between participants and not the higher-order cognitive interactions.

Chapter 5

EEG Hyperscanning Experiment

5.1 Introduction

As science continues to investigate how humans interact with each other, it is becoming increasingly important to record and interpret the neural signals of participants interacting with each other. The recording of neural signals from more than one individual is known in the literature as hyperscanning. It has been used in several different paradigms, such as musical performances, card games, and imitation of gestures as a means of investigating the neural correlates of interpersonal coordination and joint actions.

In a study by Dumas et al., participants sat in separate rooms while performing meaningless hand gestures in front of a tv screen fitted with a cam-

era, allowing participants to view each other in real-time. The experiment had 2 conditions: 1) Spontaneous imitation, participants can imitate each other whenever they want during the trial. 2) Induced imitation, participants are asked to imitate each other at specific moments during the trial. They found that phase synchronization increased in the alpha-mu, beta, and gamma frequency bands during moments of behavioural synchrony and turn taking. Synchronization was found predominantly in the temproparietal regions of the brain. Results from this experiment, along with others, have shown that the right temporoparietal regions are essential to social processes such as a sense of agency, attention, and self-other discrimination [52, 51, 53]. A comparison between different frequency bands found that changes in alpha-mu were the most robust. The alpha-mu frequency band has previously been identified as a neural correlate of the mirror neuron system[54]. Specific frequencies in the alpha-mu frequency band, Phi1, and Phi2 have also been identified as markers of social cooperation[55].

Results from these studies are fascinating and significantly advance our understanding of the neural mechanisms involved in human-human interactions. However, it is essential to note the level of restrictions that these paradigms place on the participants. One variety of paradigm attempts to hide the participants from each other. These experiments typically look at low-level mechanical coordination and skill transfer between participants [10, 30]. Other experiments have explored humans in more social and biologically plausible settings, such as playing a card game with a friend or being part of a guitar duet[61, 56]. Although these paradigms give an essential view of joint actions' neural correlations, they fail to capture the negotiations that make coordination between participants possible.

The paradigm proposed in this project allows participants to interact with each other freely. The only restriction placed on participants was that all interactions had to be done via the plastic cylinder, limiting communication between participants to a modality that can be quickly recorded and analysed. It also allowed the participants enough freedom to develop new and unique means of communicating to complete the task. Results from behavioural experiments suggest the emergence of a haptic language from the force-force interactions between paired participants. By joining hyperscanning and the coin collecting paradigm developed during this Ph.D. I aim to identify the neural correlates of the haptic communication that emerges from these interactions. The analysis was done in several parts: 1) A coarse averaging method where all inter and intrabrain connections were collected. 2) A finer-grained method where each participant's brain was divided into 6 regions of interest.

Several methods of calculating connectivity were evaluated for this project. The circular correlation was chosen over the others due to its robustness to type I errors and because it is an unbiased measurement of synchronization[16]. It was essential to choose an appropriate cut-off that could separate random synchronizations from true synchronizations. Two methods of creating distributions that describe random circular correlations were tested in this experiment: 1) Randomly shifted time series, Fig.5.2, and 2) randomly shuffled dyads, Fig.5.3. Both methods adhere to Hurtado et al. 's guidelines, stating that surrogate data must preserve some of the temporal correlations within each channel to obtain an appropriately strict cut-off [74]. Complex networks are then created using the circular correlation between pairs of electrodes as the weight of that connection. The differences

between paired participants and singles give a novel view into participants'
characteristic intra and interbrain connectivity in a complex social task.

5.2 Methods

5.2.1 Subjects

The experiment consisted of the same "coin collecting task" described in
chapter 3. In total, 10 individual participants and 5 pairs took part in
the experiment. They were all recruited from the University of Reading
student body and were all right-handed between the ages of 18 and 35.
All participants were new to the experiment and had no previous training.
Participants first completed the experiment in singles and returned a few
days later to complete it in dyads. For dyad experiments, participants were
selected so that both members were strangers and of the same sex. The
experiment was reviewed in accordance with the research ethics procedures
of the University of Reading and was given a favourable ethical opinion for
conduct. All participants gave their informed written consent to participate
in the experiment and have their data used for publication.

5.2.2 Experimental Task

This paradigm's success in identifying temporal structures in force-force
interactions provide a good starting point to investigate neural correlates
associated with emergent social interactions using the same paradigm. In
this experiment, dyads and single participants used the same peripheral

device to control a blue circular tracer. The experiment consisted of 40 trials, each lasting 40 seconds. The trials were divided into 4 groups of 10. Each group corresponds to one of the four conditions (1,2,5 or 10 coins on the screen). Each trial lasted a total of 40 seconds, with a 5-second break in between trials. After every ten trials, the participants were given a 1-minute break to rest their arms. In between each trial, participants were presented with a 5-second countdown. During this time, the participant could see their tracer and a red circle that marked the centre of the playing area. The sequence of conditions was calculated randomly during the initial planning phase of the project. The same pseudo-random sequence was used for all participants. The entire experiment lasted a total of one hour, including the briefing and debriefing of participants.

Each experiment lasted for about one 1 hour and 30 minutes, including the time taken to set up EEG equipment. The order of the trials was randomly selected once at the beginning of the experiments. The same pseudo-random trial order was used for all the experiments. The placing of new targets, however, was randomly selected during the experiment.

At the start of the experiment, participants were instructed to refrain from verbal communication and only use visual feedback from the screen and force-force interactions between them to communicate. A more detailed description of the paradigm is given in chapter3. Participants were each fitted with a 32 electrode EEG cap using a standard 10-20 layout shown in figure 5.1. All electrodes were carefully filled with gel to ensure reliable contact with the skin. The active electrode system guarantees a low transmission impedance of about 1 kOhm between the electrode and the

Figure 5.1: Locations of each of the 32 EEG channels used in this experiment and their numbers.

amplifier. All EEG equipment was purchased from g.tec medical engineering GmbH in Austria. A detailed description of the system can be found in appendix A.1.

5.2.3 Processing EEG Data

EEG data was analysed using Matlab 2017a and EEGLAB 2019. EEG data was first low and high pass filtered at 0.5 and 40 Hz, respectively. Filtered EEG data was then visually inspected for any trials with values larger than 100 mv or errors in the recording. One participant's single data had to be discarded due to a faulty gamma box that failed to receive data during the experiment; the corresponding paired data was used. Once the data had been visually inspected, ICA (independent component analysis) with automatic MARA classification was used to calculate the independent components and measure the probability that a component was noise [75]. Only components with at least an 80% probability of being noise were removed from the data.

Signals were first bandpass filtered to one of four frequencies that have been

previously identified as being correlated to social interactions. By study-ing EEG recordings of pairs of guitar players Müller and his colleagues found that in the delta (2-3 Hz) and theta (5-7 Hz) frequency bands, they were able to identify more connectivity during coordinated guitar playing [76]. Research by Tognolli et al. on visually mediated social interactions identified changes in the phi complex (9.2-11.5 Hz) related to whether the movement was uncoordinated and coordinated. They found two distinct peaks within this frequency range: Φ_1(10-12 Hz) increased during uncoordi-nated movement. Φ_2(12-12.5 Hz) increased during coordinated movement. Once the data was bandpass filtered, the Hilbert transform was applied to the entire time series, and the instantaneous phase was extracted. The Hilbert transform is described by,

$$\hat{f}(t) = \frac{1}{\pi} P \int_{-\infty}^{\infty} \frac{f(\tau)}{t - \tau} d\tau, \tag{5.1}$$

where $\hat{f}(t)$ is the Hilbert transform of a function $f(t)$ defined for all t. P is the Cauchy principle value.

EEG data was analysed using a sliding window of 2 seconds, with an overlap of 10%. This window size was chosen to accommodate the lowest frequency band analysed (2-3 Hz). A detailed description of the EEG system and its configuration can be shown in appendix A.1.

5.2.4 Calculating Circular Correlation

The circular correlation coefficient was used to calculate the synchroniza-tion between electrode pairs. This measurement is directly comparable

to the Pearson product-moment but appropriate for circular data such as phase [77, 16]. Burgess has shown that circular correlation is a more robust measure of synchronization between two EEG time series than methods such as phase locking values, partial directed correlation, and Kraskov mutual information [16]. Using both simulated and recorded data, they found that the circular correlation measurement was more resistant to changes in variance and gave an unbiased estimate of hyper-connectivity. They also found that circular correlation gave less spurious correlations than the methods such as phase locking values. The circular correlation is defined as

$$\text{CCorr}_{\phi,\psi} = \frac{\sum_{k=1}^{N} \sin(\phi - \bar{\phi}) \sin(\psi - \bar{\psi})}{\sqrt{\sum_{k=1}^{N} \sin^2(\phi - \bar{\phi}) \sin^2(\psi - \bar{\psi})}} \tag{5.2}$$

where $\bar{\phi}$ and $\bar{\psi}$ are the mean phases for channels 1 and 2 respectively. The circular correlation has been shown to be more robust to false positives; it measures the differences between two oscillators and their respective means. If both oscillators are likely to be ahead of their expected phase, then the circular correlation will be positive; the opposite is true for negatively correlated signals. If the channels are unrelated, then the correlation is zero[16].

Circular correlations were calculated for each pair of electrodes, including intra and inter-brain electrode pairs. The entire 40-second trials were used to gain an average view of the connectivity for each trial.

5.2.5   Creation of Surrogate Data

Given that EEG activity could be synchronized due to events other than social interactions, it is essential to objectively choose a cut-off that distinguished between significant and insignificant correlations. Research has shown that choosing a suitably strict cut-off depends on maintaining the correlations within each channel and breaking the correlations between channel pairs[16]. Two different methods for creating surrogate distributions were tested, one that breaks the experiment's intrinsic timing and another that keeps this timing while still breaking the pairwise interactions between channels from different participants. By comparing the two distributions and the cut-offs calculated from them, it is possible to quantify the effect that the intrinsic timing has on the correlation between channels and choose an appropriate cut-off.

Randomly shifted phases

The first method of creating a surrogate distribution broke all correlations between channels, including the intrinsic timing of executing the task. Surrogate data was created using the following method.

1. Choose a dyad to serve as a starting point.

2. Select a channel pair, called channels 1 and 2 from now on.

3. Randomly shifts the entire 40-second phase time series from channel 2 forwards or backward by a random amount. If the trial is shifted
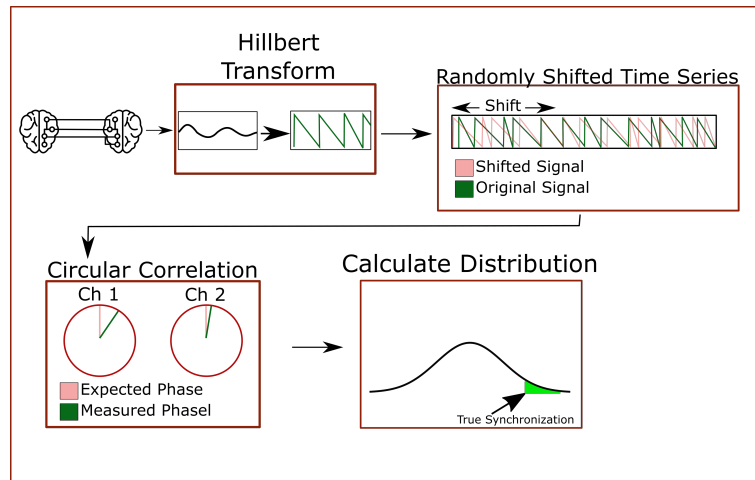
Figure 5.2: Flow chart of the method used to create distributions of circular correlations between randomly shifted phase time series. EEG recordings from paired participants were bandpass filtered, and phases were extracted using the Hilbert transform. For each channel pair, one channel had its phase time series shifted by a random amount. Circular correlations were then calculated. This procedure was repeated 200 times for each channel pair to create a distribution that represented synchronization between channels with no correlations.

past t=0 or t=N, where N is the original sequence's length, it gets wrapped back to maintain the same length.

4. Calculate the circular correlation, using Eq.5.2 for channel 1 and the randomly shifted channel 2.

Each method is repeated 200 times for each channel pair and results in 64x64x200 samples. An example of the process is shown in Fig. 5.2. Two different cut-offs were calculated, one for paired participants and one for singles.
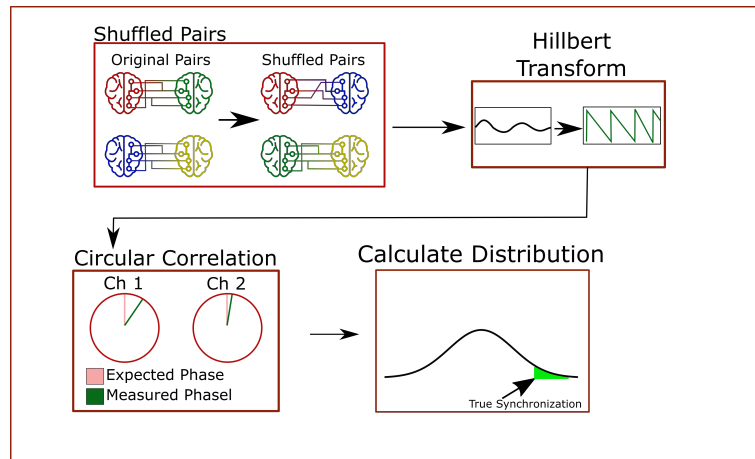
Figure 5.3: Flow chart of the method used to create distributions of circular correlations between shuffled participants. EEG recordings from paired participants were first shuffled to create surrogate pairs. The time series were then bandpass filtered, and the phases were extracted using the Hilbert transform. Circular correlations were calculated for each channel pair. By repeating this for all participants and all conditions, a distribution was created that represents correlations due to the task's timings and to chance.

Surrogate Paired Participants

The previous surrogate distribution characterized circular correlations for time series where the internal correlations of individual channels were maintained, but the intrinsic timings and any social interactions were broken. To better understand the synchronization between channel pairs, distributions of correlations for data where the intrinsic timings were still present, but no social interactions could be taking place were also analysed.

To this end, a new surrogate distribution was calculated using the following method.

1. Choose a pair of dyads to serve as a starting point.

2. Join participant 1 from pair 1 with participant 1 from pair 2 and

participant 2 from pair 1 with participant 2 from pair 2.

3. For every channel pair, calculate the circular correlation for the entire trial using Eq.5.2.

Given that the intra-brain correlations remained the same in this method, only the inter-brain correlations were considered. An example of this process can be seen in Fig. 5.3

5.2.6 Complex Weighted Networks

Networks were created by calculating the pairwise correlations between EEG channels over a 1-second window with a 10% overlap. The calculated correlations were then compared to the cut-off calculated by the randomised pair method shown in Fig. 5.3. Correlations below the cut-off were considered spurious and discarded, and all those above the cut-off were kept as links. The cut-off chosen for the remainder of the experiment was 0.27. It was chosen because so that it was stricter than the cut-offs suggested by the phase shift and random shuffle methods. The weight of the link was equal to the circular correlation between the electrodes. An example of the process used to calculate the adjacency matrices is shown in Fig.5.6. This method resulted in 20 adjacency matrices for each trial, which were averaged together to give each trial's average connectivity. An example of an average adjacency matrix can be seen in Fig. 5.4. Adjacency matrices for all conditions can be seen in figs. A.11-A.18.

Network characteristics associated with social coordination and the emergence of proto-languages were identified by calculating the correlations be-
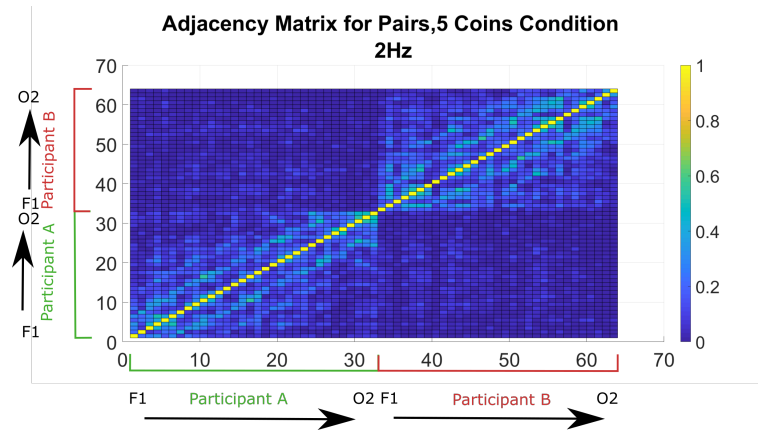
Figure 5.4: Example of an adjacency matrix showing the average inter and intra-brain correlations for all pairs in the five-coin condition. The bandpass filter that was used to calculate correlations was centred at 2Hz with a bandwidth of +/- 1Hz. Each square corresponds to an electrode; 1-32 are on participant A's scalp and 33-64 on participant B's. Inter-brain electrodes are found between (1-32, 32-64) as well as in (32-64, 1-32). Intra-brain electrodes are found between (1-32, 1-32) and (33-64, 33-64). The colour corresponds to the circular correlation averaged over all pairs and 5 coin trials.

tween paired participants and comparing them to correlations calculated between baseline pairs. The baselines are composed of two 32 channel EEG recordings from single participants combined to create one 64 channel recording, Fig. 5.5. This combined data set is treated as a pair and analysed using the same method.

5.2.7   Average Inter and Intra-brain Degrees

The adjacency matrices were divided into three distinct regions of interest, one set of inter-brain electrode pairs and two sets of intra-brain electrode pairs. Correlations between electrodes in these regions were averaged together and considered the average weighted degrees. This measurement was used to compare inter and intra-brain synchronizations between real
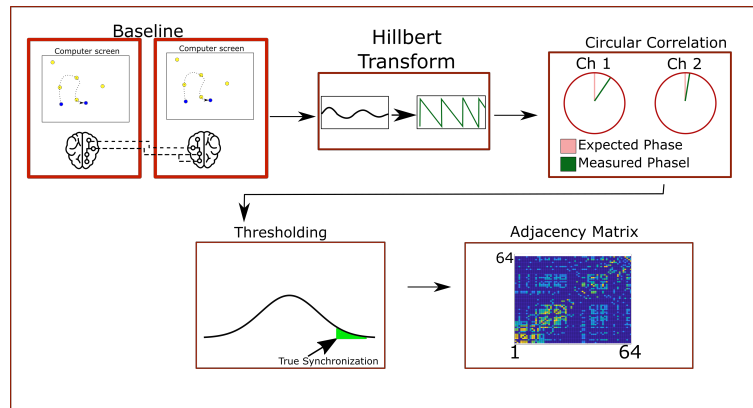
Figure 5.5: method used to calculate the weighted matrices from baseline pairs. The data sets from two single participants are combined and treated as a pair. Raw EEG recordings are bandpass filtered before having their phases extracted using the Hilbert transform. The circular correlations and calculated and thresholded to create the final weighted adjacency matrix.
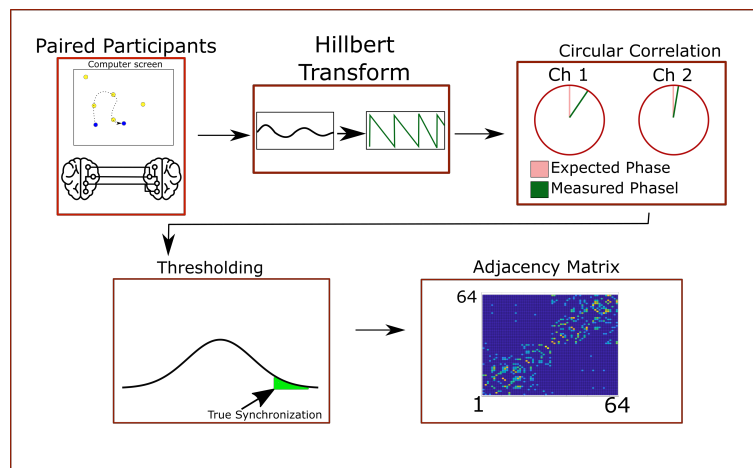
Figure 5.6: Method used to calculate the weighted matrices from paired participants. Raw EEG recordings are band pass filtered before having their phases extracted using the Hilbert transform. The circular correlations and calculated and thresholded to create the final weighted adjacency matrix.

pairs and. Inter and intra-brain degrees are calculated by

$$\text{Average Inter Brain Degree} = 1/N \sum_{i=1}^{32} \sum_{j=33}^{64} w_{i,j}$$
$$\text{Average Intra Brain Degree} = 1/N \sum_{i=1}^{32} \sum_{j=1}^{32} w_{i,j}, \tag{5.3}$$

where indexes $1-32$ index corresponds to electrodes on participant A's head, indexes $33-64$ correspond to electrodes on participant B's head and N is the total number of links.

5.2.8   Segmentation of EEG Networks Into Regions of Interest

Finer-grained analysis of the EEG data was performed by dividing each brain into six regions of interest: left frontal, right frontal, left central, right central, left parietal, and right parietal. The circular correlation of each region was calculated as the average correlation for all channels within it. These regions were chosen so that it was possible to identify the key areas associated with social interactions such as the frontal and temporoparietal areas. Other experiments have shown that the temporoparietal region is active during joint actions and social interactions between humans [51, 52, 51, 53]. A map of the regions is shown in figure 5.7.

The thresholded circular correlations for all time windows, trials, and participants were grouped together and used to determine whether the distribution of correlations for paired participants was significantly different from those of surrogate pairs. These were then compared to determine which
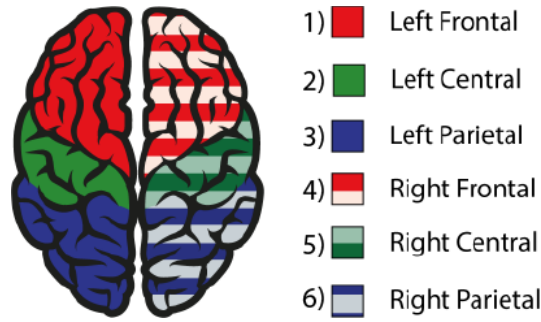
Figure 5.7: An example of the regions of interest that were analysed in this experiment. The regions are numbered 1-3 for the left side (frontal, central, and parietal) and 4-6 for the right side. The same pattern was repeated for participant B with regions numbered 7-12 to distinguish them from the regions of participant A.

regions were significantly different between paired participants and singles. Statistical significance was measured using the Kruskal-Wallis method with a p-value< 0.05 and was corrected for multiple comparisons using the Tukey-Kramer correction.

5.3 Results

5.3.1 Surrogate Distributions

Randomly Shifted

The circular correlations' distributions, calculated from randomly shifted phase time series for single and paired participants, are shown in Figs. 5.8 - 5.9 respectively. The distributions had a mean,μ, of about 0 and a standard deviation,σ, of 0.078 for both pairs and singles. The cut-off was calculated as $\mu + 3\sigma$, giving a cut-off of 0.25. The three standard deviations ensure that 99.7% of the surrogate correlation values are below the cut-off and
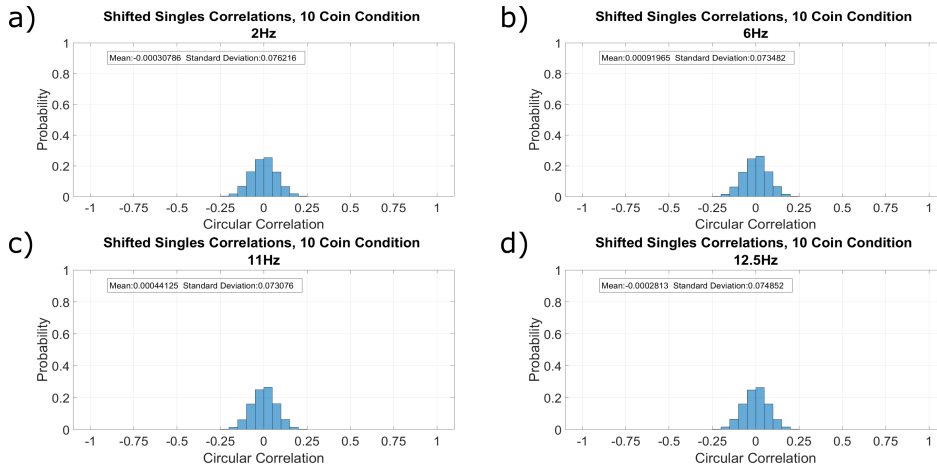
Figure 5.8: Distribution of surrogate circular correlations between two single participants. Surrogate data was created by shifting a channel's entire 40-second phase time series by a random amount. Data was taken from all trials of the 10 coin condition. A) Shows the distribution of average circular correlations for all participants. Data was filtered between 1-3 Hz. B) Shows the distribution of average circular correlations for all participants. Data was filtered between 5-7 Hz. C) Shows the distribution of average circular correlations for all participants. Data was filtered between 10-12 Hz. D) Shows the distribution of average circular correlations for all participants. Data was filtered between 11.5-13.5 Hz.

have an appropriately conservative p-value < 0.003. Distributions were created for every participant and every condition. Final cut-offs calculated from the different distributions were within 0.02 of each other. The largest cut-off was chosen to remove any links that could be due to noise. Given that all between channel correlations were broken, it was unnecessary to create a distribution for each condition. However, research has shown that synchronization between electrodes can change depending on the frequency band [51, 78]. Therefore, different distributions were calculated for the four frequencies of interest. In this case, the frequency had a negligible effect on the cut-off as shown in Figs 5.8 and 5.9. The cut-offs were calculated using combined data from all participants and were used as a global cut-off.
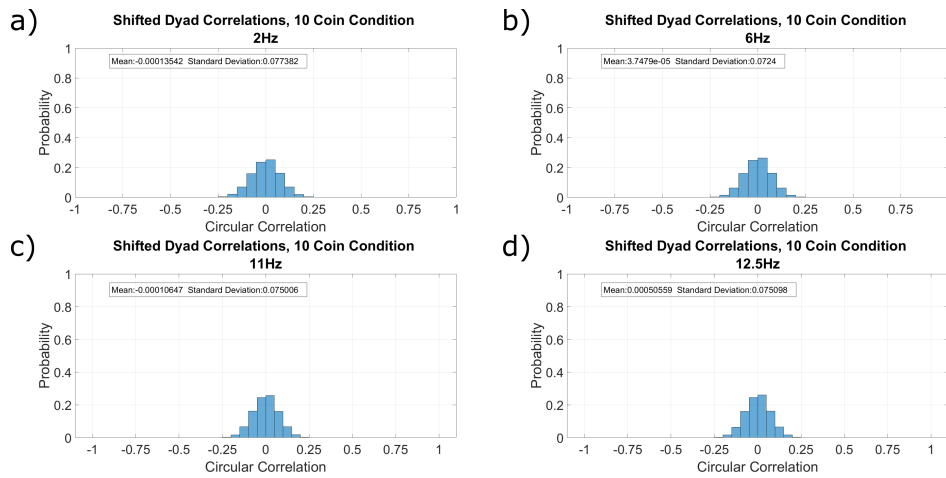
Figure 5.9: Distribution of surrogate circular correlations between paired participants. Surrogate data was created by shifting a channel's entire 40 second phase time series a random amount. Data was taken from all trials of the 10 coin condition. A) Shows the distribution of average circular correlations for all participants. Data was filtered between 1-3 Hz. B) Shows the distribution of average circular correlations for all participants. Data was filtered between 5-7 Hz.C) Shows the distribution of average circular correlations for all participants. Data was filtered between 10-12 Hz. D) Shows the distribution of average circular correlations for all participants. Data was filtered between 11.5-13.5 Hz.

Dyad Shuffle

The distributions of circular correlations calculated from randomly shuffled participants had an average mean, μ of 0, and an average standard deviation, σ of 0.07. The cut-off was calculated as $\mu+3\sigma$; this gives a cut-off limit of 0.24. Using three standard deviations ensures that 99.7% of the surrogate correlation values are below the cut-off and have a p-value < 0.003. A comparison between distributions calculated from randomised pairs and actual distributions during different conditions are shown in Fig. 5.10 (a-d). The cut-offs were calculated using combined data from all participants and were used as a global cut-off.

Results show that the standard deviation of inter-brain correlations changes depending on the frequency and the number of coins on the screen. There is a decrease in the standard deviation for paired participants in conditions with one or ten coins on the screen. The standard deviation for shuffled participants is consistently around 0.07, while for paired participants, it ranges from 0.12 to .07. The smallest σs are seen in the one and ten coin cases. Differences in σs suggest a change in synchronization between real dyads. These differences potentially depend on the number of coins on the screen. A possible explanation for this is that the strategy used to pick up coins when the density of coins is high reverts to a strategy similar to those employed in single coin cases. If the density of coins on the screen was above a certain threshold, participants could move to the closest coin to their current path. The clarity in which coin is next could simplify the strategy to the point of being similar to the strategy employed during the one coin conditions.
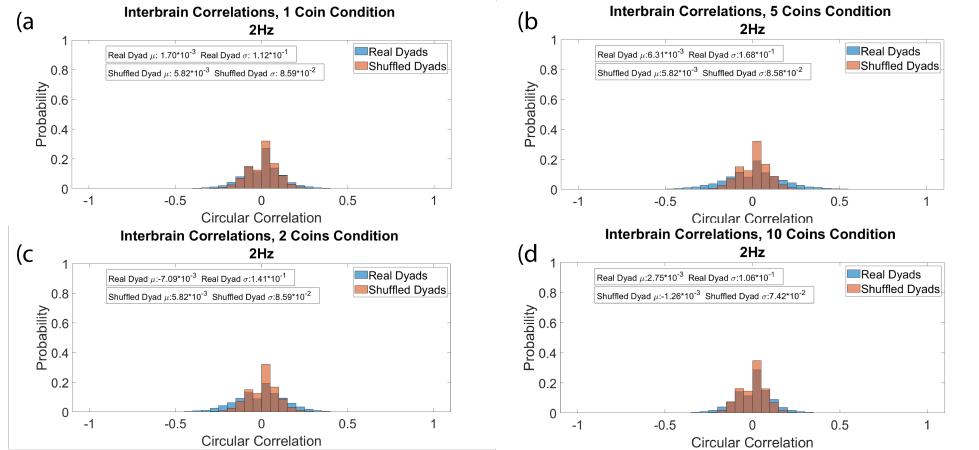
Figure 5.10: Distribution of circular correlations from real and shuffled pairs. Correlations were calculated from EEG data that was band passed between 1-3 Hz. a) Data from one coin conditions, b) data from two coin conditions, c) Data from five coin conditions, d) data from one ten conditions

5.3.2   Average Inter and Intra Brain Degree

The Data shown in this section corresponds to data from 5 pairs and 10 single participants. Circular correlations between inter-brain electrodes are shown in Fig.5.11 (a-d) and correlations for intra-brain electrodes are shown in Figs.5.12 (a-d). These figures show that the average inter-brain degrees are consistently larger for singles than pairs. The largest difference between pairs and single participants is seen in the 1-3Hz frequency band. These results coincide with results from guitar duets, which also identified that the 2Hz frequency contained the most inter-brain synchronization[61]. At this stage of the analysis, no significant differences have been found between conditions.

Differences between pairs and singles related to the bandpass frequency were analysed using data from all four conditions. Significance was tested with the Kruskal-Wallis analysis of variance with a p-value < 0.005 and
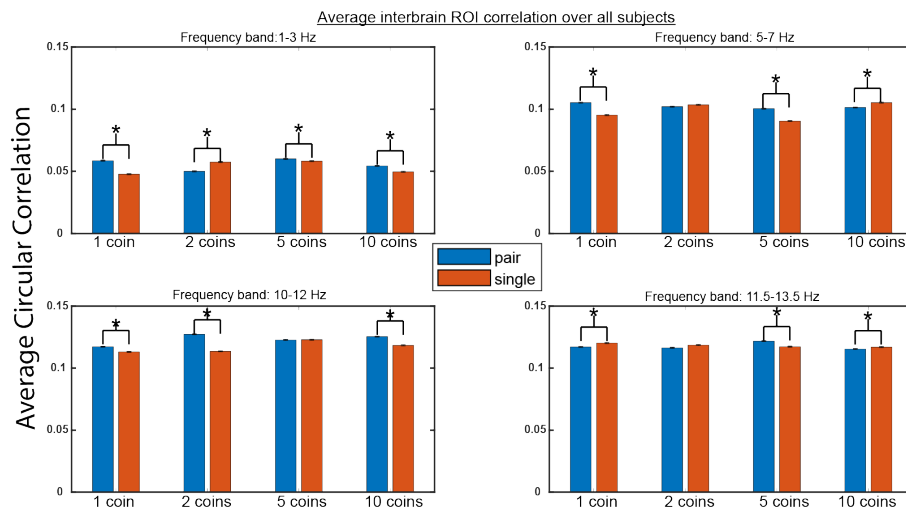
Figure 5.11: Average inter-brain degree averaged over all inter-brain electrodes and all participants. The orange bars show the values for single participants, and the blue ones show the values for paired participants. Asterisks show significant differences between paired and single participants. The error bars show the standard error for each measurement. a) Data that was bandpass filtered between 1-3 Hz, b) Data that was bandpass filtered between 5-7 Hz,c) Data that was bandpass filtered between 10-12 Hz, d) Data that was bandpass filtered between 11.5-13.5 Hz
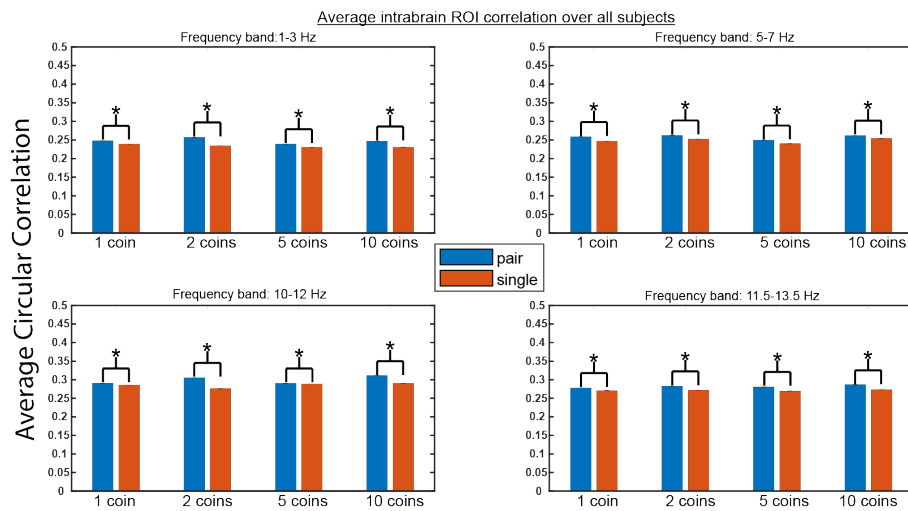
Figure 5.12: Average intra-brain degree averaged over all intra-brain electrodes and all participants. The orange bars show the values for single participants, and the blue line shows the values for paired participants. Asterisks show significant differences between paired and single participants. The error bars show the standard error for each measurement. a) Data that was bandpass filtered between 1-3 Hz, b) Data that was bandpass filtered between 5-7 Hz,c) Data that was bandpass filtered between 10-12 Hz, d) Data that was bandpass filtered between 11.5-13.5 Hz
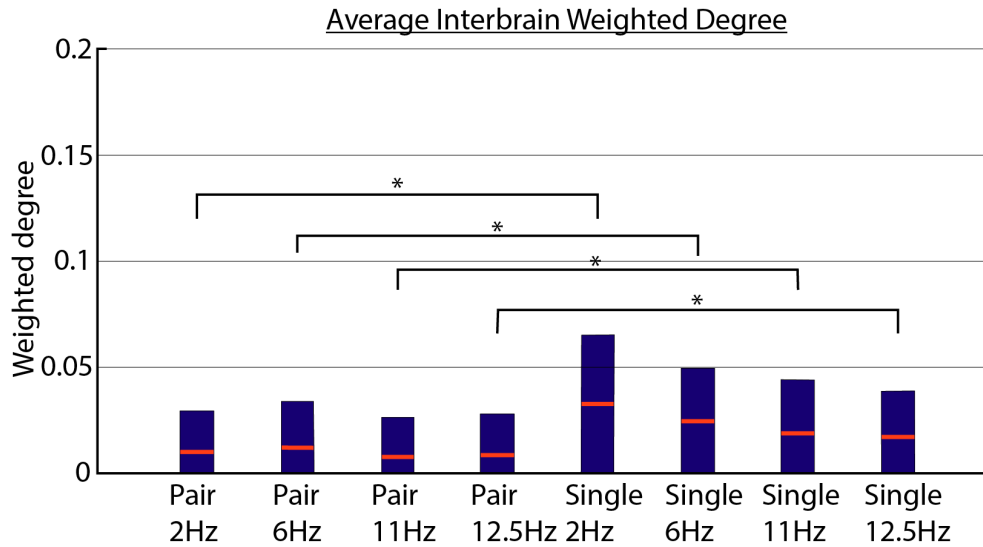
Figure 5.13: Average interbrain weighted degrees. Each box plot shows the mean(red line)) and standard deviations(blue shaded rectangle) of the interbrain weighted degrees at a given frequency averaged over all conditions and pairs. Distributions that are connected with a horizontal bar and are marked with an * are significantly different with p< 0.005 and were corrected for multiple comparisons.

corrected for multiple comparisons using the Bonferroni correction. Figure 5.13 shows that inter-brain degrees between pairs and single participants are significantly different for all frequency bands. There is also an inverse relationship between the frequency band and the average inter-brain weighted degree.

5.3.3 Region of Interest Analysis

Deciding which connections were significant was done by comparing the distributions of circular correlations of paired and single participants. An example of the distributions can be seen in figure 5.15. The correlations in figures 5.17-5.20 are only for regions where these distributions were significantly different between paired participants and baseline pairs made up
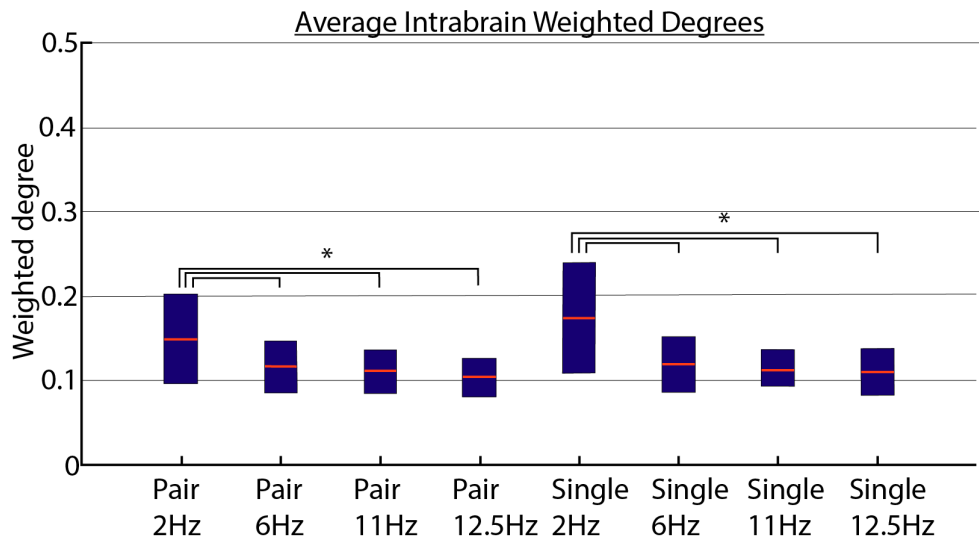
Figure 5.14: Average intrabrain weighted degrees. Each box plot shows the mean(red line)) and standard deviations(blue shaded rectangle) of the intrabrain weighted degrees at a given frequency averaged over all conditions and pairs. Distributions that are connected with a horizontal bar and are marked with an * are significantly different with p< 0.005 and were corrected for multiple comparisons.

of two singles. Significance testing was done with a Kruskall-Wallis test with a p-value of 0.05, which was corrected for multiple comparisons. An example of two significantly distributions can be seen in fig 5.15 C, while non significant distributions are shown in fig 5.15 A and B.

Figure 5.16 shows the average circular correlations over all conditions for all four frequency bands. Averaging over all conditions gives a quick overview of the connectivity in the different frequency bands. We can see that intrabrain correlations for participant B are largest during the 10-12 and 11.5 - 13.5 Hz frequency bands. The correlations in Participant A vary less between each frequency band. In both A and B participants, we can see that the highest correlations are found between central and frontal regions in both the left and right hemispheres. Connections between occipital and central regions also show large average correlations.
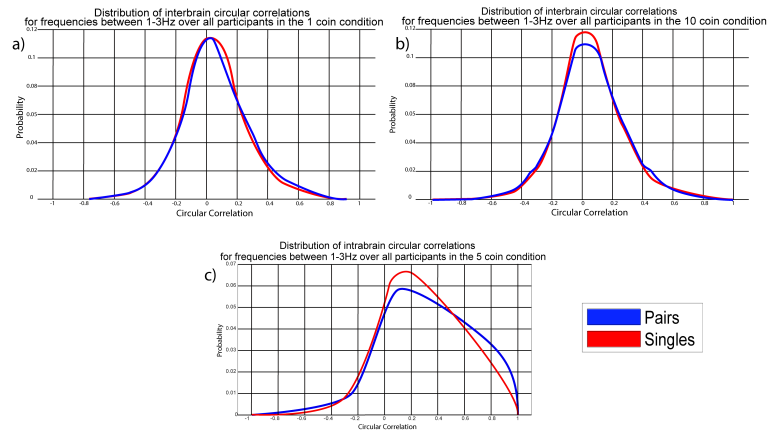
Figure 5.15: Examples of distributions taken from inter and intra brain regions of interest from paired and single participants. These distributions are average circular correlations over all participants for a single electrode. Figures a and b show distributions from two different electrodes and show distributions that were not found to be significantly different. Both a and b show interbrain electrodes. Figure C shows an example of distributions taken from a pair of intrabrain electrodes that were significantly different from each other.

By breaking the results up into conditions, we see that conditions 2 and 3 have the most instances of significant average correlations. Particularly in the higher frequency bands where we see much activity in Participant B. Table 5.1 shows that in the Phi2 frequency band, the average intrabrain correlations are larger than in any other frequency band, except for condition 3, which is largest in the phi1 frequency band. From the figures 5.17-5.20, we can see that during most conditions, participant B has more significantly different correlations and in most frequency bands. However, this is not the case during conditions 3 and 4 in the 1-3 and 5-7 Hz frequency bands where significant activity in participant B is significantly reduced compared to the other conditions. The most strongly connected regions are consistent between participants A and B. The right central region showed the largest average circular correlations with the right occipital
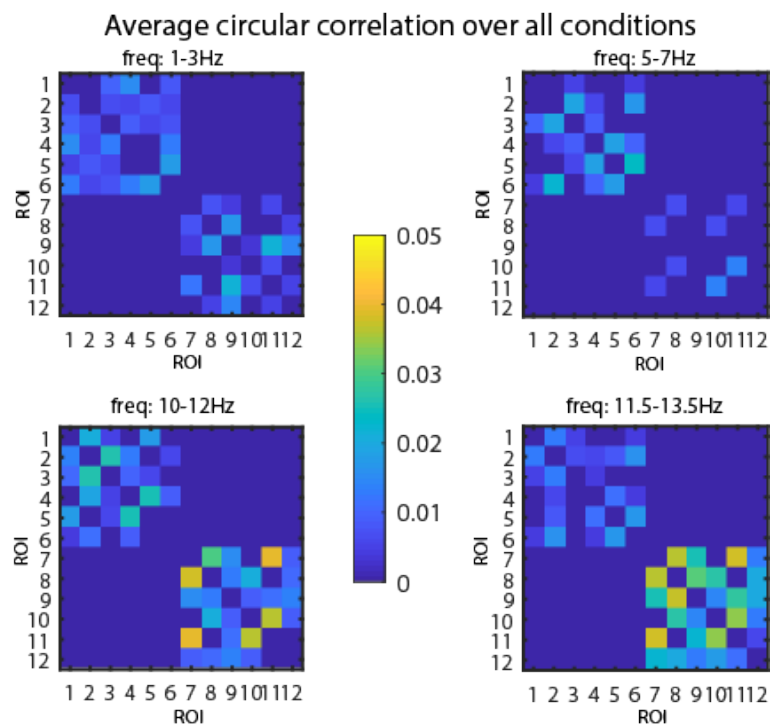
Figure 5.16: Adjacency matrix showing the average circular correlations between regions of interest. The correlations shown here were calculated as the mean over all conditions for a given frequency band. The locations of each regions are detailed in section 5.2.8, 1-6 are on participant A's head (left frontal,left central, left occipital, right frontal, right central, right parietal). Regions 7-12 are the same but located on Participant b's head.
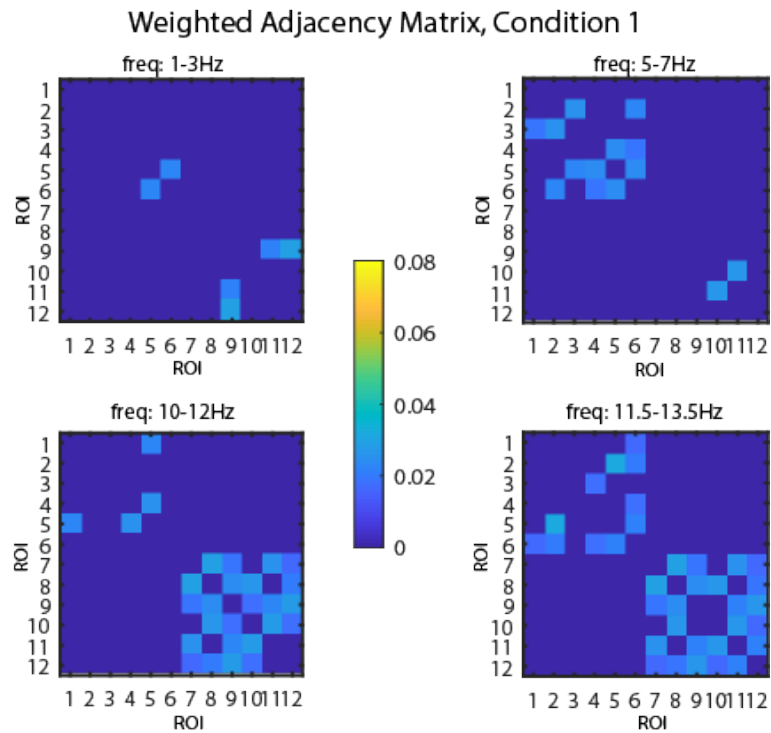
Figure 5.17: Adjacency matrix showing the average weighted circular correlations between the regions in the one coin condition. The locations of each region are detailed in section 5.2.8, 1-6 are on participant A's head (left frontal, left central, left occipital, right frontal, right central, right parietal). Regions 7-12 are the same but located on Participant b's head. Probability distributions of circular correlations were compiled from all time points, trials, and all paired participants were statistically compared to those calculated from single participants. The number of trials where a pair of regions were significantly different in pairs versus singles was used as a weight. This weight was then multiplied with the average circular correlation for that pair of regions.
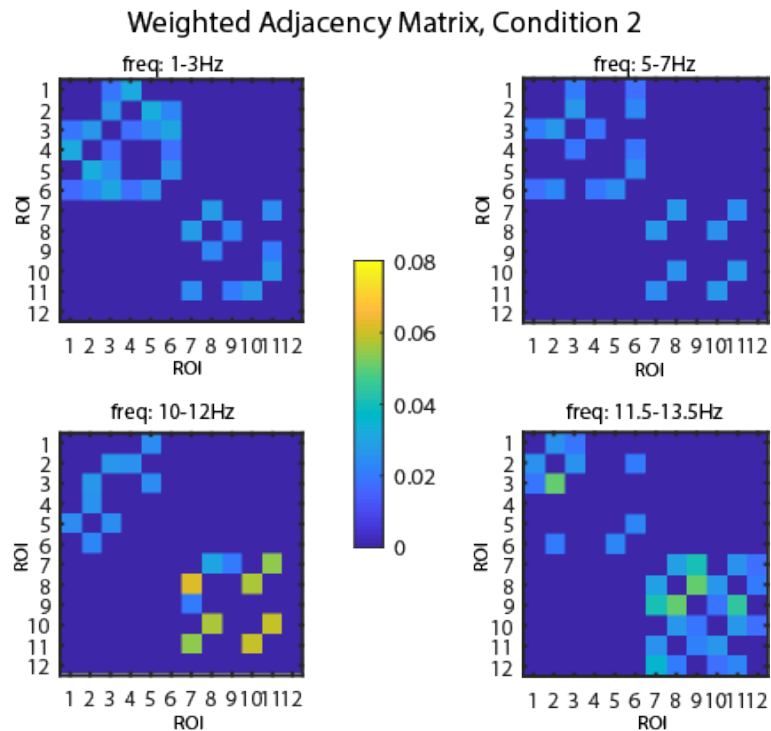
Figure 5.18: Adjacency matrix showing the average weighted circular correlations between the regions in the two coin condition. The locations of each region are detailed in section 5.2.8, 1-6 are on participant A's head (left frontal, left central, left occipital, right frontal, right central, right parietal). Regions 7-12 are the same but located on Participant b's head. Probability distributions of circular correlations were compiled from all time points, trials, and all paired participants were statistically compared to those calculated from single participants. The number of trials where a pair of regions were significantly different in pairs versus singles was used as a weight. This weight was then multiplied with the average circular correlation for that pair of regions.
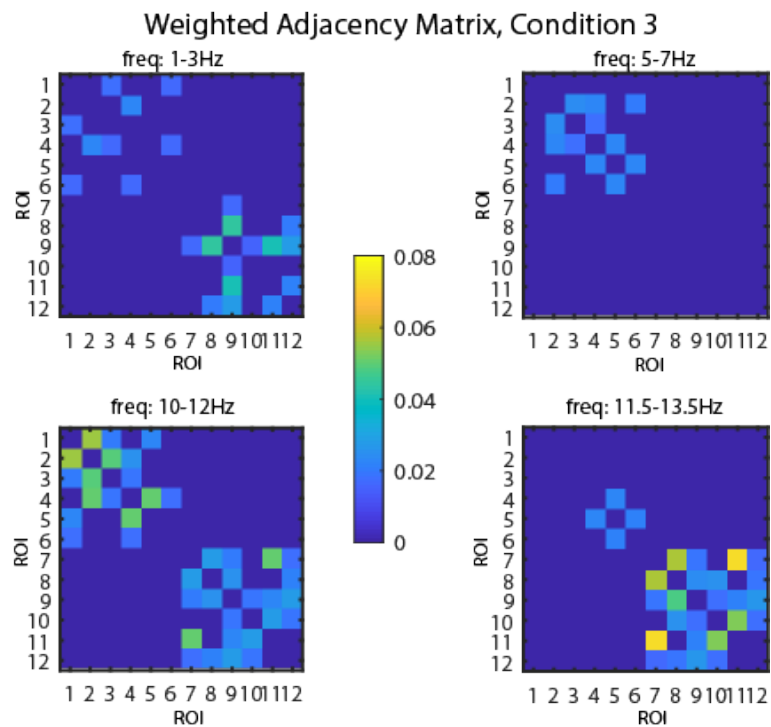
Figure 5.19: Adjacency matrix showing the average weighted circular cor-relations between the regions in the five-coin condition. The locations of each region are detailed in section 5.2.8, 1-6 are on participant A's head (left frontal, left central, left occipital, right frontal, right central, right parietal). Regions 7-12 are the same but located on Participant b's head. Probability distributions of circular correlations were compiled from all time points, trials, and all paired participants were statistically compared to those calculated from single participants. The number of trials where a pair of regions were significantly different in pairs versus singles was used as a weight. This weight was then multiplied with the average circular correlation for that pair of regions.
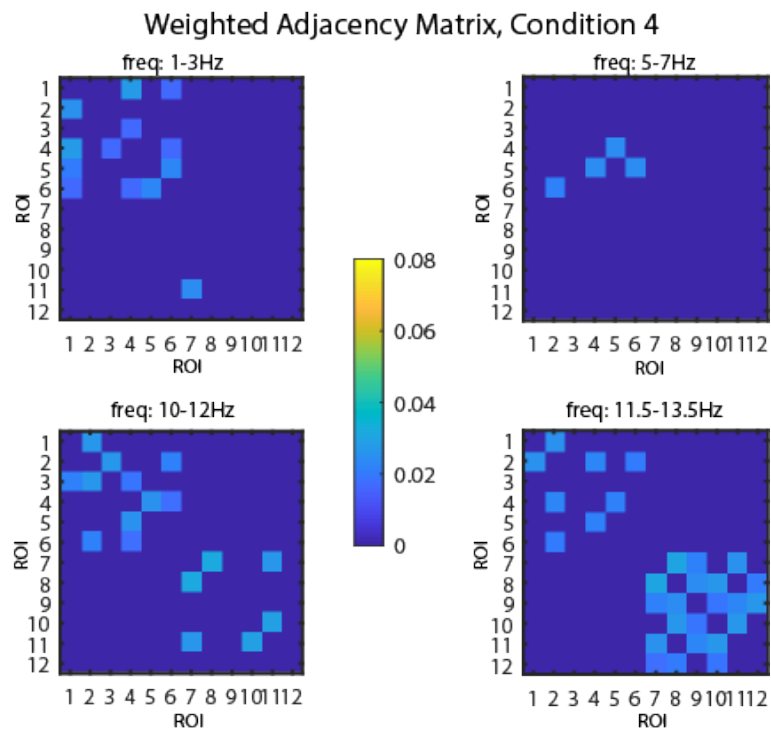
Figure 5.20: Adjacency matrix showing the average weighted circular correlations between the regions in the ten coin condition. The locations of each region are detailed in section 5.2.8, 1-6 are on participant A's head (left frontal, left central, left occipital, right frontal, right central, right parietal). Regions 7-12 are the same but located on Participant b's head. Probability distributions of circular correlations were compiled from all time points, trials, and all paired participants were statistically compared to those calculated from single participants. The number of trials where a pair of regions were significantly different in pairs versus singles was used as a weight. This weight was then multiplied with the average circular correlation for that pair of regions.

Table 5.1: Mean intrabrain circular correlation for paired participants

	1-3 Hz	5-7 Hz	10-12 Hz	11.5-13.5 Hz
1 coin	0.004	0.009	0.018	0.022
2 coins	0.020	0.013	0.018	0.024
3 coins	0.015	0.007	0.030	0.023
4 coins	0.006	0.003	0.011	0.018

Table 5.2: Mean intrabrain circular correlation for single participants

	1-3 Hz	5-7 Hz	10-12 Hz	11.5-13.5 Hz
1 coin	0.003	0.007	0.018	0.021
2 coins	0.018	0.011	0.015	0.023
3 coins	0.015	0.006	0.029	0.022
4 coins	0.006	0.002	0.010	0.018

region, having the second largest for both participants. Results show that central regions on participant B, mainly frontal central regions, identified as the location of phi1 and phi2 by Tognolli et al., were consistently connected to frontal electrodes. Interestingly, this was not seen in participant A, who generally had much lower connectivity than their partners.

By comparing tables 5.1 and 5.2, we can see that, after removing all non-significant connections, circular correlations in paired participants are higher than in single participants. These results contradict those from the coarser-grained analysis, which did not filter out statistically insignificant connections. This result shows that when two participants share physical control over a device, it can be seen as an overall increase in interbrain circular correlations. The most considerable differences occur in connections between frontal and central regions in participant B. The largest differences in Participant A are seen between central and occipital regions.

5.4   Discussion

Synchronization between different brain areas has been seen across a wide range of frequencies and experiments [55, 61, 51, 26, 79]. With the increased popularity of hyper-scanning methods, researchers have also turned to use synchronization both within one brain and between brains as a method of characterizing the connections that underlie human communication. This experiment used the paradigm introduced in chapter 4 and employed hyperscanning methods to investigate the neural correlates of social coordination and the emergence of proto-languages. The analysis in this experiment focused on identifying network characteristics associated with two participants cooperating and communicating with each other. The strength of the links between electrodes was calculated using the circular correlation eq.5.2[16]. Application the methods described in this project are relatively new and still requires more research to understand how to interpret circular correlation and how it changes depending on the participant's mental state. Because of this, there is little literature with which to compare results. Burgess and his colleague used circular correlation to distinguish between eyes open and eyes closed. They showed that resting-state EEG had a maximum circular correlation of 0.06 and 0.14 while viewing a picture of a face. It was shown that circular correlations reach up to 0.3 for intrabrain circular correlations.[16]

To create an adjacency matrix of participants, distinguishing significant correlations from random correlations was vital. This distinction was made by comparing the calculated circular correlation to a cut-off value calculated using the shuffled pairs method, Fig .5.3. This method was used

because it preserved the temporal structure unique to taking part in the game but broke any correlations between participants given that baseline pairs were made using two single participants. The cut-offs were consistent for all three methods of creating surrogate distributions, random pairs(Fig. 5.3), shifted phase(Fig. 5.2), and shifted singles(similar to shifted phases but with baseline pairs). These figures show that the cut-offs calculated using the three methods are robust and appropriate for both singles and paired participants. All three methods gave cut-offs between 0.24 and 0.27. Ultimately, the largest cut-off was chosen. This cut-off corresponded to the randomised pair method. This method preserved all correlations within individual channels and any correlations due to participants taking part in the same task. Because of the preservation of these correlations, this method gave the strictest cut-off. Hurtado et al. found similar results when testing different methods for calculating cut-off limits for phase-locking values [74]. They found that cut-offs calculated from surrogate data where the correlations within the channel had been preserved were the most effective at reducing type I errors.

In this experiment, networks from paired participants were compared to those of single participants. Using baseline pairs made up of single participants meant that baseline pairs retain the task's correlations but lacked those related to the force-force interactions. Some examples of these are the experiment's length, rhythmic movements done while taking part in the experiment, and any influence from the experiments' location. Analysing the differences between paired participants and baseline pairs reduces these confounding variables' influence and should reveal the network characteristics associated with social coordination and the emergence of proto-

languages. The primary measurement that was investigated was the inter and intra-brain degrees. They characterize the average connection strength over all inter and intra-brain electrodes.

Analysing the average intra-brain degrees shows significant differences between the 1-3Hz frequency band and the other three, both for paired participants and baseline pairs, as shown in Fig .5.14. Finding larger average correlations at lower frequencies is consistent with work done by Lindenberger et al. [61, 76, 26]. However, in Lindenberger's experiment, the increase in synchronization was found in the inter-brain electrodes of participants playing guitar in paired participants and was mostly associated with play onset. Interestingly, in the current experiment, this effect is smaller in the inter-brain network than in the intra-brain network and occurs for baseline pairs. Although Fig. 5.13 shows a negative correlation between the average inter-brain weighted degree in baseline pairs and the frequency, this effect is not significant and was not seen for paired participants. This difference may be due to the type of task that participants were performing. In Lindenberger's experiments, participants played a musical piece on the guitar as a duet. Both participants had previously practised the piece, and the only difference between them was the time of play onset for each one. Although a certain degree of interaction between the participants is required to keep each stream of music in time, each participant's motor coordination depends only on themselves and the timing imposed by a metronome and the piece of music. In Linderberger et al. experiments, the metronome and learned timing of the piece act as a powerful external driver that can create spurious neural correlations [61]. In this paradigm, there is no external driver; therefore, participants must truly cooperate

and exchange information with each other to synchronize their minds and bodies. This synchronization emerges from the haptic interactions between the participants without a common driver. In this paradigm, when participants are paired together, they must coordinate their own movements and coordinate their movements with their partners. The single case condition is the only one that only requires self coordination, making it closer to the duet condition in Lindenberger's paradigm. This difference in interbrain degrees could be related to the proficiency level that the subjects have with the task. In Lindenberger's experiment, both participants were proficient in playing guitar and had memorised a piece of music supplied by the experimenters.

The next step in the analysis was to get a more detailed spatial map of each participant. Each brain was divided into 6 regions of interest, 3 on the right hemisphere and 3 on the left, as shown in Fig. 5.7. At this point, a second method was used to keep only correlations that were different between paired participants and baseline pairs. The distributions of circular correlations for each pair of regions from paired participants were statistically compared to those from baseline pairs made up of two single participants. Only pairs of regions that were significantly different passed on to the next analysis. This strict filtering process removed all interbrain connections and many of the intrabrain connections as well. However, these results also show that the phi1 and phi2 frequency bands were the most active, particularly in participant B. An increase in connections found in frequency bands linked to social interaction could characterize the division of roles between participants. Participant B might adopt a follower role more often and thus need to be more in tune with their partner, primarily

if participant B used their non-dominant hand.

Results from individual regions show that central electrodes are the most connected, with the right occipital being the second most connected. Connections were strongest in the phi1 and phi2 frequency bands. These results corroborate what Tognolli found in his finger-wagging experiment [55]. He found that the phi complex was primarily found over the right centroparietal cortex, which in this experiment corresponds to the central region. The strongest connections were also found between the central and frontal regions. Frontal brain areas have previously been identified as being involved in modifying internal models by Menoret and his colleagues [80]. These results suggest that there may be some modification of internal models in conjunction with the processing of social cues via the mirror neuron system.

From both the coarse and more detailed analyses, it is possible to see a similarity between 1 and 10-coin conditions and between 2 and 5-coin conditions. Interestingly, participants in the 2 and 5-coin conditions show increased intrabrain connectivity. Given that we expected connectivity to increase with task difficulty we expected to see the largest circular correlations in the 10 coin condition. The similarities between the 1 and 10 coin conditions suggest that the synchronization level necessary to play this game is related to the density of points on the screen. At the lowest density, there is only one option making negotiations very simple. Here, the only limit to how well the participants perform is related to the coordination between their limbs. With more than one coin on the screen, participants must now agree on the next target, which requires extra time

to negotiate where to go next. However, when the density of coins passes a threshold, the negotiations become less critical. Potentially this is due to there always being a coin that is closest to the tracer. Having a clear target reduces the time that participants spent negotiating. Future experiments could identify the critical density where the strategy changes from a simple mechanical strategy to a more complex negotiated strategy.

Comparing the adjacency matrices of paired participants and the baseline pairs, made up of two single participants, we can see that paired participants show larger circular correlations on average. Further analysis showed that in participant A, connections between the central and occipetal regions had significantly larger circular correlations in paired participants than in the baseline pairs. In participant B, the central and frontal regions are more active in the paired participant experiments than in the single participant ones. This result suggests that participant A, the one using their dominant hand, uses visual information to plan the route through the playing area. On the other hand, Participant B is activating regions related to social interactions (central region) and regions related to manipulating internal models (frontal region). Differences between participants A and B could suggest that participant B is following participant A. Possibly, by modifying their internal model, which includes both participants and the device used to move in the virtual world.

5.5 Conclusion

In conclusion, this experiment introduces a promising research paradigm that could advance the scientific understanding of interpersonal coordination. The methods include a robust way of finding appropriate cut-off values for circular correlations and distinguishing real connections from those created by merely taking part in the same experiment. Although many other studies have also created baseline pairs by shuffling the participants, this is one of the first studies to create baseline pairs from single participants. It is also one of the first to compare the distributions of circular correlations between single and paired participants. The analysis was carried out in two parts: 1) A coarse-grained analysis where all interbrain connections were averaged together, and all intrabrain connections were also averaged together. 2) A localized analysis that divided the brain into 6 regions of interest. The coarse-grained analysis showed that single participants had larger circular correlations both in intra and interbrain connections. This effect was not seen when comparing the mean circular correlations between different regions in paired participants and singles. Instead, the results show that paired participants have larger interbrain circular correlations than single participants. Evidence from both the coarse-grained average results and the region of interest analysis shows similarities between the 1 and 10 coin conditions and between the 2 and 5 coin conditions. It is hypothesized that these similarities are related to the density of coins on the screen and explored further in future experiments. As a whole, these results show an excellent set of preliminary results that have introduced some interesting points for discussion. The current study is one of the first to

investigate both single participants and paired participants simultaneously and compare their behavioural and neural characteristics.

5.6   Future Work

Work on this research will continue in two ways. The first will be by continuing to work on the data that was collected for this thesis. Given the complexity of the data that was collected, there remain many avenues to be explored. The first would be to find neural correlates for each haptic state present in the behavioural data set. It gives a much clearer picture of each participant's role and how they coordinated their efforts to achieve a common goal. It would also be interesting to compare the results obtained using single participants as a baseline with those obtained by comparing trials of each experiment with their corresponding rest periods. Another aspect of the data that still needs to be explored is the network dynamics and their correlations to the haptic data set.

This paradigm could also be modified in exciting ways to better understand human interpersonal coordination and the development of strategies in a group. One interesting modification would be to vary the density of coins on the screen systematically. By doing this, it should be possible to identify the critical value where the 1/10 coin strategy shifts to a 2/5 coin strategy.

Chapter 6

Conclusion

6.1 Research Contributions

This project's aim can be split into three distinct areas: 1)To develop a paradigm designed to allow participants the freedom to interact with each other in a meaningful way and carry out a goal-oriented task that required cooperation. 2)Investigate how pairs used force-force interactions to communicate and create mental models of each other's movements and intentions. 3)Investigate the neural correlates associated with communication via force-force interactions.

The behavioural experiment presented in this project is the first study to investigate the temporal correlations of haptic interactions during a cooperative task. This work introduces two new concepts, haptic states and haptic signals, which can characterize force-force interactions. Chapter 4 showed that haptic signals are a useful tool to analyse haptic communications between two individuals. By reducing force-force interactions to 16

haptic signals, a time series representing bi-directional interactions between participants can be constructed. Analysis of the proportion of short and long-range temporal correlations was used to identify signals that were more likely to be necessary for communication. If the distribution of distances for a given signal had many more long-range correlations than short-range ones, the q value would be larger than 1.

These experiments show that the haptic signals used by paired participants have both long and short-range temporal correlation. On the other hand, haptic signals for single participants mostly show only short-range temporal correlations. This difference is shown by the larger Δq values and a larger proportion of haptic signals whose distributions can be fit by the q-exponential function (Fig. 4.12a). Combinations of longer and shorter-range temporal correlations have been identified as fundamental characteristics of emerging simple languages[33]. The presence of the same behavioural pattern suggests that haptic signals are being used by paired participants to communicate. The results also suggest that the emergence of this protolanguage is due to the real-time coupling of action-perception loops between paired participants, creating a richer possibility of states that pairs can use to exchange information.

The paradigm developed during this Ph.D. was also applied to a hyperscanning methodology designed to build complex networks. This methodology characterized the interactions between paired participants and identified the network characteristics associated with true social interactions. This experiment is the first to look into social interactions and the emergence of protolanguages. Building the networks relied on using circular correlation

as a measure of synchronization between EEG channels and choosing an appropriate cutoff value to remove any spurious correlations. Choosing the cutoff is a vital step in defining the links between pairs of electrodes. Many possible sources of spurious correlations between oscillators and interpretation of and measure of synchronization must take these into account [16]. Researchers typically choose a cutoff calculated from a distribution of synchronizations where there were no real interactions in the underlying data to address this problem. Therefore any synchronization found in this distribution is purely due to chance. In this project, two different methods of creating the surrogate data were tested: randomly shifting data in time and shuffling members of pairs. The first method broke all correlations between channels but maintained the correlations within the channels. The second method kept all correlations due to the task and the within channel correlations. The only between channel correlations that were kept in the second method was the intra-brain correlations. Method 2 gave the most conservative cutoff of 0.27, which was the cutoff used in the rest of the experiment. This cutoff ensured that the links identified by this method corresponded to synchronizations stronger than those only associated with the task or random synchronizations. Networks from paired participants were compared to those calculated from single participants. This comparison was made to ensure baseline data was related to the task and free from any social interactions.

The hyperscanning experiments show larger average correlations at lower frequencies in both inter and intra-brain networks of single participants. These results are consistent with the work done by Lindenberger et al. [61, 76, 26]. Although in Lindenberger's experiment, the increase in syn-

chronization was only found in the interbrain electrodes of participants playing guitar in pairs and was mostly associated with play onset. In this project's experiments, the interbrain degrees were significantly smaller for pairs than for singles. This effect requires more analysis to be fully understood. The low synchronization between pairs could be due to behavioural differences in the task. One crucial difference is that single participants used both hands to interact with the computer, while paired participants only used one. On the other hand, paired participants only used one hand. The comparatively low synchronization in pairs could also be due to the dynamics of the networks. Due to time constraints, only average networks were studied during this project. A detailed investigation of the inter and intrabrain network dynamics would focus on identifying neural correlates of different haptic signals or types of haptic signals, such as purely receptive or unilaterally receptive. It is also important to note that unlike in Lindenberger et al. experiments, the coin collecting paradigm does not introduce a common source of coupling, such as a metronome, making interpreting the results from the current paradigm more straightforward.

Another novel result that has not been reported in other studies is the possible dependence of behavioural strategy and interbrain synchronization on the density of coins on the screen. Both behavioural and EEG results show an effect which, although not significant, suggests that this is indeed the case. Figs. 5.10(a-d) show an increase in the standard deviation of the weighted degree in the 2 and 5 coin conditions. On the other hand, the 1 and 10 coin conditions show a lower standard deviation. These results reflect the similarities seen in transition probabilities during the 2 and 5 coin conditions, Figs. 4.6a -4.7a, and between the 1 and 10 coin conditions,

Figs. 4.5a -4.8a. These results suggest that paired participants have two behavioural modes, which are possibly reflected in the inter-brain circular correlations' standard deviation. These results suggest that the behavioural mode used by paired participants is related to the density of coins in the target area.

However, there remain many questions yet to be answered. For example, why do paired participants show lower overall synchronizations than single participants? There are three possible reasons for this difference: 1) Larger synchronization between limbs creates more synchronization between inter-brain electrodes. 2) The task and environment that singles are subject to are identical. On the other hand, each member of a pair is doing a slightly different task. The differences in the task could contribute to reducing the synchronization between them, or even creating negative correlations. 3) Correlations in pairs change cyclically over time and give low averages, while correlations for singles are more constant and give larger averages over the entire trial. Points 1 and 2 will be addressed by analysing behavioural and EEG data using the same methods detailed in this thesis. Correlations in either the forces applied to the cylinder or in the cursor's movements could affect the synchronization measured between participants. The third point will be addressed by repeating the current analysis using overlapping windows and characterising the resulting networks' dynamics.

6.2   Applications

Understanding the temporal structures present in haptic communication between humans could help us implement the same algorithms to Human-Robot interfaces. Research has shown that people repeating a specific motor task benefit from being haptically linked to experts in that task [10, 31, 13]. Although these effects are only seen if the coupling is between two humans, it is possible that by maintaining the temporal structure of the haptic interactions, they could also be seen in human-robot interactions [81]. This new modality of interaction between humans and robots could also be applied to robots in the home. The increased attention that robots will have to the forces applied to it will allow them to be more compliant and less dangerous. I anticipate that developing this technology will allow humans to feel as comfortable and secure interacting with a robot as with a human.

6.3   Future Work

The paradigm developed for this thesis presents new ways of studying humans cooperating in a genuinely social setting. It opens up several new research areas that will significantly advance our understanding of how humans can use haptic signalling as a means of communication. Studying how the behavioural and neural markers identified in this thesis change as a function of social variables could reveal interesting interpersonal dynamics related to levels of friendship, sensitivity to haptic cues, or between same-sex and mixed sex pairs. Understanding these differences will help decode

the signalling behaviours that humans use to communicate via force-force interactions.

During the experiment, it was apparent that some participants found it difficult to apply enough pressure to the device. Typically, this was due to not wanting to appear too forceful with their partner. Although keeping these social dynamics was intentional, it would be beneficial to our understanding of the results to compare the current paradigm with others that address this issue. One possibility would be to record more than just one force vector for each participant. A device could be built that surrounds the finger and records both horizontal and vertical forces. These changes would make the device more comfortable to hold and provide more data about the participants' interactions. Future work also includes further analysis of data collected from the hyperscanning experiments. It will focus on understanding why paired participants show lower average synchronization than singles.

Appendix A

Appendix

A.1 EEG recording system

EEG data will be recorded using two 16 channel g.tec (g.tec medical engineering GmbH Austria) g.BSamp bio-signal amplifiers per participant. Every channel on both amplifiers had the same initial settings, which were specified using a set of DIP switches on the rear of the amplifier. Internal low pass filters were set to 0.1 kHz; notch filters at 60Hz were turned on to remove as much electrical noise before amplifying the signal, high pass filter was set to 0.5 Hz, and the sensitivity to 0.5 mV. The electrodes used during the experiment are g.tec g.LADYbird active electrodes which are connected to a g.EXTENSIONbox, one for each set of 16. This system greatly reduced the time needed to get channel impedances to a reasonable level and reduced the setup time in half.

During preliminary testing of the EEG system, it was discovered that due to the sensitive nature of the active electrodes used during the experiments,

special care needed to be taken to reduce the system's noise as much as possible. After extensive testing, it was determined that the two most crucial noise sources were a problem with the input and output impedances of the g.EXTENSIONbox and the g.BSamp, the second source of noise, were large ground loops in the system due to our attempts to ground all the equipment. Special cables sent from g.tec fixed the impedance issues, and battery packs will power the amplifiers and isolate them from any ground loops that could create more noise in the system.
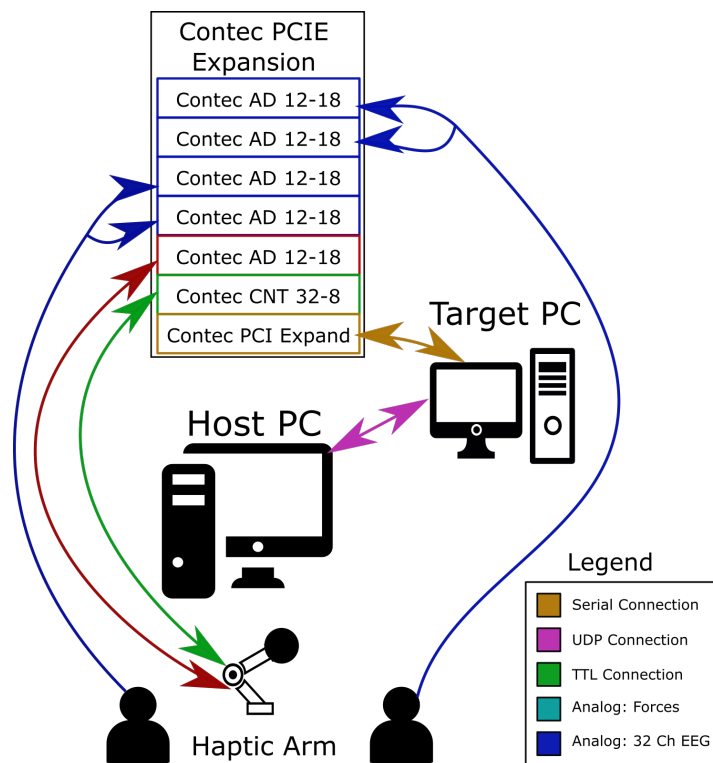
Figure A.1: Experimental set up used during hyperscanning. The set up for behavioural experiments excluded the analogue EEG connections but included all the others. All data was first sent to the Contec PCIe expansion board, where it was synchronized and timestamped. The host PC was able to access the data via a UDP connection and display the haptic arm's movement on the screen. The data that was to be analysed was kept on the target PC until the experiment's end.

Amplified signals are sent to a Contec PCI-E breakout box, which houses six Contec AD 12-16 (16 channel,12 bit) and one Contec Counter board CNT32-8. The PCIe breakout box is connected to a pc running XPC Target, which records the data and communicates with the host pc running the paradigm. This system allows for high precision, real-time co-registration of all the data streams being recorded during the experiment, ensuring that all the data is time-locked. Finally, all data is sent to the host pc using a UDP protocol. The system was connected, as shown in Fig.A.1. All data used during this analysis was collected and stored on the target computer while the experiment was running. This method had the advantage of removing distortion due to dropped packets.

A.2   Force Sensor Testing

The testing of the force/acceleration sensor system was done under the simplest possible conditions. The cylinder was disconnected from the haptic arm to ensure that the system's dynamics did not include the haptic arm. If it were not removed, unnecessary complexity would be introduced to the relationship between force and acceleration. Three different conditions were tested with the simplified system, up and down motions, side to side, and no movement. If the sensor system is working correctly, the net force's cross-correlation in the x direction will be strongly correlated at 0 lag with the acceleration in the x direction when moving side to side. Figure A.3, A.2 and A.4 show the results of the cross-correlation between $F_{Net} = F_L - F_R$ and acceleration for each test condition. We can see a higher average correlation when the movement is side to side, confirming

that the equipment is working correctly.
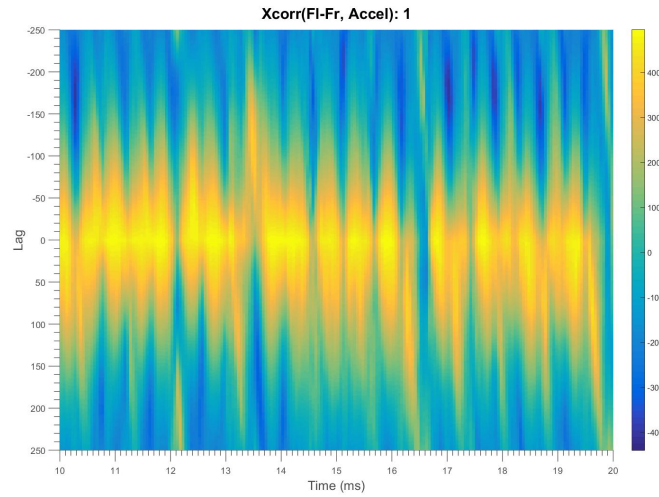
Figure A.2: Cross correlation of net force and acceleration when moving side to side along the x axis. Each time point is the cross correlation of a 1 second window. The colour corresponds to the cross correlation of net force and acceleration in that given time window for a specific lag.
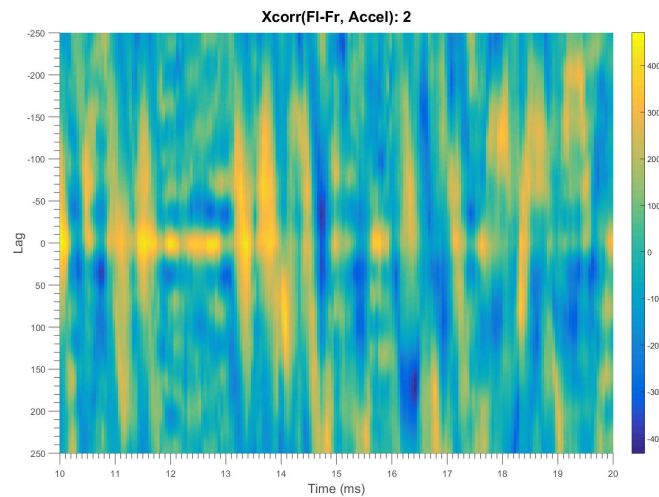
Figure A.3: Cross correlation of net force and acceleration when moving up and down. Each time point is the cross correlation of a 1 second window. The colour corresponds to the cross correlation of net force and acceleration in that given time window for a specific lag.
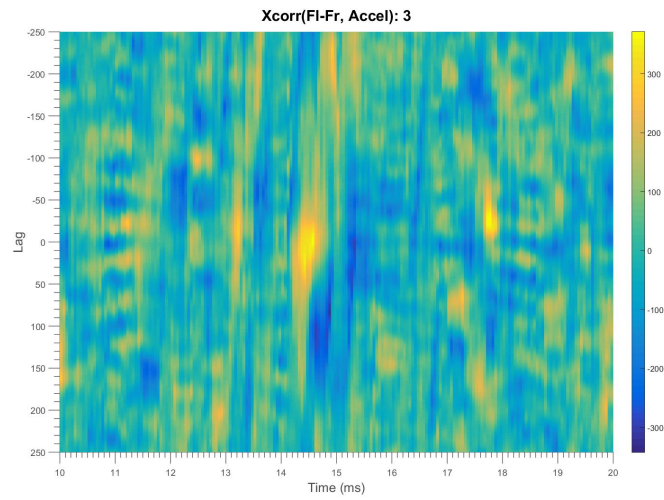
Figure A.4: Cross correlation of net force and acceleration when not moving. Each time point is the cross correlation of a 1 second window. The colour corresponds to the cross correlation of net force and acceleration in that given time window for a specific lag.

A.3   △ q Values
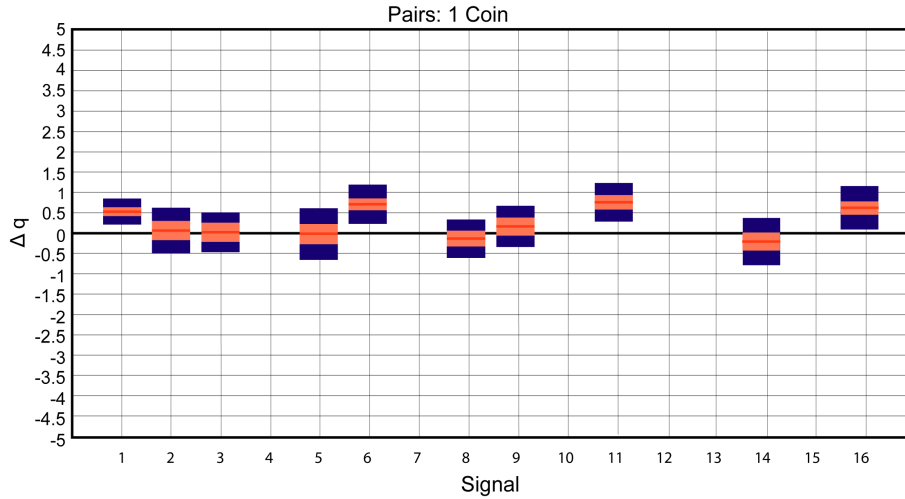
(a) Δq values for dyads.
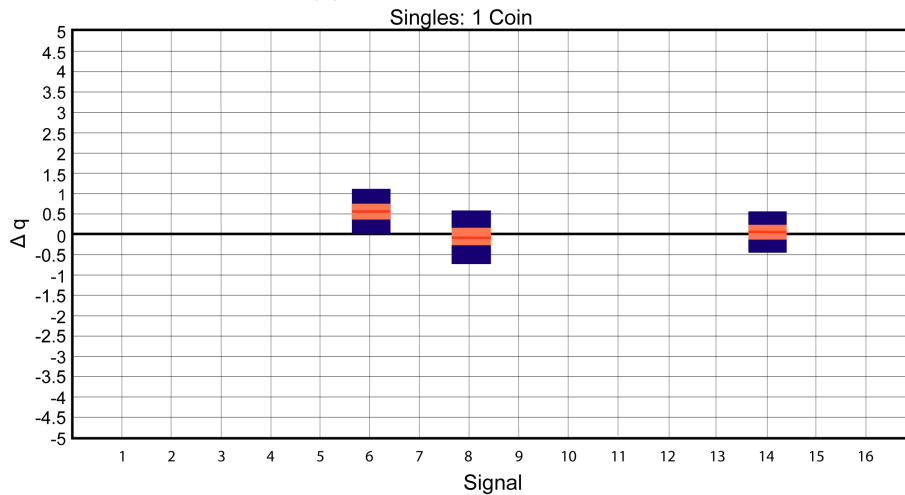
(b) Δq values for singles.

Figure A.5: Δq for all one coin trials and over all paired and single partici-
pants. The red line shows the average of all data for a particular signal. The
red outline shows the 95% confidence interval of the average value, and the
blue outline shows the standard deviation. Signals that appeared less than
5 trials over all participants have been removed. Although both paired
and single participants show temporal correlations which are longer and
shorter than a random distribution, only pairs have long-range correlations
in signals that include a receptive state (signals 1-5). Single participants
only show long-range correlations for signals where pressure is applied to
both sides of the device and where participants are only applying force on
Fa. It is important to note that only 30% of the identified haptic signals
have any long-range correlations in single participant experiments, while
80% have long-range correlations in paired participant experiments.
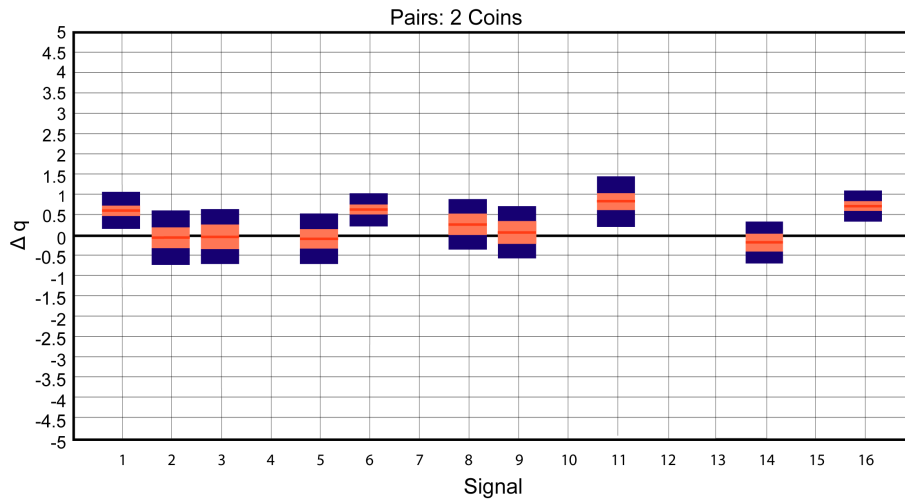
(a) Δq values for dyads.
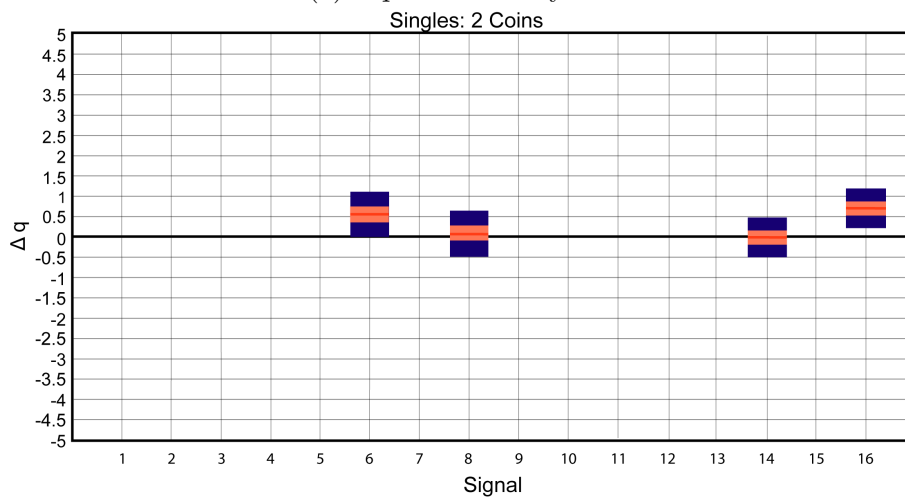
(b) Δq values for singles.

Figure A.6: Δq for all two coin trials and over all paired and single participants. The red line shows the average of all data for a particular signal. The red outline shows the 95% confidence interval of the average value, and the blue outline shows the standard deviation. Signals that appeared less than 5 trials over all participants have been removed. Although both paired and single participants show temporal correlations longer and shorter than a random distribution, only pairs have long-range correlations in signals, including a receptive state (signals 1-5). Single participants only show long-range correlations for signals where pressure is applied to both sides of the device and signal 6 where participants are only applying force on Fa. It is important to note that only 30% of the identified haptic signals have any long-range correlations in single participant experiments, while 80% have long-range correlations in paired participant experiments.
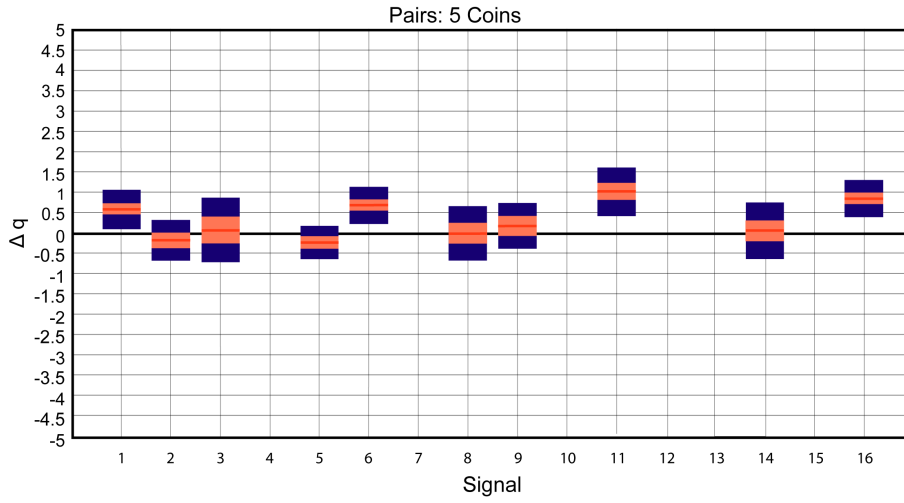
(a) Δq values for dyads.
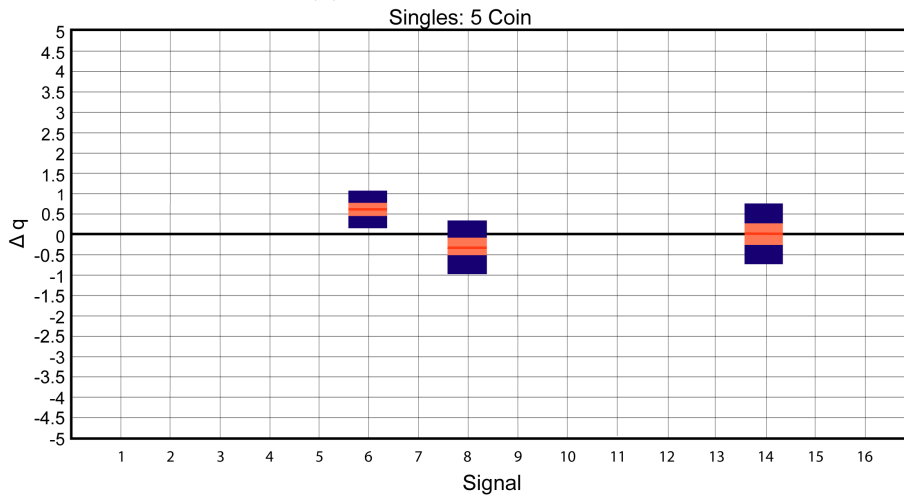
(b) Δq values for singles.

Figure A.7: Δq for all five coin trials and over all paired and single partic-
ipants. The red line shows the average of all data for a particular signal.
The red outline shows the 95% confidence interval of the average value,
and the blue outline shows the standard deviation. Signals that appeared
less than 5 trials over all participants have been removed. Although both
paired and single participants show temporal correlations that are longer
and shorter than a random distribution, only pairs have long-range correla-
tions in signals, including a receptive state (signals 1-5). Single participants
only show long-range correlations for signals where pressure is applied to
both sides of the device and signal 6 where participants are only applying
force on Fa. It is important to note that only 30% of the identified haptic
signals have any long-range correlations in single participant experiments,
while 80% have long-range correlations in paired participant experiments.

A.4 EEG System Testing

A.4.1 Introduction

During testing of the EEG equipment, we identified two main noise sources that could have negative effects on the data recorded with this system. The following section will outline the three sources of noise identified, how the system was tested, and any implemented solutions.

A.4.2 Active Electrode Testing

To find faulty electrodes, we connected the ground, reference, and test electrodes to the amplifier. All other channels were left with nothing connected. The three electrodes were placed in a plastic cup with a solution of water and non-abrasive electrolytic gel. One second of data was recorded from each electrode and visually inspected. This procedure was completed for 70 electrodes by replacing the test electrode and maintaining the other two. Of 70 electrodes, we identified 4 faulty ones that were replaced by the manufacturer.

Figs A.9 and A.8 show examples of a working and a faulty electrode. Faulty electrodes show a characteristic sharp increase in voltage and a subsequent overshoot in the opposite direction. When looking at recordings from working electrodes, there is a constant environmental noise of +/- 2 mV with no larger peaks.
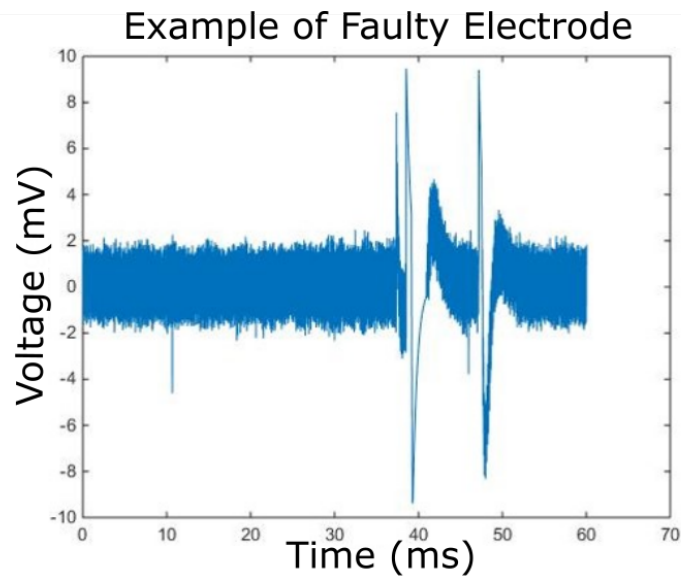
Figure A.8: Example of a recording made from a faulty electrode. The test electrode was submerged in a solution of water and non-abrasive electrolytic get and all electrical equipment was kept as far as possible.
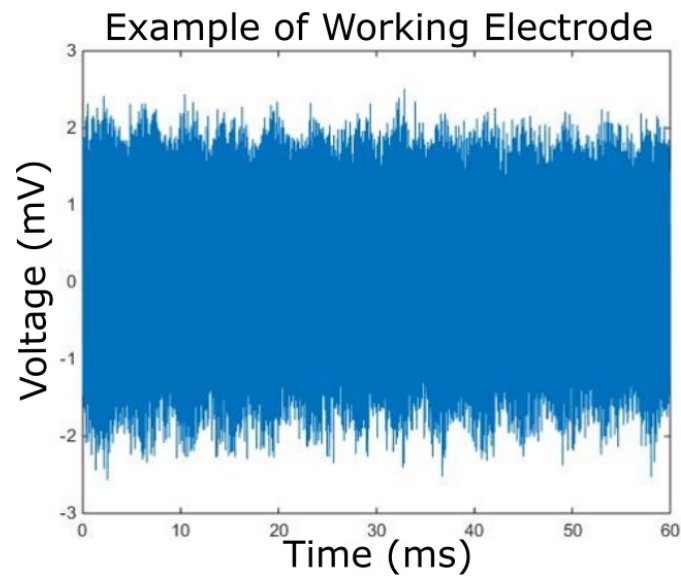
Figure A.9: Example of a recording made from a working electrode. The test electrode was submerged in a solution of water and non-abrasive electrolytic get and all electrical equipment was kept as far as possible.

A.4.3 Data Acquisition System Testing

Testing of the data acquisition system(DAQ) was done by introducing a sine wave into the system at different points. To test the entire system, including the amplifiers, a sine wave function generator, supplied by gTech, was used as an input for the gTech amplifiers. To test the digital recording and storage of the data, the analogue amplifier and A/D converter were removed from the system, and a digital function generator, implemented in SIMULINK, was used. four different conditions were tested:

1. The test signal was generated using an analogue sine wave signal generator manufactured by gTech. To record the signal, we used gTech BsAmps and a SIMULINK host/target PC system. The data was collected using the Target PC and streamed in real-time to the Host PC for storage and processing using the UDP protocol.

2. The test signal was generated using a digital sine wave signal generator implemented in SIMULINK. The signal was sent to the target PC and recorded in the same manner as the analogue signal. The only difference here is the absence of an analogue amplifier. The recorded data was again streamed in real-time to the host PC using the UDP protocol.

3. This test used a digital signal and only the SIMULINK system to record it. The data was stored in the target PC during the test and only recovered once the experiment was over.

4. The test signal was generated and recorded using the analogue system. It was stored in the target PC and recovered only at the end of

the experiment.

Results in Fig. A.10 show that using the UDP transfer protocol to stream the data to the host PC distorted the sine wave in all cases. This distortion occurred due to the nature of the UDP protocol. The UDP protocol has no means of error correction. If it encounters a corrupt package or a problem at the transmitter, it will simply repeat the previously sent packet. This repetition causes SIMULINK to receive the previous value and create a stepped distortion in the sine wave. This issue can be easily solved by storing a copy of the data on the target PC and using this copy when doing subsequent analysis.
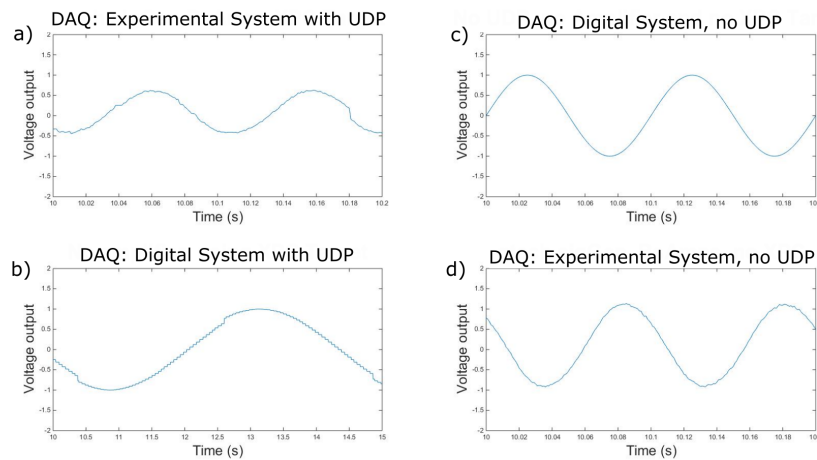
Figure A.10: a) The signal source used during this test was the gTech signal generator. The data acquisition system was a gTech BsAmp and a SIMULINK target/host system. Data was collected by the target PC and streamed to the host PC via an ethernet cable using a UDP protocol. b) The signal source used during this test was the SIMULINK digital signal generator. The data acquisition system was only the SIMULINK target/host system. Data was collected by the target PC and streamed to the host PC via an ethernet cable using a UDP protocol. c) The signal source used during this test was the gTech signal generator. The data acquisition system was a gTech BsAmp and a SIMULINK target/host system. Data was collected on the target PC and recovered once the experiments were done. d) The signal source used during this test was the SIMULINK digital signal generator. The data acquisition system was only the SIMULINK target/host system. Data was collected on the target PC and recovered once the experiments were done.

A.4.4 Complex Networks

Baseline Pairs

The following graphs show the average adjacency matrices over all participants for baseline pairs. They were calculated using the procedure outlined in Fig. 5.5.
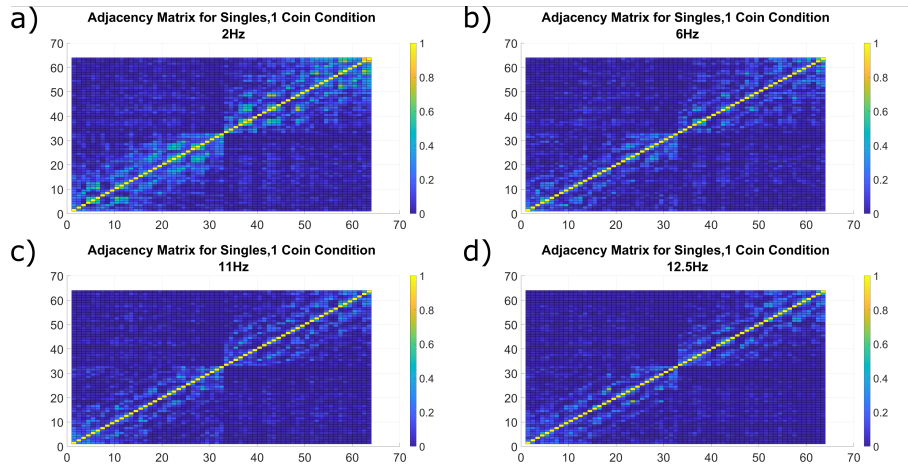
Figure A.11: Average weighted adjacency matrices for all baseline pairs in the one coin condition. Each sub figure shows the matrix for a particular frequency band whose central frequencies are a)2Hz, b)6Hz, c)11Hz, d)12.5Hz +/- 2Hz. The yellow range of the scale is equal to a circular correlation of 1
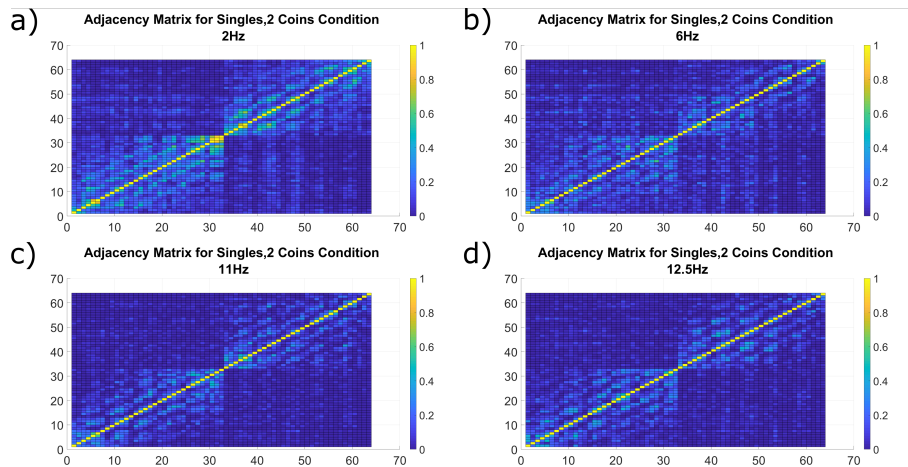
Figure A.12: Average weighted adjacency matrices for all baseline pairs in the two coin condition. Each sub figure shows the matrix for a particular frequency band whose central frequencies are a)2Hz, b)6Hz, c)11Hz, d)12.5Hz +/- 2Hz. The yellow range of the scale is equal to a circular correlation of 1
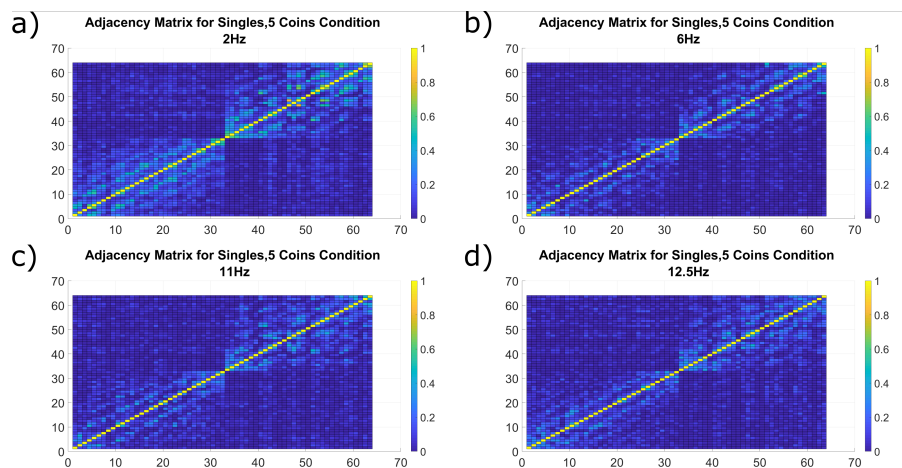
Figure A.13: Average weighted adjacency matrices for all baseline pairs in the five coin condition. Each sub figure shows the matrix for a particular frequency band whose central frequencies are a)2Hz, b)6Hz, c)11Hz, d)12.5Hz +/- 2Hz. The yellow range of the scale is equal to a circular correlation of 1
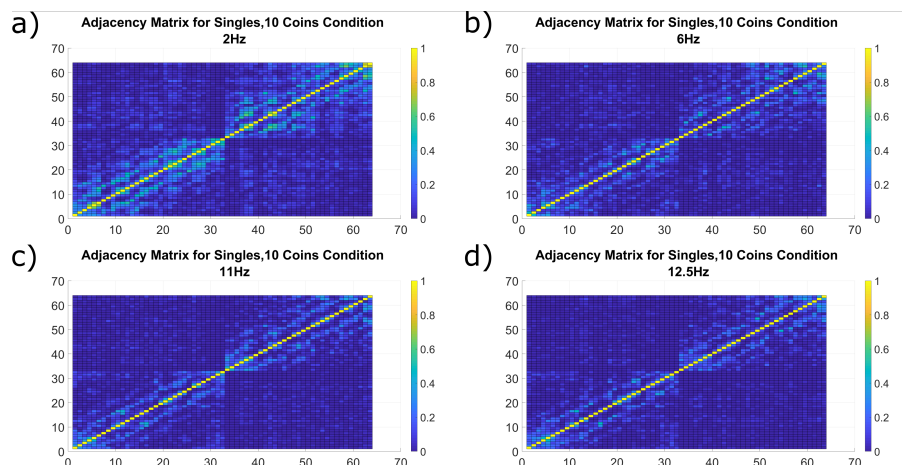
Figure A.14: Average weighted adjacency matrices for all baseline pairs in the ten coin condition. Each sub figure shows the matrix for a particular frequency band whose central frequencies are a)2Hz, b)6Hz, c)11Hz, d)12.5Hz +/- 2Hz. The yellow range of the scale is equal to a circular correlation of 1

Paired Participants

Average adjacency matrices over all participants for pairs.
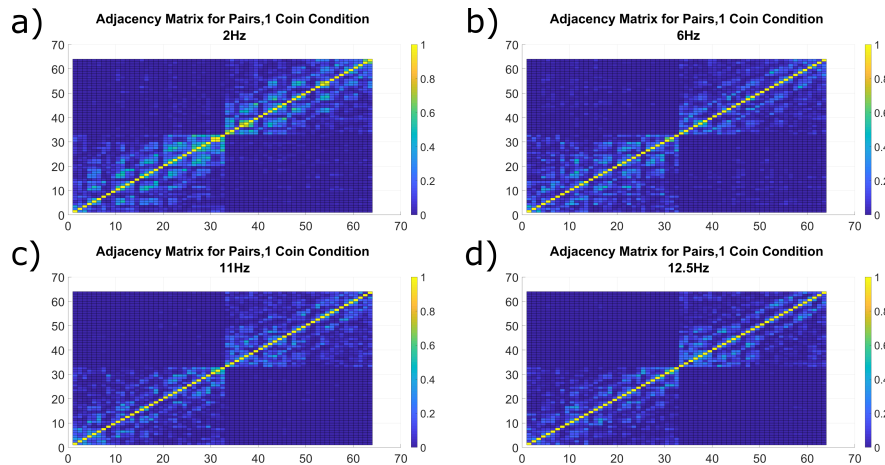
Figure A.15: Average weighted adjacency matrices for all paired participants in the one coin condition. Each sub figure shows the matrix for a particular frequency band whose central frequencies are a)2Hz, b)6Hz, c)11Hz, d)12.5Hz +/- 2Hz. The yellow range of the scale is equal to a circular correlation of 1
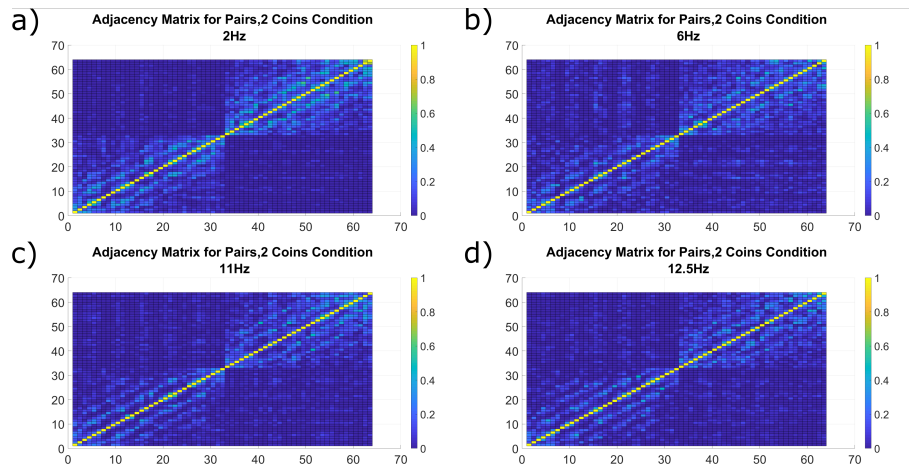
Figure A.16: Average weighted adjacency matrices for all paired participants in the two coin condition. Each sub figure shows the matrix for a particular frequency band whose central frequencies are a)2Hz, b)6Hz, c)11Hz, d)12.5Hz +/- 2Hz. The yellow range of the scale is equal to a circular correlation of 1
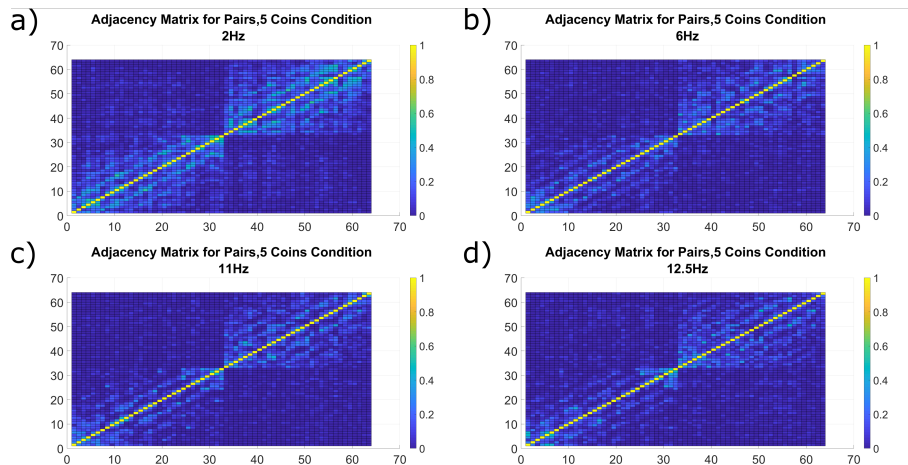
Figure A.17: Average weighted adjacency matrices for all paired participants in the five coin condition. Each sub figure shows the matrix for a particular frequency band whose central frequencies are a)2Hz, b)6Hz, c)11Hz, d)12.5Hz +/- 2Hz. The yellow range of the scale is equal to a circular correlation of 1
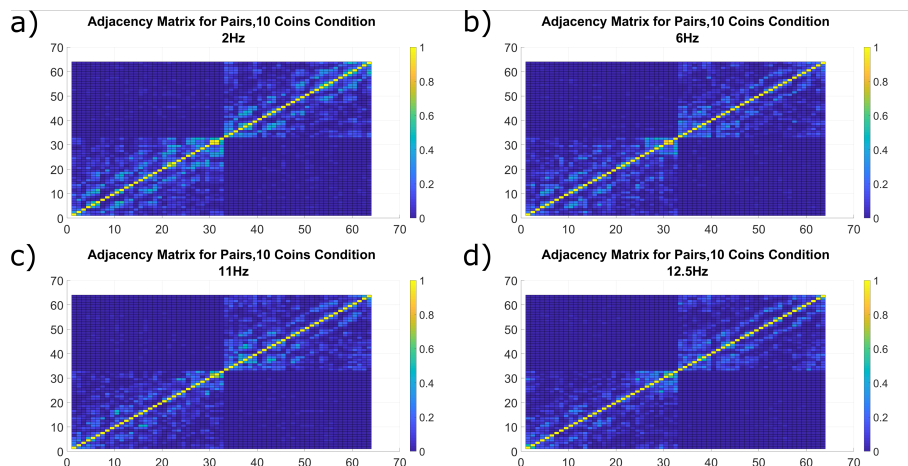
Figure A.18: Average weighted adjacency matrices for all paired participants in the ten coin condition. Each sub figure shows the matrix for a particular frequency band whose central frequencies are a)2Hz, b)6Hz, c)11Hz, d)12.5Hz +/- 2Hz. The yellow range of the scale is equal to a circular correlation of 1

A.5   Ethical Approval

A.5.1   behavioural Experiments

Ethical approval for the behavioural experiments was given by the School of Systems Engineering of the University of Reading. Unfortunately, the original documentation regarding the ethical approval of this experiment have been lost.

A.5.2   EEG Experiments

Ethical approval for the EEG experiments was given by the School of Psychology and Clinical Language Sciences of the University of Reading. The following is a copy of the accepted ethical request form.

University of **Reading**

SECTION 1: APPLICATION DETAILS

1.1   Project and Dates

Project title: Neural correlates of haptic signalling in a cooperative task.

Date of submission: 27-04-2018   Start date: 04-05-2018   End date: 04-10-2018

1.2   Applicant Details

Principal Investigator

Name:	Dr Juliane Honisch	Position:	Academic Staff
Institution/Department:	Psychology	Email:	j.j.honisch@reading.ac.uk
Office room number:	253	Telephone:	

(Please note that an undergraduate or postgraduate student cannot be a named principal investigator for research ethics purposes. The supervisor must be declared as Principal Investigator)

Other Applicants

Name	Institution/Department	Position	Email
Nicolas Thorne	School of Bio Sciences	PHD Student	N.A.ThorneTerry@pgr.reading.ac.uk

Right-click to insert more rows as needed.

1.3   Project Submission Declaration

On behalf of my co-applicants and myself,

- I confirm that to the best of my knowledge I have made known all information relevant to the Research Ethics Committee and I undertake to inform the Committee of any such information which subsequently becomes available whether before or after the research has begun
- I understand that it is a legal requirement that both staff and students undergo Disclosure and Barring Service checks when in a position of trust (i.e. when working with children or vulnerable adults)
- I confirm that if this project is an interventional study, a list of names and contact details of the participants in this project will be compiled and that this, together with a copy of the Consent Form, will be retained within the School for a minimum of five years after the date that the project is completed

10/05/2018

(Signed, Principal Investigator)   *Date*

1.4   University Research Ethics Committee Applications

Projects expected to require review by the University Research Ethics Committee (such as, for example, research involving NHS patients, research involving potential for distress to participants) must be reviewed by the Chair of the School Ethics Committee or the Head of School before submission. Please ask PCLSethics@reading.ac.uk if unsure whether your project needs UREC approval.

11-Jun-2018

(Signed, Chair of School Research Ethics Committee)   *Date*

dd-mmm-yyyy

(Signed, Head of School)   *Date*

1.5   External Research Ethics Committees

Please provide details below of other external research ethics committees to which this project has been submitted, or from whom approval has already been granted (e.g. NHS Committee)

Name of committee	Date of submission/approval	Reference	Status
	dd-mmm-yyyy		

University of
Reading

SECTION 2:   PROJECT DETAILS

2.1   Lay Summary

Please provide a summary of the project in non-specialist terms, which includes a description of the scientific background to the study (existing knowledge), the scientific questions the project will address and a justification of these. Please note that the description must be sufficient for the committee to take a reasonable view on the likely scientific rigour and value of the project.

The ability for humans to coordinate together is the corner stone of many of our daily activities [1], it has been studied in psychology as joint action which has been defined as any activity where two or more actors coordinate their actions in real time in order to successfully complete a task. In order to carry out a joint task as a group it is important to understand where our partners are focusing their attention to. Studies on children 12-18 months old have shown that the ability to cooperate pre-dates the full development of a child's theory of mind and lays the foundation for our ability to understand our partner's goals. Studies have shown that watching the actions of others activates a representation in the observer's action neural system [2, 3]. This representation enables the understanding and prediction [4, 5] of observed actions. Another important source of information about another's actions is obtained by forming a shared representation of the task at hand [6]. With this representation, dyads are able to know what actions will be performed. Studies looking at EEG activity in motor areas have found that although a partner's actions where hidden [7] the observer was still able to anticipate their partner's movements. The last piece of the joint action puzzle is to understand what our own abilities are and how they are affected by the abilities of our interacting partners[8].

This experiment is an extension to a previous work as part of my PhD. Here I will investigate the behavioural mechanisms at play when pairs of participants are asked to coordinate their movements together to accomplish a joint action task. Participants will be asked to participate in a simple coin collecting computer game using a plastic cylinder mounted at the tip of a Phantom Haptic Arm as the interface. The experiment will be divided in two parts each taking place on separate days, the first one will involve one participant as a control experiment and the second one will use pairs of participants. During both experimental session EEG recordings will be taken as a mean of examining the emergence of synchronised brain signals during each trial. These signals will be correlated with the pairs' task performance.

References:

1 N. Sebanz, H. Bekkering, and G. Knoblich. Joint action: bodies and minds moving together. Trends in cognitive sciences, 10(2):70–76, 2006
2. Grezes, J. L. Armony, J. Rowe, and R. E. Passingham. Activations related to "mirror" and "canonical" neurones in the human brain: an fmri study. Neuroimage, 18(4):928–937, 2003.
3. G. Rizzolatti and L. Craighero. The mirror-neuron system. Annu. Rev. Neurosci., 27:169–192, 2004.
4. M. Wilson and G. Knoblich. The case for motor involvement in perceiving conspecifics. Psychological bulletin, 131(3):460, 2005.
5. J. M. Kilner, C. Vargas, S. Duval, S.-J. Blakemore, and A. Sirigu. Motor activation prior to observation of a predicted movement. Nature neuroscience, 7(12):1299, 2004.
6. P. Cisek and J. F. Kalaska. Neural correlates of mental rehearsal in dorsal premotor cortex. Nature, 431(7011):993, 2004.
7. N. Ramnani and R. C. Miall. A system in the human brain for predicting the actions of others. Nature neuroscience, 7(1):85–90, 2004.
8. K. L. Marsh, M. J. Richardson, R. M. Baron, and R. Schmidt. Contrasting approaches to perceiving and acting with others. Ecological Psychology, 18(1):1–38, 2006.

2.2   Procedure

Please briefly describe what the study will involve for your participants and the instruments and methodology to be undertaken.

The experiment will be split into two separate sessions. In the first session participants will complete an experimental task on their own whereas in the second session participants will complete this task with a randomly allocated partner (another participant).

The project will constitute of an EEG experiments on healthy adults without any motor impairments. During both experimental sessions 32 non-invasive gel based electroencephalography (EEG) electrodes will be placed on the participant's scalp to record EEG related to social cooperation between pairs. Participants will be asked to play a simple target reaching task on the computer. The peripheral device used to play the game

University of **Reading**

is a phantom haptic arm with a 3d printed cylinder attached to the end. The haptic arm is only used to record the position and no feedback is being given. Each participant uses their index finger to apply pressure on the circular end of the cylinder and coordinate their movements to successfully lift the device off the table and moved in a 2d plane in front of the computer screen. The cylinder is fitted with force sensors on either circular end of the cylinder and an accelerometer at the centre. In the second session, participants will be seated side by side holding the device with the index finger of their dominant hand. Participants will be asked to refrain from discussing the experiment until the end.

Four different conditions will be tested during each experimental session, corresponding to a different number of targets on the screen, one target, two targets, five targets and ten targets. Each condition is repeated ten times and the succession of conditions is chosen at random. In total, each experiment consists of 40 trials lasting 40 seconds each. One minute rest periods are given after every ten trials and 5 second rests are given after each individual trial.

At the start of the experiment both singles and paired participants will be given consent and information forms to fill in Paired participants will also be asked to fill in a questionnaire aimed at understanding each participant's impressions of the turn taking behaviours and communication during the experiment at the end of their second session. In total the duration, including the time necessary to prepare each participant for EEG, will be 2:30 hours for pairs and 2:00 hours for singles. During the course of the experiment we will be collecting data from 15 pairs and 30 singles.

The research and experiments will be conducted by 3rd year PhD student Nicolas Thorne, who is supervised by Dr Juliane Honisch , Dr Yoshikatsu Hayashi, and Prof Slawomir Nasuto, Biomedical Engineering Section.

2.3 Location

Where will the project take place? The EEG experiment will take place in the Brain Embodiment Lab (BEL) EEG recording room located in G60, Polly Vacher building. The EEG recording rooms are well equipped for performing EEG based experiments with human participants and have passed the health, safety and risk analysis. Due precautions will be taken for the safety of the participants as well as the researchers such as – securing the connector cables to avoid tripping, measuring head size to avoid any discomfort while putting the EEG cap on participant, making sure there is comfortable seating for the participant, the ambient lighting is proper, monitors are kept at safe distance to avoid stress on eyes. Sufficient breaks will be given to the participants. There are no major risks associated with the experiment. The experiment operator will be present with the participant at all times.

If the project is to take place in schools, please confirm that you have informed the SREC (*PCLSethics@reading.ac.uk*):   no

If you plan to do home visits for the data collection, you need to perform a risk assessment and provide information about what safety measures you will take: Click here to enter text.

2.4 Funding

Is the research supported by funding from a research council or other external sources (e.g. charities, business)?   no

If "Yes":   (a)   please give details of the funding body:
                    Click here to enter text.
            (b)   does your funder stipulate review by UREC (see note below)?
                    no

Some Research Councils or other external funding sources may require that the project is reviewed by the University Research Ethics Committee. If this is the case, then the project should be submitted to UREC. This does not apply to postgraduate activity funded by Research Councils.

2.5 Ethical Issues

Could this research lead to any risk of harm or distress to the participants? Please explain why this is necessary and how any risk will be managed.

There are no ethical issues, apart from matters related to data storage, usage and confidentiality – these are discussed in Sections 2.8 and 2.9.

2.6 Deception

Will the research involve any element of intentional deception at any stage (i.e. providing false or misleading information about the study)?   no

If "Yes", please justify why: Click here to enter text.

University of Reading

Please note you must append a description of the debriefing procedure if the study involves deception.

2.7   Payment

Will you be paying your participants for their involvement in the study?   yes

If "Yes", please justify the amount paid: Participants will receive either 1.5 university credits for each part of the experiment or 5 pounds an hour in appreciation of their time. The payment is purely to encourage students to take part due to the time it takes to set up and do the experiment.

Please note that excessive payment may be considered coercive and therefore unethical. Travel expenses need not to be declared.

2.8   Data Protection, Confidentiality, Disposal of Data

What steps will be taken to ensure participant confidentiality? How will the data be stored? When will the data be destroyed?

Data collected in this experiment is of two categories- 1) Digital: EEG, Kinematic and Haptic data. 2) Hard copy: questionnaire.

1) Digital data storage and confidentiality

EEG data: The EEG data recorded from the experiment will be anonymised. Each participant will be assigned an anonymous user ID, and all electronic data from the study will be stored, processed, and reported using this anonymous user ID. This dataset will be stored on a secure shared drive for BEL located on the internal University server, accessible to members of the research team now and in the future. This internal server is managed by central IT and access is available only to the BEL researchers approved for access. Participants cannot be identified by their EEG data which is purely numeric in nature. There is no confidential information in EEG data.

These anonymised data will be stored indefinitely. The data may also be made publicly available via a research data repository, where this is a requirement for a journal, for example.

Kinematic and Haptic data: Kinematic and haptic data will be stored using the anonymous user ID. The files will be stored in the secure shared BEL drive detailed above indefinitely, accessible to members of the research team.

Information linking the participant's identity with their research data will NOT be stored on the shared BEL drive (see next section about storage of the consent forms).

   2) Hard copy of questionnaire:

Questionnaire: Questionnaire asks for age, gender and handedness of the participants along with the confirmation that they have normal/corrected to normal vision, no motor or communication impairments and no medications affecting brain chemistry. The questionnaire is also targeted at determining the level of cooperation and non-verbal communication between participants. The aggregate of this information is required for publishing the scientific results of this study. Questionnaire itself will not be shared with anybody. Questionnaires will be anonymised with the unique identifier of the participant just like EEG data. Questionnaires will be stored securely in BEL in a locked cabinet dedicated for this purpose, separate from the cabinet for consent forms.

Please note that consent forms have to be kept for 5 years after the end of the study. There is no requirement for data, such as paper questionnaires, to be kept for 5 years.

2.9   Consent

Please describe the process by which participants will be informed about the nature of the study and the process by which you will obtain consent.

Written information sheet outlining the experiment procedure will be presented to the participant. Experiment would be explained to the participant by the researcher and then the written consent would be obtained from the participants by completing the consent form at the beginning of the experiment. Participants reserve the right to withdraw from the experiment at any time without giving any reason.

The consent form is the only document that will contain the participant's name. Signed consent forms will be stored securely in the locked cabinet storage facility in BEL dedicated for this purpose. All data will be stored anonymously. Consent forms will not be shared with third parties.

The consent forms will be stored for 5 years after completion of the PhD, and then destroyed securely.

Please note that a copy of consent forms and information letters for all participants must be appended to this application.

University of Reading

SECTION 3: PARTICIPANT DETAILS

3.1 Sample Size

How many participants do you plan to recruit? Please provide a brief justification for this number.

Target sample size of the participants in this EEG experiment is 30 and 400 EEG trials will be recorded from each participant. This was selected to get statistically significant results. Similar sample size is used in EEG BCI research on healthy humans according to the literature review. Sample size of EEG was calculated using the following formula for 95% confidence level and 5% confidence interval:

Sample size = ((z-score *SD*(1-SD))/error margin)2

Where, z-score for 95% confidence level is 1.96, standard deviation is unknown and hence considered as 0.5 and the error margin is ±5%. This gives the sample size of 384.16 which was rounded off to 400 EEG trials per person to account for noisy trials.

3.2 Sample Characterisation

Will the research involve children or vulnerable adults (e.g. with mental health or neurological conditions)?   no

If "Yes", how will you ensure these participants fully understand the study and the nature of their involvement in it and freely consent to participate?

Click here to enter text.

Please append letters and, if relevant, consent forms, for parents, guardians or carers. Please note: information letters must be supplied for all participants wherever possible, including children. Written consent should be obtained from children wherever possible in addition to that required from parents.

3.3 Sample Age

Will your research involve children under the age of 18 years?   no

Will your research involve children under the age of 5 years?   no

3.4 NHS and Social Services Involvement

Will your research involve NHS patients or clients of Social Services?   no

Please note that if your research involves NHS patients or Clients of Social Services your application will have to be reviewed by the University Research Ethics Committee and by an NHS research ethics committee.

3.5 Recruitment

Please describe the recruitment process and append any public advertising if used.

Participant recruitment will be done by advertising using emails and poster.

University of **Reading**

University of Reading

Brain Embodiment Laboratory

Participants needed for
EEG experiment in social cooperation

As a participant you would be asked to take part in an EEG
experiment where you will play a simple coin
collection game on the computer. Your participation
will involve two sessions (one alone and one
with a partner),each session will be aproximately 2 hours.

You will recieve **£10** for each session
in appreciation for your time

For more information or to volunteer for this
study **please contact Nicolas Thorne** :
N.A.ThorneTerry@pgr.reading.ac.uk

Advertisements on the Research Panel do not need to be appended.

University of Reading

IMPORTANT NOTES

1. *The Principal Investigator must complete the Checklist below to ensure that all the relevant steps have been taken and all the appropriate documentation has been appended*

2. *If you expect that your application will need to be reviewed by the University Research Ethics Committee you must also complete the* <u>*Project Submission Form*</u>

3. *For template consent forms and information sheets see the document "example consent forms and information letters"*

4. *If the research is being carried out by undergraduates for their Final Year project, a special consent form must be used. This is shown in the "example consent forms and information letters" document*

CHECKLIST

This form <u>must</u> be completed by the Principal Investigator.
This form should be used if you submit your application to the School Research Ethics Committee
Please tick to confirm that the following information has been included and is correct. Indicate (N/A) if not applicable:

Information Sheet

Is on headed notepaper and the information in the header is up-to-date	Yes
Includes Investigator's name and email / telephone number	Yes
Includes Supervisor's name and email / telephone number	Yes
Does not include student mobile phones / personal e-mails	Yes
Includes the title of the study	Yes
Includes the aims of the study	Yes
Includes information about what the participants will be asked to do	Yes
Statement that participation is voluntary	Yes
Statement that participants are free to withdraw their co-operation	Yes
Reference to the ethical process using the sentence: *'This application has been reviewed by the University Research Ethics Committee and has been given a favourable ethical opinion for conduct.'*	Yes
Reference to Disclosure using the following sentence: *'All investigators on this project have had criminal records checks and have been approved by the School to work with children.'*	Yes
Reference to confidentiality, storage and disposal of personal information collected. Note, consent forms have to be kept for 5 years	

Consent Form(s)

Please note that if researchers are undergraduates, you must use the "Undergraduate Project Consent Form" in Blackboard, and include researcher names	N/A

Other Relevant Material

Questionnaires	Yes
Interviews	N/A
Letters	N/A
Other (please specify)	N/A
Click here to enter text.	
Expected duration of the project (months)	Yes

PRINCIPAL INVESTIGATOR
Name: Dr Juliane Honisch

10/05/2018

_____   _____
(Signed, Principal Investigator)   *Date*

Bibliography

[1] Hayashi, Y. & Kondo, T. Mechanism for synchronized motion between two humans in mutual tapping experiments: Transition from alternative mode to synchronization mode. *Physical Review E* **88**, 022715 (2013).

[2] Hayashi, Y. & Sawada, Y. Transition from an antiphase error-correction mode to a synchronization mode in mutual hand tracking. *Physical Review E* **88**, 022704 (2013).

[3] Wing, A. M., Endo, S., Bradbury, A. & Vorberg, D. Optimal feedback correction in string quartet synchronization. *Journal of The Royal Society Interface* **11**, 20131125 (2014).

[4] Codrons, E., Bernardi, N. F., Vandoni, M. & Bernardi, L. Spontaneous group synchronization of movements and respiratory rhythms. *PLoS One* **9**, e107538 (2014).

[5] Van Dijk, J., Kerkhofs, R., Van Rooij, I. & Haselager, P. Special section: Can there be such a thing as embodied embedded cognitive neuroscience? *Theory & Psychology* **18**, 297–316 (2008).

[6] J. Varela, F., Thompson, E. & Rosch, E. *The embodied mind : cognitive science and human experience* (book, 2018).

[7] Auvray, M. & Rohde, M. Perceptual crossing: the simplest online paradigm. *Frontiers in human neuroscience* **6**, 181 (2012).

[8] Froese, T., Iizuka, H. & Ikegami, T. Embodied social interaction constitutes social cognition in pairs of humans: a minimalist virtual reality experiment. *Scientific reports* **4**, 3672 (2014).

[9] van der Wel, R. P., Knoblich, G. & Sebanz, N. Let the force be with us: dyads exploit haptic coupling for coordination. *Journal of Experimental Psychology: Human Perception and Performance* **37**, 1420 (2011).

[10] Ganesh, G. *et al.* Two is better than one: Physical interactions improve motor performance in humans. *Scientific reports* **4** (2014).

[11] Míreles, E. J. A., De Santis, D., Morasso, P. & Zenzeri, J. Transferring knowledge during dyadic interaction: The role of the expert in the learning process. In *Engineering in Medicine and Biology Society (EMBC), 2016 IEEE 38th Annual International Conference of the*, 2149–2152 (IEEE, 2016).

[12] Mireles, E. J. A., Zenzeri, J., Squeri, V., Morasso, P. & De Santis, D. Skill learning and skill transfer mediated by cooperative haptic interaction. *IEEE Transactions on Neural Systems and Rehabilitation Engineering* **25**, 832–843 (2017).

[13] Galofaro, E., Morasso, P. & Zenzeri, J. Improving motor skill transfer during dyadic robot training through the modulation of the expert

role. In *Rehabilitation Robotics (ICORR), 2017 International Conference on*, 78–83 (IEEE, 2017).

[14] Sebanz, N., Bekkering, H. & Knoblich, G. Joint action: bodies and minds moving together. *Trends in cognitive sciences* **10**, 70–76 (2006).

[15] Varela, F., Lachaux, J.-P., Rodriguez, E. & Martinerie, J. The brainweb: phase synchronization and large-scale integration. *Nature reviews neuroscience* **2**, 229 (2001).

[16] Burgess, A. P. On the interpretation of synchronization in eeg hyperscanning studies: a cautionary note. *Frontiers in human neuroscience* **7**, 881 (2013).

[17] Haken, H. Synergetics. *Physics Bulletin* **28**, 412 (1977).

[18] Haken, H., Kelso, J. S. & Bunz, H. A theoretical model of phase transitions in human hand movements. *Biological cybernetics* **51**, 347–356 (1985).

[19] Engström, D. A., Kelso, J. S. & Holroyd, T. Reaction-anticipation transitions in human perception-action patterns. *Human movement science* **15**, 809–832 (1996).

[20] Hayashi, Y., Tamura, Y., Sase, K., Sugawara, K. & Sawada, Y. Intermittently-visual tracking experiments reveal the roles of error-correction and predictive mechanisms in the human visual-motor control system. *Transactions of The Society of Instrument and Control Engineers* **46**, 391–400 (2010).

[21] Shockley, K., Santana, M.-V. & Fowler, C. A. Mutual interpersonal postural constraints are involved in cooperative conversation. *Journal*

of Experimental Psychology: Human Perception and Performance **29**, 326 (2003).

[22] Frischen, A. & Tipper, S. P. Orienting attention via observed gaze shift evokes longer term inhibitory effects: implications for social interactions, attention, and memory. *Journal of Experimental Psychology: General* **133**, 516 (2004).

[23] Bayliss, A. P. & Tipper, S. P. Gaze and arrow cueing of attention reveals individual differences along the autism spectrum as a function of target context. *British Journal of Psychology* **96**, 95–114 (2005).

[24] Richardson, M. J., Marsh, K. L. & Baron, R. M. Judging and actualizing intrapersonal and interpersonal affordances. *Journal of experimental psychology: Human Perception and Performance* **33**, 845 (2007).

[25] Ikegami, T. & Ganesh, G. Shared mechanisms in the estimation of self-generated actions and the prediction of other's actions by humans. *Eneuro* **4** (2017).

[26] Sänger, J., Müller, V. & Lindenberger, U. Intra-and interbrain synchronization and network properties when playing guitar in duets. *Frontiers in human neuroscience* **6** (2012).

[27] Masumoto, J. & Inui, N. Bidirectional transfer between joint and individual actions in a task of discrete force production. *Experimental brain research* **235**, 2259–2265 (2017).

[28] Sallnäs, E.-L., Rassmus-Gröhn, K. & Sjöström, C. Supporting presence in collaborative environments by haptic force feedback. *ACM*

Transactions on Computer-Human Interaction (TOCHI) **7**, 461–476 (2000).

[29] Basdogan, C., Ho, C.-H., Srinivasan, M. A. & Slater, M. An experimental study on the role of touch in shared virtual environments. *ACM Transactions on Computer-Human Interaction (TOCHI)* **7**, 443–460 (2000).

[30] De Santis, D., Zenzeri, J., Masia, L., Squeri, V. & Morasso, P. Human-human physical interaction in the joint control of an underactuated virtual object. In *2014 36th Annual International Conference of the IEEE Engineering in Medicine and Biology Society*, 4407–4410 (IEEE, 2014).

[31] Wahn, B., Karlinsky, A., Schmitz, L. & König, P. Let's move it together: A review of group benefits in joint object control. *Frontiers in psychology* **9** (2018).

[32] Galantucci, B. An experimental study of the emergence of human communication systems. *Cognitive science* **29**, 737–767 (2005).

[33] Uno, R., Suzuki, K. & Ikegami, T. An interactive wall game as an evolution of proto language. In *ECAL*, 813–819 (2011).

[34] Bugoon, J., Buller, D. B. & Woodall, W. G. Nonverbal communication: The unspoken dialogue (1996).

[35] Hertenstein, M. J., Verkamp, J. M., Kerestes, A. M. & Holmes, R. M. The communicative functions of touch in humans, nonhuman primates, and rats: a review and synthesis of the empirical research. *Genetic, social, and general psychology monographs* **132**, 5–94 (2006).

[36] Bosga, J. & Meulenbroek, R. G. Joint-action coordination of redundant force contributions in a virtual lifting task. *Motor control* **11**, 235–258 (2007).

[37] Tang, A., McLachlan, P., Lowe, K., Saka, C. R. & MacLean, K. Perceiving ordinal data haptically under workload. In *Proceedings of the 7th international conference on Multimodal interfaces*, 317–324 (ACM, 2005).

[38] Chan, A., MacLean, K. & McGrenere, J. Designing haptic icons to support collaborative turn-taking. *International Journal of Human-Computer Studies* **66**, 333–355 (2008).

[39] Peng, C.-K. *et al.* Long-range correlations in nucleotide sequences. *Nature* **356**, 168–170 (1992).

[40] Schenkel, A., Zhang, J. & Zhang, Y.-C. Long range correlation in human writings. *Fractals* **1**, 47–57 (1993).

[41] Tsallis, C. & Brigatti, E. Nonextensive statistical mechanics: A brief introduction. *Continuum Mechanics and Thermodynamics* **16**, 223–235 (2004).

[42] Abe, S. & Suzuki, N. Zipf-mandelbrot law for time intervals of earthquakes. *arXiv preprint cond-mat/0208344* (2002).

[43] Abe, S. & Suzuki, N. Law for the distance between successive earthquakes. *Journal of Geophysical Research: Solid Earth* **108** (2003).

[44] Mehri, A. & Darooneh, A. H. Keyword extraction by nonextensivity measure. *Physical Review E* **83**, 056106 (2011).

[45] Jamaati, M. & Mehri, A. Text mining by tsallis entropy. *Physica A: Statistical Mechanics and its Applications* (2017).

[46] Moghaddasi, H., Khalifeh, K. & Darooneh, A. H. Distinguishing functional DNA words; a method for measuring clustering levels. *Scientific Reports* **7** (2017).

[47] Duane, T. D. & Behrendt, T. Extrasensory electroencephalographic induction between identical twins. *Science* (1965).

[48] Montague, P. R. *et al.* Hyperscanning: simultaneous fmri during linked social interactions (2002).

[49] Rilling, J. K., King-Casas, B. & Sanfey, A. G. The neurobiology of social decision-making. *Current opinion in neurobiology* **18**, 159–165 (2008).

[50] Rilling, J. K. & Sanfey, A. G. The neuroscience of social decision-making. *Annual review of psychology* **62**, 23–48 (2011).

[51] Dumas, G., Nadel, J., Soussignan, R., Martinerie, J. & Garnero, L. Inter-brain synchronization during social interaction. *PloS one* **5**, e12166 (2010).

[52] Decety, J. & Lamm, C. The role of the right temporoparietal junction in social interaction: how low-level computational processes contribute to meta-cognition. *The Neuroscientist* **13**, 580–593 (2007).

[53] Blakemore, S.-J. & Frith, C. Self-awareness and action. *Current opinion in neurobiology* **13**, 219–224 (2003).

[54] Pfurtscheller, G., Woertz, M., Supp, G. & da Silva, F. L. Early onset of post-movement beta electroencephalogram synchronization in the supplementary motor area during self-paced finger movement in man. *Neuroscience letters* **339**, 111–114 (2003).

[55] Tognoli, E., Lagarde, J., DeGuzman, G. C. & Kelso, J. S. The phi complex as a neuromarker of human social coordination. *Proceedings of the National Academy of Sciences* **104**, 8190–8195 (2007).

[56] Babiloni, F. *et al.* High resolution EEG hyperscanning during a card game. In *2007 29th Annual International Conference of the IEEE Engineering in Medicine and Biology Society*, 4957–4960 (IEEE, 2007).

[57] Varela, F. J. Resonant cell assemblies: a new approach to cognitive functions and neuronal synchrony. *Biological research* **28**, 81–95 (1995).

[58] Destexhe, A., Contreras, D. & Steriade, M. Spatiotemporal analysis of local field potentials and unit discharges in cat cerebral cortex during natural wake and sleep states. *Journal of Neuroscience* **19**, 4595–4608 (1999).

[59] Roelfsema, P. R., Engel, A. K., König, P. & Singer, W. Visuomotor integration is associated with zero time-lag synchronization among cortical areas. *Nature* **385**, 157 (1997).

[60] Lachaux, J.-P., Rodriguez, E., Martinerie, J. & Varela, F. J. Measuring phase synchrony in brain signals. *Human brain mapping* **8**, 194–208 (1999).

[61] Lindenberger, U., Li, S.-C., Gruber, W. & Müller, V. Brains swinging in concert: cortical phase synchronization while playing guitar. *BMC neuroscience* **10**, 22 (2009).

[62] Strogatz, S. H. Exploring complex networks. *nature* **410**, 268 (2001).

[63] Newman, M. E. The structure and function of complex networks. *SIAM review* **45**, 167–256 (2003).

[64] Sporns, O., Chialvo, D. R., Kaiser, M. & Hilgetag, C. C. Organization, development and function of complex brain networks. *Trends in cognitive sciences* **8**, 418–425 (2004).

[65] Toppi, J. *et al.* Investigating cooperative behavior in ecological settings: an EEG hyperscanning study. *PloS one* **11**, e0154236 (2016).

[66] Tsallis, C. Possible generalization of boltzmann-gibbs statistics. *Journal of statistical physics* **52**, 479–487 (1988).

[67] Tognoli, E. EEG coordination dynamics: neuromarkers of social coordination. In *Coordination: Neural, Behavioral and Social Dynamics*, 309–323 (Springer, 2008).

[68] Interlink Electronics. *FSR Force Sensing Resistor Integration Guide and Evaluation Parts Catalog*. Rev. D.

[69] Hertenstein, M. J. Touch: Its communicative functions in infancy. *Human Development* **45**, 70–94 (2002).

[70] Tan, H. Z., Durlach, N. I., Reed, C. M. & Rabinowitz, W. M. Information transmission with a multifinger tactual display. *Attention, Perception, & Psychophysics* **61**, 993–1008 (1999).

[71] Tsallis, C. Nonextensive statistics: theoretical, experimental and computational evidences and connections. *Brazilian Journal of Physics* **29**, 1–35 (1999).

[72] Luhn, H. P. The automatic creation of literature abstracts. *IBM Journal of research and development* **2**, 159–165 (1958).

[73] Takagi, A., Ganesh, G., Yoshioka, T., Kawato, M. & Burdet, E. Physically interacting individuals estimate the partner's goal to enhance their movements. *Nature Human Behaviour* **1**, 0054 (2017).

[74] Hurtado, J. M., Rubchinsky, L. L. & Sigvardt, K. A. Statistical method for detection of phase-locking episodes in neural oscillations. *Journal of neurophysiology* **91**, 1883–1898 (2004).

[75] Winkler, I., Haufe, S. & Tangermann, M. Automatic classification of artifactual ica-components for artifact removal in eeg signals. *Behavioral and Brain Functions* **7**, 30 (2011).

[76] Müller, V., Sänger, J. & Lindenberger, U. Intra-and inter-brain synchronization during musical improvisation on the guitar. *PloS one* **8**, e73852 (2013).

[77] Jammalamadaka, S. R. & Sengupta, A. *Topics in circular statistics*, vol. 5 (world scientific, 2001).

[78] Chavez, M., Besserve, M., Adam, C. & Martinerie, J. Towards a proper estimation of phase synchronization from time series. *Journal of neuroscience methods* **154**, 149–160 (2006).

[79] Konvalinka, I. *et al.* Frontal alpha oscillations distinguish leaders from followers: multivariate decoding of mutually interacting brains. *NeuroImage* **94**, 79–88 (2014).

[80] Ménoret, M. *et al.* Neural correlates of non-verbal social interactions: a dual-EEG study. *Neuropsychologia* **55**, 85–97 (2014).

[81] Hatem, S. M. *et al.* Rehabilitation of motor function after stroke: a multiple systematic review focused on techniques to stimulate upper extremity recovery. *Frontiers in human neuroscience* **10**, 442 (2016).